THE UNIVERSITY
of EDINBURGH

Investigation of PML locus on chr15 for susceptibility to Paget's disease of Bone

Sachin WANI (M.B.B.S., M.Sc.)

A thesis submitted for the degree of Doctor of Philosophy

The University of Edinburgh

2019

Declaration

I hereby declare that this thesis has been composed by myself and the work described within, except where specifically acknowledged, has been carried out entirely by myself and it has not been submitted for any previous degree application. The information obtained from sources other than this study is acknowledged in the text or included in the references.

Sachin Wani

Dedication

To my family and friends and all those who are contributing to make the world a better place in their own way.

Acknowledgements

I would like to thank my supervisors Dr. Omar Albagha and Prof. Stuart Ralston for giving me this opportunity to study for a PhD in relation to bone disease. Omar has always supported me and advised me on how to best approach the questions I have during this work and conduct experiments accordingly. Stuart has been very supportive and enthusiastic in providing necessary input regularly. For e.g. access to patient records and samples, secure mice from abroad as well as encouragement to do and achieve more all the time. Both of them pointed me in the right direction in relation to paper publishing and presentations at various levels.

I would also like to thank my bone group members (Rob Van't Hof, Aymen Idris and Philip Riches) and lab members (Asim Azfer, Micaela Rios, Antonia Sophocleous, Maheva Vallet, Lorraine Rose, Euphemie, Silvia Marino, Anna Torquivst, Fiano Kierans, Nerea Alonso, Beatrice) for helping and facilitating my doctoral work and creating a friendly and conducive environment. I would like to thank my administrators (Belinda, Rosa) and technicians (Stephen, Helen, Joyce, Shaun, Evelyn, Derek and his team) as well as IGMM researchers (Bernie Ramsahoye, Alex Adams, Rahul Kalla, Toby Hurd, Matthieu Vermeren, Mandy Johstone, Liz Freyer, Simon Wilkinson, Noor Gammoh and Dasa) for help and support to ensure a smooth performance of experiments and achievement of relevant results.

I would like to thank GENEPAD ERC and FAST/ERC PDB for the funding as well as University of Edinburgh staff scholarship for payment of PhD tuition fees. I would like to thank Pauline, Kathy Evans and Cathy Abbott for their advice and support related to postgraduate study/administration. I would also like to thank my supervisory committee (Elaine Nimmo and Prof. Donald Salter) for their excellent independent, impartial advice and constructive criticism to ensure my doctoral work was always heading in the right direction. Lastly, I would like to thank my friends and family members especially my wife Purva and son Parth for their support in achieving this milestone in my professional career as well as personal life. Thank you all.

Table of Contents

Presentations from this thesis

- **S. Wani** (2018) Exploring function of *Promyelocytic Leukaemia*, a susceptibility gene for Paget's disease of Bone. Oral presentation at CGEM away day, IGMM, University of Edinburgh Jan 2018, Edinburgh, UK. **Received Best oral presentation**.
- **S. Wani**, D.M. Salter, S.H. Ralston and O.M.E. Albagha (2017) The Paget's disease susceptibility gene *PML* regulates osteoclast activity *in vitro*. Presented as poster at European Calcified Tissue Society Conference (ECTS), May 2017, Salzburg, Austria
- **S. Wani**, D.M. Salter, S.H. Ralston and O.M.E. Albagha (2016) Investigation of Paget's disease susceptibility locus on chromosome 15q24 using Targeted next generation DNA sequencing approach. Presented as poster at ECTS conference, May 2016, Rome, Italy. **Received Best poster prize in genetics/epigenetics category**.

Publications from this thesis

- **S. Wani**, D.M. Salter, S.H. Ralston and O.M.E. Albagha (2019) Tumour suppressor *Promyelocytic Leukaemia*, a susceptibility gene for PDB, regulates bone metabolism by negatively regulating osteoclastogenesis. In preparation for submission.

Abbreviations

µCT Microcomputed tomography scanning
1,25-$(OH)_2$ vitamin D3 Vitamin D3
ALP Alkaline phosphatase
A-MuLV Abselon leukaemia virus
AP-1 Activator protein-1
APL Acute promyelocytic leukaemia
ATG5 Autophagy-related gene 5
ATP Adenosine triphosphate
ATP6v0d2 A subunit of ATPase
Bcl6 B-cell lymphoma 6
Blimp1 B-lymphocyte induced maturation protein 1
BMDM Bone marrow derived macrophages
BMP Bone morphogenetic protein
BMSC Bone marrow stromal cells
BSA Bovine serum albumin
BSP Bone sialoprotein
BWA Burrows-Wheeler alignment tool
C57Bl6 An inbred mouse strain (C57 Black 6)
CAII Carbonic anhydrase II
CASR Calcium sensing receptor
Ctsk Cathepsin K
CCL7 Chloride channel 7
cDNA Complementary DNA
CEBP β CCAAT-enhancer-binding protein β
chr Chromosome
CK2 Casein kinase 2
CSF1 Colony stimulating factor 1
c-Src SRC Proto-oncogene, non-receptor tyrosine kinase
CTX Carboxy-terminal collagen crosslinks
CYLD Cylindromatosis lysine 63 deubiquitinase
DC STAMP Dendritic cell-specific transmembrane protein
DMEM Dulbecco's modified eagle's medium
DTT Dithiothreitol
ENCODE Encyclopedia of DNA elements
EoPDB Early onset familial Paget's disease of bone
ER Endoplasmic reticulum
ERK Extracellular signal-regulated kinase
ESH Expansile skeletal hyperphosphatasia
ESR1 Estrogen receptor 1
EtOH Ethanol
FCS Fetal calf serum
FEO Familial expansile osteolysis
FFPE Formalin fixed paraffin embedded
FGF Fibroblast growth factor

FM Fibrovascular marrow
GAS IFN-γ activated site
GATK Genome analysis toolkit
GOLGA6A Member of golgin family of proteins
HCl Hydrochloric acid
HET Heterozygote
hMSC Human mesenchymal stem cells
HOM Homozygote
IBMPFD Inclusion body myopathy, Paget's disease and Frontotemporal dementia
IBSP Integrin-binding sialoprotein
Ids Inhibitors of differentiation/DNA binding
IFN-γ Interferon γ
IGF1 Insulin like growth factor 1
IHC Immunohistochemistry
Ihh Indian hedgehog
IKBα Nuclear factor of kappa light polypeptide gene enhancer in B-cells inhibitor, alpha
IL Interleukins
IRF 8 Interferon regulatory factor-8
ISLR Immunoglobulin superfamily containing leucine rich repeat
ISLR2 Immunoglobulin superfamily containing leucine rich repeat 2
ISRE Interferon stimulated response element
JAK-STAT Janus kinase/signal transducer and activator of transcription
JNK c-Jun N-terminal kinase
JPD Juvenile Paget's disease
KO Knockout
LC3 Light chain 3 gene
LD Linkage Disequilibrium
LOXL1 Lysyl oxidase Like 1
LRP5 Lipoprotein receptor-related protein 5
mAb Monoclonal antibody
MafB v-maf musculoaponeurotic fibrosarcoma oncogene family protein B
M-CSF Macrophage colony stimulating factor
MITF Microphthalmia-associated transcription factor
MKK6 Mitogen-activated protein kinase kinase 6
MMP9 Matrix metalloproteinase 9
MNC Multinucleated
mRNA Messenger RNA
MSC Mesenchymal stem cells
MVNP Measles virus nucleocapsid gene
NCI National cancer Institute
NES Nuclear export signal
NF-kB Nuclear factor Kappa B
NHLBI National Heart, Lung, and Blood Institute

NLS Nuclear localization sequence
NTC No DNA template control
NUP205 Nucleoporin 205kDa
OPG Osteoprotegerin
OPTN Optineurin
ORF Open reading frame
OSCAR Calcitonin receptor, osteoclast-associated receptor
OSx Osterix
PCR Polymerase chain reaction
PDB Paget's disease of bone
PDGF Platelet derived growth factor
PI3-Akt Phosphoinositide-3-kinase–protein kinase B
PINP Procollagen type I N propeptide
PML Promyelocytic Leukemia
PPARγ Peroxisome proliferator activator γ
PTH Parathyroid hormone
qPCR Quantitative Polymerase Chain Reaction
qRT-PCR Quantitative Real-Time Polymerase Chain Reaction
RANKL Receptor activator of the nuclear factor NF-kB ligand
RANK Receptor activator of NF-kB
Rb Retinoblastoma
RF Ruffled border
RIN3 Ras and Rab interactor 3
RING Really interesting new gene
ROI Region of interest
rRNA Ribosomal RNA
Runx2 Runt related transcription factor 2
SD standard deviation
SEM standard error of mean
Sema 4D Semaphorin 4D
SIFT Sorting intolerant from tolerant
SIM SUMO interacting motif
SNP Single nucleotide polymorphism
Sp1 Sphingosine-1-phosphate
SQSTM1 Sequestosome 1
STOML1 Stomatin like 1
SZ Sealing zone
TAB2 TGF-Beta activated kinase 1 binding protein 2
TAK1 TGF-Beta activated kinase 1
TB Trabecular bone
TBST TBS-tween
TF Transcription factor
TGF-β Transforming growth factor β
TNFA Tumor Necrosis Factor alpha
TNFRSF11A TNF receptor superfamily member 11a
TNFRSF11B TNF receptor superfamily member 11b

TRAcP Tartrate resistant acid phosphatase
TRAF6 TNF-receptor associated factor 6
TRIM TRI-partite motif
UBA Ubiquitin-binding domain
VCP Valosin containing protein
Vit.C Vitamin C
Wnt Wingless
WT Wild type
ZIPP Zoledronate in the prevention of Paget's
αMEM Minimal essential medium eagle - Alpha modification
αVβ3 Integrin vitronectin receptor
βGP β-glycerol phosphate

List of Figures

List of Tables

List of Appendices

Lay Abstract

Bone in our body constantly undergoes change in a process called bone turnover or remodelling. Bone remodelling involves breaking down of bone (bone resorption) by bone cells called osteoclasts followed by replacement with new bone (bone formation) by bone cells called osteoblasts.

This process is usually under control but sometimes becomes abnormal and results in skeletal disorders like Paget's disease of bone (PDB). PDB usually affects people later in life (age of onset > 55 years of age). In PDB, the osteoclasts become overactive and erode the bone too fast which in turn leads to accelerated and disorganised bone formation by osteoblasts. The resulting bone formed is weak and results in symptoms and complications such as bone pain, osteoarthritis, bone deformity, compression of nerves and fractures.

The exact cause of PDB is not fully understood but studies have shown that it most likely occurs as a result of genetic changes with an influence from several environmental factors. At present, DNA mutations in one of the genes called *SQSTM1* result in 10% of PDB cases without family history and up to 40% of cases with family history of PDB. Therefore, more genes remain to be explored to determine their contribution to PDB development and improve the diagnosis, treatment and prevention of this late-onset chronic metabolic bone disease.

Studies in our laboratory have identified new genes, abnormalities of which may result in increased susceptibility to PDB. My doctoral study involves investigating one of these genes called *PML* in relation to bone metabolism and PDB.

I found a few genetic variations in *PML* which when inherited, may increase the risk of getting PDB. *Pml* was found to be expressed in osteoclasts and osteoblasts from mouse and human tissue. PDB patients had lower levels of *PML* compared to healthy controls.

Mice with a deletion of *Pml* in their DNA showed increase in osteoclast formation and activity compared to normal control mice. Also, osteoblasts from these mice showed increased bone mineralisation compared to controls thereby neutralising the bone resorption by osteoclasts. Indeed, I did not find any signs of bone lesions and changes in bone microstructure in these mice. Further experiments in these mice suggested that changes in *Pml* expression was altering the response of immune cells in maintaining osteoclast development and activity but more in-depth studies will be needed to understand how genetic variations in *PML* increase susceptibility to disease.

Thus, my PhD study has found a novel role of PML in regulating bone metabolism by inhibiting osteoclast formation and activity. Alterations in *PML* expression in association with environmental factors could increase risk of developing PDB and warrants further investigation.

Abstract

Paget's disease of bone (PDB) is a common bone disorder. The disease is characterised by localised abnormalities in bone turnover (Ralston et al. 2008). Genetic factors are important for PDB. Genome-wide association studies (GWAS) identified a susceptibility locus for PDB on chromosome 15q24.1 in addition to six other loci (Albagha et al. 2010; Albagha et al. 2011). The strongest signal for disease association from this locus is located within Promyelocytic Leukemia (*PML*). *PML* is a tumour suppressor gene involved in chromosomal translocation leading to acute promyelocytic leukaemia (APL). PML is involved in multiple cellular functions like cell growth, senescence, DNA repair, antiviral response and apoptosis but has never been implicated directly in bone metabolism. The aim of my PhD was to explore role of PML in bone biology.

Fine mapping of the 15q locus was performed using targeted next generation sequencing. In chapter 4, Targeted DNA sequencing of the PDB susceptibility locus on chr15 identified variants within *PML* that are associated with the disease. In chapter 5, expression analysis revealed expression of *Pml* in bone cells from murine and human tissue and its expression varies during the development and differentiation of these cells. *PML* expression was found to be downregulated in patients with PDB. In chapters 6 and 7, experiments with RAW 264.7 cell line and *Pml* knock out mice point to a negative regulatory role of PML in osteoclast differentiation. Osteoclasts from *Pml* knockout mice show increased formation, fusion and activity in response to RANKL compared to wt mice. The expression levels of osteoclast related genes such as *Ctsk* (*Cathepsin K*), *Dcstamp* and *Nfatc1* were also higher in *Pml* knockout mice. Osteoblasts differentiated from these mice show increased mineralised nodule formation *in vitro* compared to wt mice. Skeletal phenotyping by micro CT revealed no significant differences in structure and bone density between *Pml* knockout and wt mice irrespective of age.

Interferon gamma (IFN-γ) is a cytokine which is known to induce Interferon Regulatory Factor 8 (IRF-8) and PML in mouse peritoneal macrophages (Dror et al. 2007). IRF-8 is a transcription factor downregulated during RANKL mediated osteoclastogenesis (Zhao et al. 2009) and an essential regulator of *PML* gene in activated macrophages (Dror et al. 2007). In chapter 8, it was found that IFN-γ inhibited osteoclastogenesis in wt mice but failed to have a pronounced effect on osteoclasts in mice lacking *Pml*. Thus, lack of *PML* possibly renders IFN-γ and IRF-8, ineffective in suppressing osteoclastogenesis.

Thus, PML controls osteoclast development probably by modulating response of IRF-8 and IFN-γ in association with direct or indirect regulation of osteoclast related genes such as *Ctsk* (encoding Cathepsin K), *Dcstamp* and *Nfatc1*. Osteoclasts are already primed for increased formation, differentiation, fusion and activity due to upregulation of these factors in absence of PML.

My doctoral study therefore identifies PML as a novel regulator of bone metabolism. Functional genetic variants within *PML* gene possibly contribute to reduced *PML* expression thereby predisposing to PDB by increasing osteoclast differentiation and activity with an increase in osteoblast mineralisation possibly to counteract increased bone resorption.

CHAPTER ONE

Introduction

1 Introduction

1.1 Bone

Bone is a dynamic organ that supports and protects various tissues of the body. It forms an integral part of the skeletal system along with network of ligaments, tendons and joint tissue (cartilage and synovium). It enables body movements and is also a specialised connective tissue involved in haematopoietic cell production, mineral and fat storage as well as other metabolic and endocrine functions (Burr & Akkus 2013; Kini and Nandeesh 2012).

Formation of new bone is termed ossification. Bone development occurs by two important processes during embryonic development as well as postnatally: Intramembranous ossification is characterised by formation of bone from mesenchymal connective tissue giving rise to flat bones of the skull as well as scapula, mandible and clavicle whereas endochondral ossification involves development of bone from cartilage. This results in long bone formation of tibia, femur, radius and humerus (Kini and Nandeesh 2012; Allen & Burr 2013).

Bone can be divided into several types based on anatomy and structure. Structurally, bone is divided into cortical (compact) bone and trabecular (cancellous or spongy) bone and microscopically/histologically into lamellar and woven bone. Anatomically, based on shape, the bone is divided into long, short, flat, irregular and sesamoid bones (Clarke 2008).

Cortical bone surrounding the marrow space, is solid, dense whereas trabecular bone appears spongy and consists of a network of interconnected trabeculae within the bone marrow. Cortical bone constitutes 80% of the skeleton and has a low surface area and lower remodelling rate and is found in outer layer of flat bones and diaphysis of long bones. Cortical bone has an outer periosteum and inner endosteum. The basic units of cortex are called osteons or haversian systems which are cylindrical structures composed of a series of concentric lamellae of collagen fibres surrounding a central

haversian canal containing nerves, blood vessels and lymphatics. In contrast, trabecular bone is less dense, has a much larger surface area and higher remodelling rate though it constitutes only 20% of the skeleton. Lamellae within trabecular bone run parallel to each other. Trabecular bone is found in flat bones, metaphyseal ends of long bones and vertebrae (Burr & Akkus 2013; Ralston 2017).

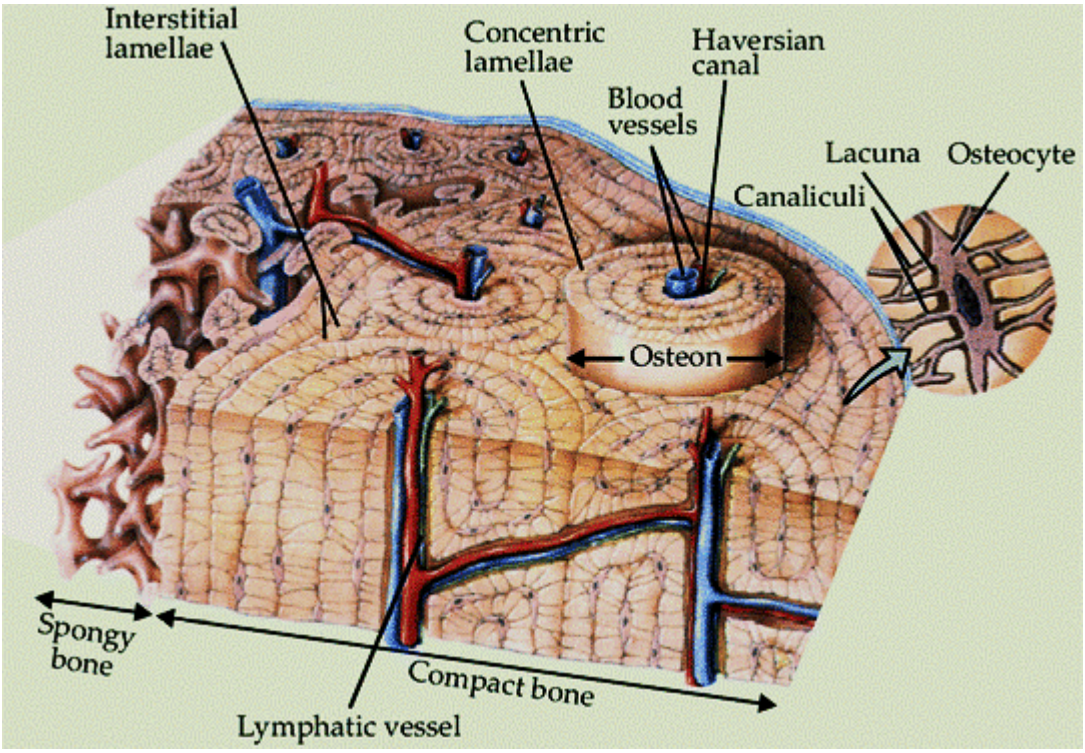

Figure 1.1 Microscopic sub-structure of cortical bone.
Image obtained from (Ritchie et al. 2009).

Lamellar bone is characterised by regular parallel arrangement of collagen into sheets/lamellae. This is absent in woven bone wherein the collagen fibrils are arranged in a random manner. This results in lamellar bone being much stronger but less metabolically active compared to woven bone (Kini and Nandeesh 2012). Woven bone is normally produced during primary bone formation but is also seen in abnormal high bone turnover conditions like Paget's disease of bone and hyperparathyroidism (Clarke 2008).

The different parts of long bone (femur) are shown in Figure 1.2. The main cylindrical part of the long bone surrounding the medullary cavity is called

diaphysis. The cavity contains yellow bone marrow and the diaphyseal walls are composed of hard, dense compact bone. The ends of long bones are called epiphyses which are covered by articular cartilage and filled with spongy/cancellous bone and red marrow. Metaphysis is the zone between diaphysis and epiphysis. During bone growth, a layer of hyaline cartilage called growth plate separates epiphysis from metaphysis which eventually forms the epiphyseal line at the end of growth period. Medullary cavity is lined by endosteum, a thin layer of connective tissue where bone growth, repair and remodelling occur. Periosteum, a fibrous connective tissue layer covering outer surface of bone, contains blood vessels, nerves, lymphatics as well as progenitor cells and protects and nourishes the bone (OpenStax Anatomy & Physiology 2016). Flat bones are composed of spongy bone enclosed within two thin layers of compact bone and have marrow.

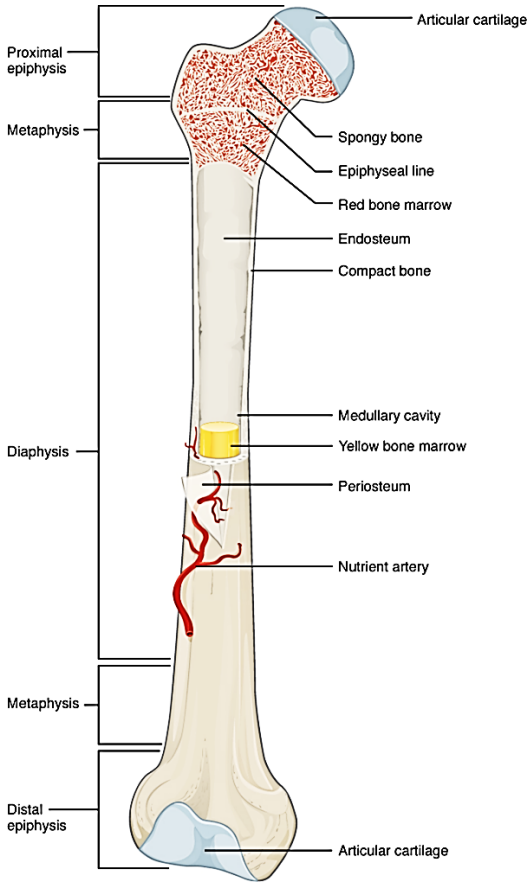

Figure 1.2 Structure of a long bone.
(OpenStax Anatomy & Physiology 2016)

Bone is therefore composed of cortical bone, cancellous bone, bone marrow, extracellular matrix, blood vessels, nerves, lymphatics and bone cells. Bone matrix consists of organic and inorganic components. Organic component is termed osteoid with Type 1 collagen constituting 90% and remainder 10% formed by proteoglycans and non-collagenous proteins including bone sialoprotein, osteopontin, osteonectin and osteocalcin. The inorganic component is mainly composed of minerals calcium and phosphorus that link together to form crystals of hydroxyapatite deposited within the organic matrix. Bone cells include osteoblasts, osteoclasts, osteocytes and osteoprogenitor stem cells within the bone marrow (Burr & Akkus 2013).

1.2 Bone cells

1.2.1 Osteoclasts

Osteoclasts are the primary bone resorbing cells of haematopoietic origin derived from monocyte-macrophage lineage precursor cells. They are involved in bone modelling as well as remodelling. Decreased osteoclast activity results in increased bone mass and vice versa. During bone modelling, recruitment of osteoclast precursors to bone occurs where they undergo proliferation and differentiation followed by fusion into multinucleated mature cells. Osteoclasts are polarised with attainment of functional domains at the bone surface, followed by acidification and degradation of mineralised bone matrix. The average lifespan of an osteoclast is about 12 days (Rosenberg et al. 2012). Post bone resorption, osteoclasts undergo apoptosis (Bellido et al 2013). Osteoclastogenesis is regulated by several signalling pathways involving multiple components, abnormalities of which results in various bone diseases.

Macrophage colony stimulating factor (M-CSF) and Receptor activator of the nuclear factor NF-kB ligand (RANKL) are the two most important cytokines involved in differentiation of haematopoietic precursors to functional osteoclasts. M-CSF which is secreted by the bone marrow stromal cells

(BMSCs), osteoblasts as well as osteocytes, contributes to osteoclast differentiation, migration and survival (Tanaka et al. 1993; Insogna et al 1997). M-CSF binds to its receptor colony stimulating factor 1 receptor (c-fms) which is present on osteoclast precursors. It also controls the spreading, motility, cytoskeletal organisation and apoptosis of the mature resorbing cell via association with c-Src and PI3-Akt axis stimulation (Fig.3) (Insogna et al 1997; Teitelbaum & Ross 2003).

Haematopoietic stem cells differentiate into early osteoclast precursors in presence of transcription factor PU.1 especially their commitment to myeloid lineage. PU.1 also induces c-fms expression in osteoclast precursors. M-CSF binding to c-fms induces expression of RANK on osteoclast precursors thereby inducing them to differentiate into osteoclasts in response to RANKL stimulation. *Csf1* knockout mice show osteopetrosis (Yoshida et al. 1990) but recover with age from decrease in osteoclast activity and number (S. Niida et al 1999; Myint et al. 1999; Teitelbaum & Ross 2003). However, *Tnfsf11* (RANKL) knockout mice have osteopetrosis that does not improve with age indicating that M-CSF alone is not enough to drive osteoclast precursors to osteoclasts *in vivo* and RANKL is the more dominant cytokine (Begg et al. 1993; Kong et al. 1999; Kearns et al. 2008). RANKL is expressed on surface of osteoblasts as well as osteocytes and dendritic cells but is also secreted in soluble form (Kearns et al. 2008). It binds to its receptor RANK on osteoclast precursors leading to their activation and differentiation into multinucleated osteoclasts (Lacey et al. 1998; Wada et al. 2006; Kohli & Kohli 2011).

RANK (which is a member of TNF receptor superfamily like RANKL) is expressed on osteoclast precursors as well as mature osteoclasts (Li et al. 2000). RANK as well as RANKL knockout mice show osteopetrosis (Dougall et al. 1999; Kong et al. 1999) due to lack of osteoclast formation and loss of function mutations in humans' results in a similar phenotype (Sobacchi et al. 2007; Guerrini et al. 2008).

RANK-RANKL interaction results in activation of several signalling pathways which play an important role in osteoclast formation, activation and survival.

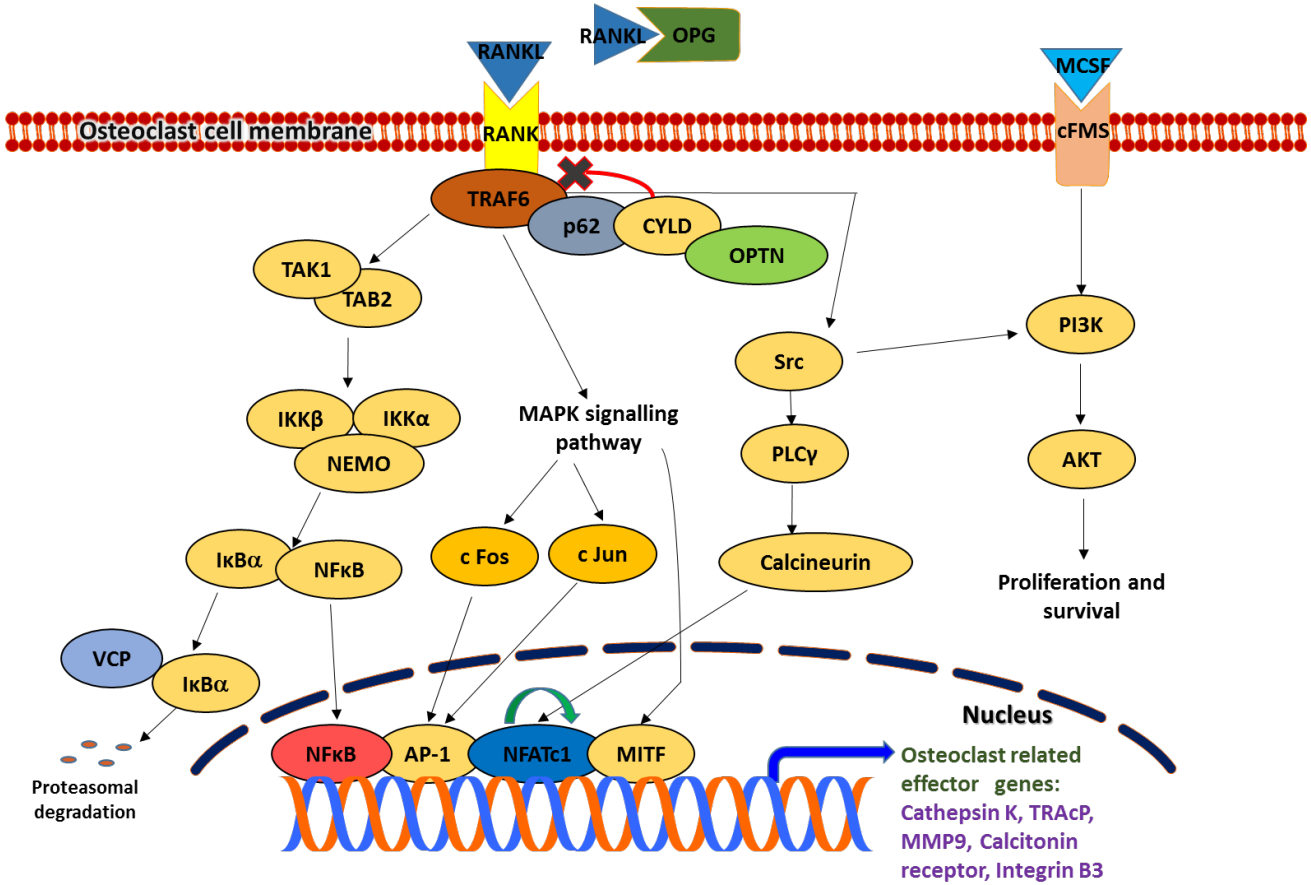

Figure 1.3 Signal transduction pathways involved in osteoclastogenesis.

Curved green arrow indicates NFATc1 autoamplification and red marker with cross indicates deubiquitination of TRAF6 leading to inhibition of RANK signalling. See text for further description.

One of the most important signalling pathways for osteoclast formation is nuclear factor Kappa B (NF-κB) which resides in an inactive state in the cytoplasm complexed to IKBα. RANKL binds to its receptor RANK resulting in recruitment of TNF-receptor associated factor 6 (TRAF6) to RANK's cytoplasmic domain. TRAF6 polyubiquitination and p62 create a platform for assembly of TAK1-TAB2 complex. The deubiquitinating enzyme CYLD inhibits RANK signalling by binding to complex of TRAF6 and p62 (via its ubiquitin domain) (Jin et al 2008). Optineurin (OPTN) is involved in inhibition of NF-κB in immune cells mediated via its interaction with CYLD (Nagabhushana et al 2011) and negative regulation of osteoclast differentiation in mice (Obaid et al. 2015). Phosphorylation of TAK1 results in K63 mediated polyubiquitination of NEMO and phosphorylation of IKKα. This in turn leads to phosphorylation and proteasomal degradation of IKBα liberating NF-κB which enters the nucleus to activate expression of target genes. NF-κB has two signalling pathways induced by RANKL: Canonical RelA/p50 pathway and non-canonical RelB/p52 pathway. Lack of these NF-κB subunits renders the mice unable to form osteoclasts. (Franzoso et al. 1997)

Along with NF-κB, RANK/TRAF mediated signalling also activates:

1. c-Fos / c-Jun N-terminal kinase (JNK): the activator protein-1 (AP-1) complex and calcineurin / PLCγ / NFATc1 pathways which play an important role in osteoclast formation;
2. Mitogen-activated protein kinase kinase 6 (MKK6) / p38 mitogen-activated protein kinase (MAPK) / microphthalmia-associated transcription factor (MITF) along with Src involved in osteoclast activation and
3. Extracellular signal-regulated kinase (ERK) as well as Src which are involved in osteoclast survival. (Boyce et al 2013).

Thus, activated NF--κB, AP-1 complex and MITF transcription factors in conjunction with NFATc1 upon entering the nucleus, promote expression of genes responsible for osteoclast differentiation, resorption and survival including, tartrate resistant acid phosphatase (TRAcP), calcitonin receptor, matrix metalloproteinase 9 (MMP9), Cathepsin K, dendritic cell-specific transmembrane protein (DC-STAMP), chloride channel 7 (CLC-7), osteoclast-associated receptor (OSCAR) and β3 integrins. NFATc1 is the master transcription factor for osteoclastogenesis which is upregulated in response to NF-κB, c-Fos and increased intracellular calcium/calcineurin and leads to its own autoamplification as well (Mellis et al. 2011; Boyce et al 2013).

Hormones such as vitamin D (1,25-$(OH)_2$ vitamin D3) and parathyroid hormone (PTH) as well as cytokines such as Interleukins (IL-6, IL-1 and IL-11) enhance osteoclastogenesis by upregulating expression of RANKL (Bellido et al 2013).

Osteoclastogenesis is also inhibited by inflammatory factors, cytokines and transcriptional repressors which play a crucial role in bone homeostasis by fine tuning remodelling of bone and preventing excessive bone resorption. RANKL signalling induces downregulation of osteoclast inhibitory factors. These include v-maf musculoaponeurotic fibrosarcoma oncogene family protein B (MafB), Eos (*IKAROS Family Zinc Finger 4)*, inhibitors of differentiation/DNA binding (ids), B-cell lymphoma 6 (*Bcl6*), and interferon regulatory factor-8 (*IRF-8*) (Boyce et al 2013). Bcl6, Inhibitor of DNA binding 1 (Id1) and IRF8 deficient mice therefore exhibit decreased bone mass and increased osteoclastogenesis. Also, NFATc1 induces B-lymphocyte induced maturation protein 1 (Blimp1) in response to RANKL stimulation, which in turn suppresses *MafB*, *IRF8* and *Bcl6* expression. Loss of Blimp1 in murine osteoclasts leads to *Bcl6* up-regulation and they exhibit osteopetrosis resulting from impaired osteoclastogenesis (Miyauchi et al. 2010; Zhao & Ivashkiv 2011).

Thus, RANKL/RANK mediated upregulation of *NFATc1* leads to promotion of osteoclastogenesis directly, as well as indirectly by suppression of negative regulators (Boyce et al 2013).

Osteoblasts and osteocytes also secrete osteoprotegerin (OPG). OPG acts as a decoy receptor of RANKL preventing its binding to RANK receptor on osteoclasts leading to inhibition of osteoclastogenesis and bone resorption (Yasuda et al 1998, Lacey et al 1998). Therefore, ratio of RANKL to OPG determines the rate of osteoclast differentiation (Boyce et al 2013).

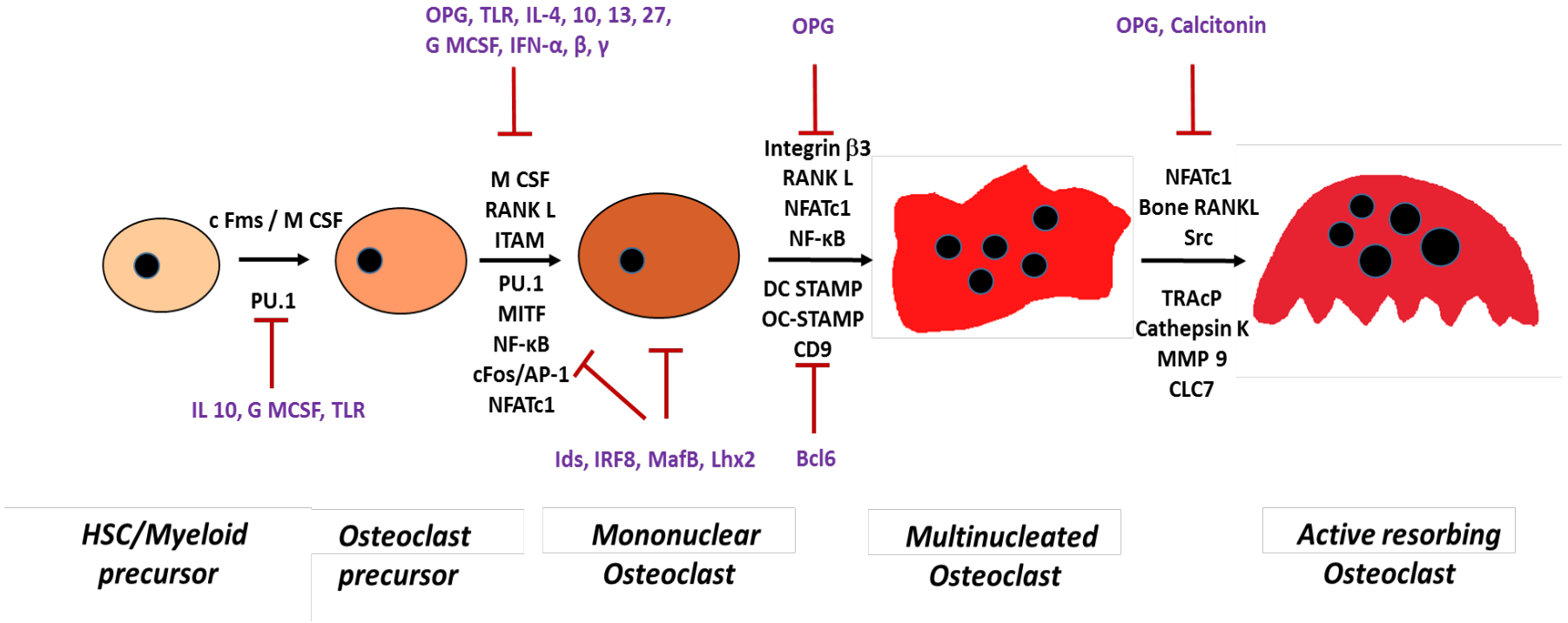

Figure 1.4 Regulation of osteoclastogenesis.

Myeloid precursors differentiate into osteoclast precursors in presence of M-CSF. RANKL stimulation promotes formation of mononuclear osteoclasts which fuse to form multinucleated osteoclasts. These secrete various factors and function as active polarised bone resorbing cells. This process is regulated at various stages by multiple genes encoding transcription factors, receptors and cytokines as shown above. Inhibitors of osteoclastogenesis (red markers) are shown in purple.

A characteristic feature of mature osteoclasts is multinucleation that results from fusion of mononuclear precursors. Various proteins such as DC-STAMP, OC-STAMP, ATP6v0d2 (a subunit of ATPase) and CD9 are known to be involved in this process. Activation involves cytoskeletal and membrane reorganisation resulting in osteoclast polarisation. An apical membrane is formed in close contact with the bone surface and a basolateral domain pointing away from the bone. Osteoclasts form tight circular ring-like sealing zones (SZ) using actin filament rich podosomes that secures them to the bone surface forming a cavity or resorption pit underneath (also known as Howship's lacunae). Within the sealing zone, cytoplasmic membrane of osteoclast is thrown into finger-like processes called the ruffled border (RB) which increases the cell surface area thereby facilitating secretion and uptake of components required for dissolution of bone matrix and minerals. The cytoplasm is filled with vesicles and vacuoles including lysosomes which contain the acid phosphatase TRAcP, a cellular and histologic marker of actively resorbing osteoclasts. Attachment to bone matrix is facilitated by the vitronectin receptor αVβ3 Integrin via a special motif present in bone matrix proteins bone sialoprotein (BSP) and osteopontin (OP). Extracellular compartment is acidified by secretion of chloride ions and protons across ruffled border. Protons generated by action of cytosolic carbonic anhydrase II (CA), are transported by V-ATPase at the ruffled border membrane and chloride ions are transported via the CLC-7 ion transporter. Mitochondria provide the energy in the form of ATP. Hydroxyapatite (mineralised) portion of the bone matrix is dissolved by HCl formed in the resorption lacuna. The remaining organic portion of matrix (composed mainly of Type I collagen) is digested enzymatically by the secreted matrix metalloproteinases (MMP) such as MMP9, MMP14, Cathepsin K and TRAcP (tartrate resistant acid phosphatase). Though unclear, TRAcP is thought to be involved in dephosphorylating bone matrix proteins thereby facilitating integrin binding and at the same time, generate reactive oxygen species for matrix degradation. The degraded products in the resorption zone are internalised into the cell and then either undergo lysosomal degradation or get

transcytosed via the basolateral membrane (Fig.1.5) (Mellis et al. 2011, Bellido et al 2013; Boyce et al 2013).

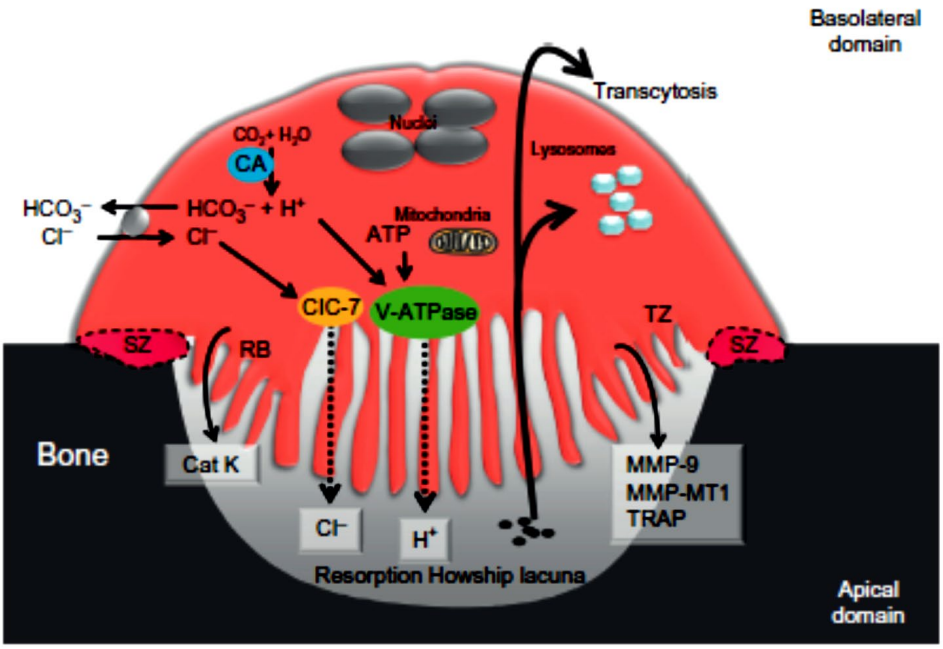

Figure 1.5 Schematic representation of an active resorbing osteoclast describing its morphology and function.

TZ is the transition zone. Figure obtained from Bellido et al. 2013. See text for description.

1.2.2 Osteoblasts

Osteoblasts are mononuclear cells involved in bone formation. They secrete bone matrix proteins and subsequently mineralise the bone matrix. They originate from the mesenchymal stem cells (MSCs) of bone marrow which can differentiate into several cell types such as osteoblast, adipocyte, chondrocyte, fibroblast and myocyte. MSCs commitment to osteoblast lineage, differentiation of osteoblasts from osteoprogenitor cells /preosteoblasts and osteoblast differentiation are regulated by various factors including Runx2, Osterix, BMPs, Wnt/B-catenin pathway, Notch signalling, growth factors (IGF1, TGF-β and FGFs) and hormones (estrogen, PTH, glucocorticoids). Mutations in the above mentioned factors have been reported in human diseases with skeletal deformities such as craniofacial

dysplasia, low/high bone mass as well as joint and limb deformities (Kini and Nandeesh 2012; Boyce et al 2013).

Runx2 belongs to Runt family of transcription factors (TFs). It is the earliest TF responsible for commitment of MSCs to osteoblast lineage and binds to osteocalcin promoter thereby regulating bone formation. *Runx2* knockout mice are devoid of osteoblasts resulting in no bone formation in the ribs at birth leading to death from respiratory failure (Otto et al. 1997; Komori et al. 1997). Osterix (Osx) is a zinc finger transcription factor that acts downstream of Runx2 and regulates differentiation of osteoblast progenitors to osteoblasts. Mice with a conditional deletion of *Osx* showed abnormal postnatal bone growth and bone homeostasis including osteoblast differentiation (Nakashima et al. 2002; Zhou et al 2010).

Bone morphogenetic proteins (BMPs) such as BMP2 and BMP7 augment expression of Runx2 and Osx in MSCs to promote osteoblast differentiation. (Datta et al. 2008)

Wnt (Wingless) is another major signalling pathway that promotes osteoblast differentiation. Wnt ligands act by canonical (through B catenin mediated gene transcription) or noncanonical pathways (B catenin independent gene transcription) to inhibit osteoblast apoptosis. Wnts stimulate differentiation of MSCs to osteoblast lineage and those of preosteoblasts. They prevent apoptosis of mature osteoblasts as well as osteocytes and increase expression of OPG from osteoblasts thereby inhibiting osteoclast mediated bone resorption. Low-density lipoprotein receptor-related protein 5 (LRP5) and frizzled proteins act as Wnt ligand receptors. Mutations with a gain of function in *LRP5* in patients results in high bone mass associated with strong bones resistant to fracture whereas children affected by osteoporosis-pseudoglioma syndrome due to loss of function mutations in *LRP5* have low bone mass associated with decreased Wnt signalling in osteoblasts (Gong et al 2001; Boyden et al 2002).

Indian hedgehog (Ihh) regulates osteoblast function by increasing expression of Runx2 (Shimoyama et al. 2007). Fibroblast growth factor (FGF) and

connexion 43 also regulate osteoblast differentiation. *FGF-2* knockout mice show lower bone mass and FGF18 upregulates osteoblast differentiation in an autocrine manner. Connexin 43 is the bone specific connexin and mutations of gene encoding it impair osteoblast differentiation and lead to skeletal malformation in mice (Florencio-Silva et al. 2015).

Notch family of transmembrane receptor signalling inhibit osteoblast differentiation by maintaining mesenchymal cells in progenitor stage. Depletion of Notch in osteoblast progenitors led to high bone mass in younger mice that progressed to severe osteopenia with ageing. Also, Notch depletion in osteoblast increased osteoclastogenesis due to reduced OPG production. Several other osteoblast negative regulatory factors act by inhibiting the BMP, Wnt or Smad signalling pathways. These include inhibitors of BMP such as gremlin, noggin and chordin and Wnt inhibitors sclerostin and dickkopf 1 (DKK1) (Boyce et al 2013).

Insulin like growth factor 1 (IGF1) also regulates Osx expression in osteoblastic cells (Celil & Campbell 2005) whereas Transforming growth factor β (TGF-β) has a dual effect on Runx2 activity as well as on osteoclast-osteoblast function. TGF-β supports osteoprogenitor cell proliferation and early differentiation but also inhibits later stages of osteoblast maturation, osteoblast mineralization, and its transition into osteocyte. TGF-β binds directly with its receptors on osteoclast to promote osteoclastogenesis but also inhibits their differentiation by decreasing RANKL/OPG secretion ratio (Wu et al. 2016). MicroRNAs regulate gene expression in osteoblasts leading to stimulation or inhibition of osteoblast differentiation (Florencio-Silva et al. 2015). For example, miR-218 stimulates Wnt signalling pathway to promote osteoblast differentiation (Hassan et al. 2012) whereas miR-335 represses Runx2 to inhibit osteogenic differentiation from hMSCs. (Tomé et al. 2011).

PTH enhances osteoblast number and activity by phosphorylating and activating Runx2, inducing IGF1 synthesis, stimulating Wnt/B-catenin pathway by inhibiting sclerostin and reducing the negative effects of peroxisome proliferator activated receptor gamma (PPARγ) on osteoblast

differentiation whereas continued excess secretion leads to enhanced bone resorption (Franceschi et al. 2003; Lombardi et al. 2011). Vitamin D is the main regulator of calcium homeostasis and skeletal health which indirectly enhances bone formation by increasing calcium absorption from the intestine and directly inhibits bone formation by regulating osteoblast differentiation and function via downregulation of *Runx2* (Kim et al. 2016). Oestrogen stimulates Runx2 activity and synergises with Wnt/B-catenin pathway to promote osteoblast differentiation of MSC-progenitor cells (McCarthy et al. 2003; Gao et al. 2013). Glucocorticoids have a dual role in bone turnover. They induce rapid bone loss transiently by delaying osteoclast apoptosis but ultimately lead to suppression of bone formation due to decreased osteoblastogenesis and osteoclastogenesis as well as increased osteoblast-osteocyte apoptosis (Bellido et al 2013).

Osteoblasts secrete bone matrix proteins Type1 collagen, osteocalcin (OCN), osteonectin, osteopontin and bone sialoprotein. They also secrete alkaline phosphatase (ALP), an enzyme involved in bone mineralisation. OCN regulates bone formation whereas circulating levels of OCN and ALP are used as biomarkers of bone formation (Kuo & Chen 2017).

Mature osteoblasts are cuboidal in shape with large round nuclei, enlarged Golgi and extensive ER. Upon completion of bone matrix formation, they either become quiescent flat-shaped lining cells of the bone surface or die from apoptosis whilst the remainder get embedded in the bone matrix to form osteocytes which are the most abundant cells of the bone tissue (Bellido et al 2013; Florencio-Silva et al. 2015). Lifespan of an osteoblast ranges from a few to about 100 days (Rosenberg et al. 2012).

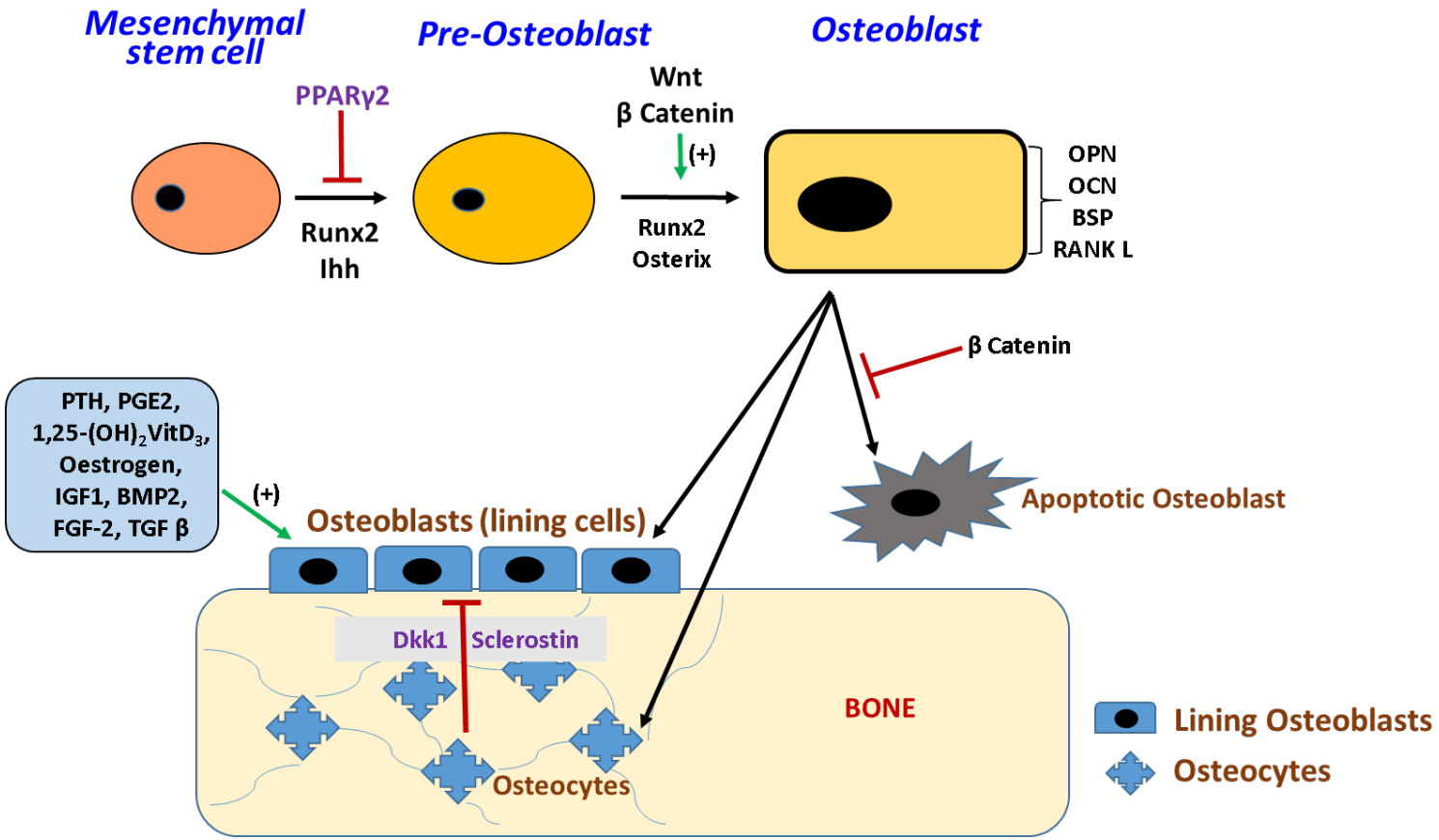

Figure 1.6 Regulation of osteoblast differentiation.

See text for further description. (PGE2, Prostaglandin E2; DKK1, Dickkopf 1).

Bone formation is also regulated by osteoclast-osteoblast communication factors. Osteoclast mediated bone resorption releases coupling factors from bone matrix such as IGF1 and TGF-β which induce migration of osteoblasts to resorbing surfaces along with sphingosine-1-phosphate (S1P) and BMP6 expressed by osteoclasts. Ephrins and semaphorins are another class of osteoblast-osteoclast communication factors that regulate bone formation (Boyce et al 2013). Ephrin B2 which is expressed by osteoclasts acts on its receptor Ephrin B4 on osteoblasts to promote bone formation while simultaneously inhibiting bone resorption whereas semaphorin 4D (Sema 4D) released by osteoclast inhibits bone formation by binding to Plexin B1 on osteoblasts (Negishi-Koga et al. 2011; Ralston 2017). Osteoblasts also regulate osteoclast function by secreting many factors such as RANKL, M-CSF and OPG (Bellido et al 2013; Florencio-Silva et al. 2015).

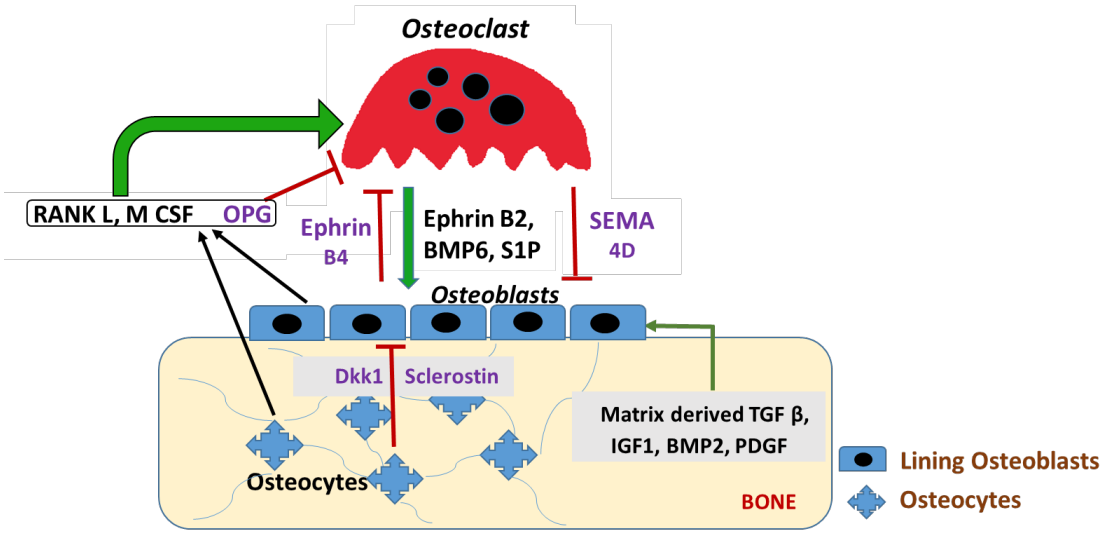

Figure 1.7 Schematic representation of different factors involved in osteoclast, osteoblast and osteocyte interaction.

See text for description. (PDGF, platelet derived growth factor)

1.2.3 Osteocytes

Osteocytes are mature osteoblasts which become embedded in the newly formed bone matrix during bone formation. These are the most long-lived and abundant cells of the bone which act as mechanosensors and coordinate osteoblast and osteoclast function in response to mechanical signals (strain and fluid flow) and circulating factors (ions and hormones).

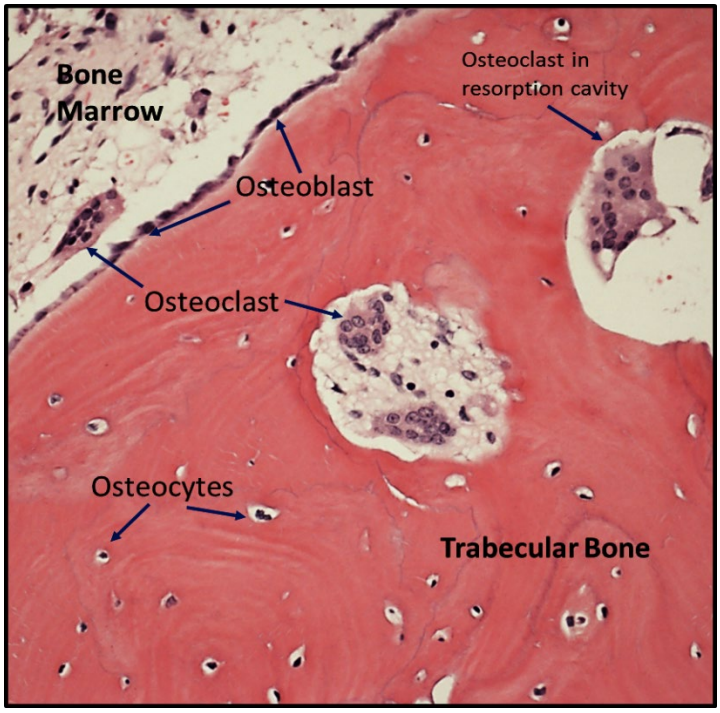

Figure 1.8 Haematoxylin & eosin stained histology section of a human bone. Shows various cell types: Osteoclasts resorbing bone, osteoblasts lining the bone and osteocytes embedded in the bone matrix (Courtesy of Prof. Donald Salter).

Osteocytes respond to microdamage by activating osteoclasts by producing RANKL to remove damaged bone as part of bone remodelling. In addition, they produce M-CSF and OPG to regulate bone resorption. They also regulate osteoblast mediated bone formation by secreting sclerostin and DKK1 as well as express genes that regulate phosphate and mineral metabolism such as *phosphate regulating endopeptidase homolog X-linked* (*PHEX), dentin matrix acidic phosphoprotein 1* (*DMP1*) and *fibroblast growth*

factor 23 (*FGF23*). Osteocytes eventually undergo apoptosis and their reduced viability results in decreased remodelling and fragile bone conditions associated with glucocorticoid excess, mechanical disuse and oestrogen withdrawal (Bellido et al 2013).

1.3 Bone modelling and remodelling

Bone undergoes change in shape and mass known as modelling to enable it to grow and withstand biomechanical forces. This process is in action during childhood and adolescence but slows down in adult life except in conditions such as hypoparathyroidism, renal osteodystrophy and anabolic therapy. Also, bones undergo constant turnover called remodelling. This lifelong process involves replacing any old, damaged bone with new bone to maintain structural integrity of the skeleton and mineral homeostasis. Remodelling process is tightly regulated with osteoclast bone resorption coupled to osteoblastic bone formation. A normal remodelling cycle last 4-6 months with osteoclast resorption occurring between 3-6 weeks and the remainder taken up by bone formation. Abnormalities in this bone turnover cycle results in a variety of bone disorders like Paget's disease of bone and Osteoporosis. Remodelling cycle is divided into the following sequential phases (Allen & Burr 2013):

Activation: This is initiated by microdamage or mechanical stress or osteocyte apoptosis or random non-signalling event. All of these events result in osteoclast precursors' migration to the bone surface where they proliferate, differentiate and fuse to become fully functional osteoclasts.

Resorption: Once mature osteoclasts form, bone lining cells retract and allow osteoclast attachment to the bone surface, seal the remodelling site and dissolve the mineralised bone to release collagen fragments. Measuring these fragments in urine and blood can serve as useful biomarkers for assessment of bone remodelling. This phase is regulated by release of cytokines M-CSF, RANKL and OPG from osteoblast lineage cells including osteocytes.

Reversal: Osteoclasts complete their resorption, undergo apoptosis and bone formation is initiated by osteoblasts. The bone lining cells clean the residual bone matrix from the resorption lacuna and lay down a new thin layer of bone matrix called the cement line which delineates the older matrix from surrounding new bone.

Formation: Bone formation by osteoblasts begins with deposition of organic unmineralised matrix composed mainly of Type I collagen fibres (osteoid) followed by inorganic hydroxyapatite crystal deposition. Mineralization of osteoid occurs in two phases:

Primary mineralization lasts for 2-3 weeks and starts when calcium and phosphate ions incorporate into the collagen matrix and accounts for 70% of the final mineral content. Osteoid turns into mature mineralised matrix during secondary mineralization thereby giving bone its rigidity, stiffness and durability (up to a year or more).

Bone forming osteoblasts meet one of three fates: Majority (90%) become apoptotic and die to be replaced by new osteoblasts as long as bone formation proceeds at the local remodelling site. Of the remaining ones, some get embedded in the bone matrix to form osteocytes and the remainder form inactive bone lining cells (that retain the capacity to become activated and capability to produce bone matrix).

Quiescence: The last stage of the remodelling cycle results in bone lining cells or surface osteocytes covering the remodelled bone surface. Over time, the matrix within the remodelling unit will mineralize. Majority of bone surfaces within the body are in a quiescent state at any given time, though capable of activating in the next bone remodelling cycle.

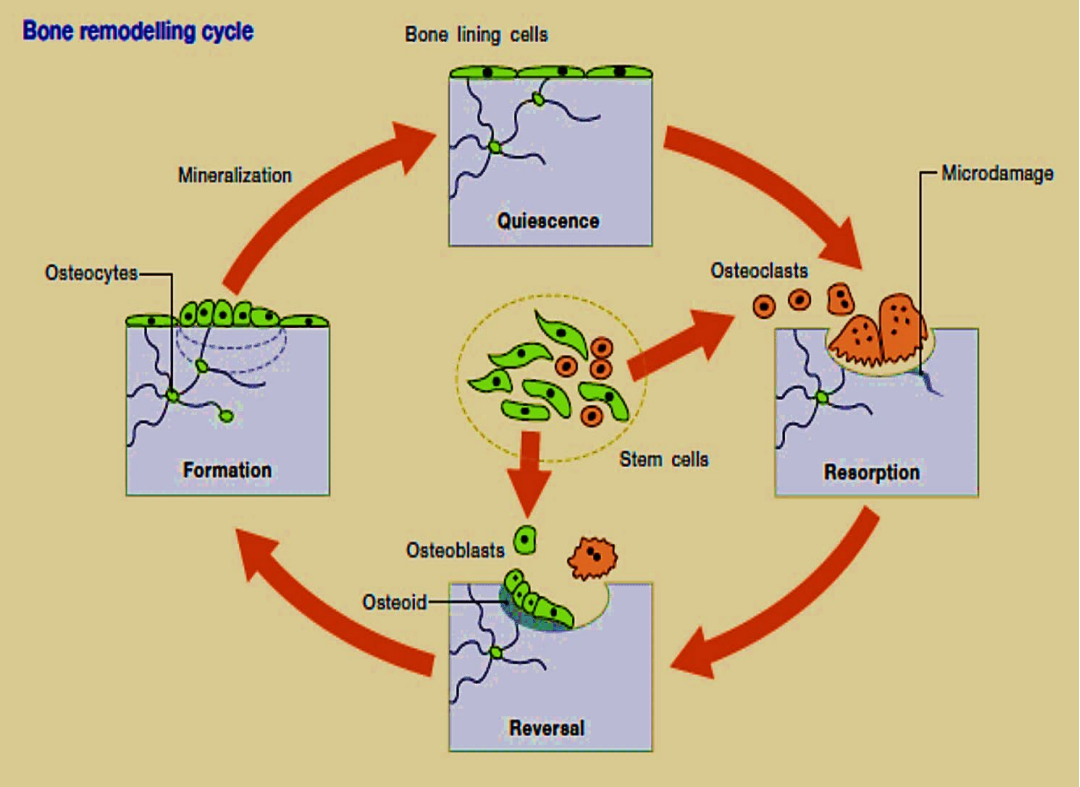

Figure 1.9 The bone remodelling cycle.

This is initiated by various signals that recruit osteoclast precursors to affected bone surface where they develop into mature osteoclasts and bone resorption takes place. This is followed by recruitment of osteoblast precursors to the resorbed site where they proliferate and differentiate into mature osteoblasts. Osteoblasts secrete osteoid following by mineralisation of bone matrix giving rise to new bone. Finally, bone enters the resting phase wherein the remodelled bone is covered by bone lining cells thereby completing the remodelling cycle (Ralston 2017).

1.4 Paget's disease of Bone (PDB)

1.4.1 Introduction

PDB was initially described by Sir James Paget in late 19th century as "osteitis deformans", a chronic inflammation of the bone leading to deformities (Paget 1877). It is a common metabolic bone disorder second only to osteoporosis and is characterised by focal abnormalities of increased bone turnover and abnormal bone remodelling (Ralston et al. 2008; Alonso et al. 2017).

1.4.2 Epidemiology

PDB affects 1-2% of Caucasians aged 55 years and above. The risk of developing PDB increases with age. It affects men more than women especially in UK (van Staa et al. 2002). The disease occurs worldwide but distribution varies widely between geographic regions. UK has the highest prevalence of PDB in the world. However, the disease is also observed frequently in western and southern Europe (Detheridge et al. 1982) and in British migrant colonies of Australia, South Africa and New Zealand (Barker 1984). However, it is rare in Asia, Scandinavia and Africa (Dahniya 1987; Takata et al. 2006). Several studies have recently observed a decline in PDB prevalence and clinical severity in several places such as New Zealand, UK and some other European countries over the past two and a half decades (Poór et al. 2006; Corral-Gudino et al. 2013) as well as delayed onset of disease in individuals with a family history of PDB (Bolland et al. 2007), while in other places such as Italy and US (Tiegs et al. 2000; Gennari et al. 2005), there are no major changes in the incidence. The exact mechanisms behind these changes are not understood, but environmental factors such as changes in ethnic make-up of the population resulting from migration, less exposure to viral infections / zoonoses, more sedentary lifestyle and improved nutrition are suggested to play a role (Ralston & Layfield 2012; Corral-Gudino et al. 2013; Alonso et al. 2017).

1.4.3 Clinical features

PDB has a late-onset and many patients (80%) are asymptomatic. Bone pain is the commonest presentation possibly due to increased bone turnover (primary pain) or secondary to complications such as osteoarthritis, spinal stenosis, pseudofractures or co-existing musculoskeletal condition. Clinical signs include bone deformity and the skin overlying an affected bone feels warm (Ralston 2013).

Pagetic lesions are focal in nature. The disease mainly affects the axial skeleton and the most commonly affected sites include pelvis (70% of cases), femur (55% of cases), lumbar spine (53% of cases), skull (42% of cases) and tibia (32% of cases) (Kanis 1992). The disease either affects a single skeletal site (monoostotic) or most often multiple noncontiguous sites (polyostotic) (Bolland & Cundy 2013).

Complications commonly resulting from PDB include bone fracture, bone deformity, deafness due to skull involvement, nerve compression and secondary osteoarthritis. These complications can be extremely disabling due to loss of mobility and can result in a substantial reduction in quality of life. Its late-onset and asymptomatic nature means long term permanent skeletal damage may have already occurred by the time it is diagnosed. Rare complications include osteosarcoma (less than 1% of cases), high-output cardiac failure, obstructive hydrocephalus and hypercalcemia in immobilized patients (Ralston et al. 2008).

1.4.4 Pathology

Pagetic lesion is initiated by an increased bone resorption at affected site(s). The primary abnormality lies in osteoclasts, the cells responsible for bone resorption which are enlarged and numerous, hypernucleated and hyperactive. This is accompanied by rapid new bone formation by osteoblasts which seem to be normal (Roodman & Windle 2005; Ralston & Layfield 2012).

Many osteoclasts also contain nuclear inclusion bodies that have been compared to viral nucleocapsids. These have been proposed to result from a persistent viral infection. The exact nature of these inclusion bodies is not established since they are not specific to PDB and also found in other conditions such as hereditary oxalosis (Bianco et al. 1992), osteopetrosis (Mills et al. 1988) and neurodegenerative diseases (Sieradzan et al. 1999). Recently, they have also been suggested to be non-degraded protein by-products of dysregulated autophagy, a novel pathway associated with PDB pathogenesis. There is also evidence of marrow fibrosis and bone hypervascularity (Ralston & Layfield 2012).

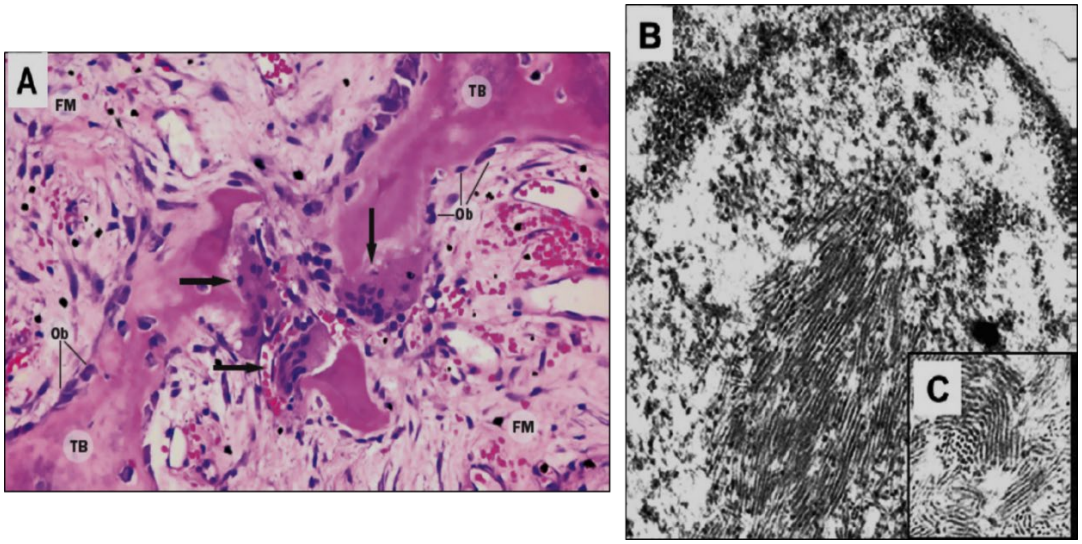

Figure 1.10 Microscopic images of a Pagetic bone.

A) 20X magnified H&E image of a Pagetic bone biopsy showing hypernucleated osteoclasts (arrows), Osteoblasts (Ob) lining trabecular bone (TB) and fibrovascular marrow (FM). Image reproduced from (Singer 2015).

(B) Typical nuclear inclusions seen in osteoclasts from patient with PDB using electron microscopy.

(C) Magnified high power image of the inclusion seen in (B). Images reproduced from (Ralston 2008).

Increase in bone turnover results in 3 phases of PDB all of which can be observed at the same time but at different sites in an affected individual:

- Osteolytic phase: increased bone resorption leading to lytic changes seen in radiographs.
- Mixed phase: consisting of sclerotic bone resulting from new bone formation accompanying the osteolysis.
- Sclerotic phase: is observed due to a reduction in bone turnover and cells (Ooi & Fraser 1997).

Newly formed collagen fibres are arranged in a chaotic fashion rather than linear to form more primitive woven bone. The resulting bone has a characteristic mosaic appearance consisting of abnormal woven bone and few areas of lamellar bone linked in a disorderly fashion by numerous cement lines from previous osteolysis (Misra et al. 2013). There is increased osteoid in the bone matrix without much alterations in mineralisation. The disrupted architecture of pagetic bone leads to loss of structural integrity (Zimmermann et al. 2015; Alonso et al. 2017).

1.4.5 Diagnosis

PDB diagnosis is incidental in most cases, the first indication often being an elevated serum alkaline phosphatase (ALP) or an abnormal X-ray/radiograph in an individual who is being investigated for other reasons (Guma et al. 2002; Ralston et al. 2008).

Plain radiograph (X-ray) typically shows areas of focal osteolysis mixed with sclerotic areas along with bone expansion, coarsened trabeculae and thickened cortices (Ralston 2013). Technetium 99m bone scanning (Tc^{99m}) identifies areas of increased uptake of radiolabelled bisphosphonate and is associated with areas of high bone remodelling. Tc^{99m} along with targeted X-rays (of abdomen, facial bones, skull and tibiae) is recommended to fully and accurately determine the extent of metabolically active disease (Ralston et al. 2019). It is highly sensitive and non-specific but has the advantage of detecting lesions even in early stages of PDB (Selby et al. 2002).

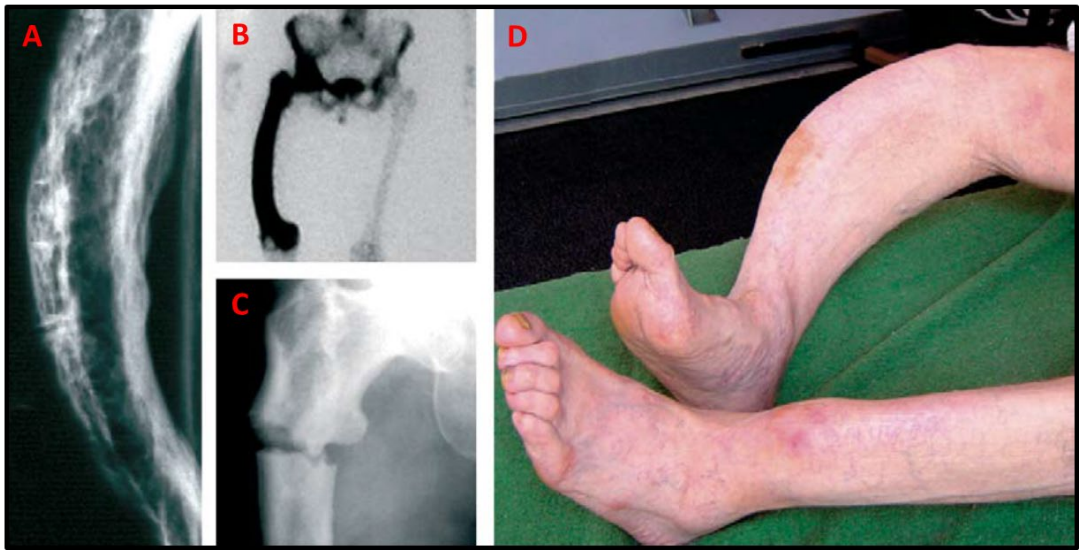

Figure 1.11 Diagnostic features of PDB

A) Radiograph of tibial bone affected by PDB which shows bone expansion, deformity and areas of osteolysis as well as osteosclerosis.
(B) Increased tracer uptake in PDB affected femur using radionuclide scan.
(C) Pathological fracture in PDB affected femur bone.
(D) Severe bone deformity of PDB affected tibia. Pictures obtained from (Ralston et al. 2008).

Serum total ALP is recommended as the first line biochemical test for screening metabolically active PDB in combination with Liver function tests (LFTs). Elevated serum ALP in isolation in absence of liver disease and otherwise normal biochemical results is typical of PDB. MRI and CT are rarely required except for assessing complications like spinal stenosis and osteosarcoma. Other biochemical laboratory tests for calcium, albumin and 1,25-$(OH)_2$ Vitamin D3 are often normal though vitamin D deficiency is common in older patients with PDB. Elevation of specialised biomarkers such as bone specific alkaline phosphatase, PINP and CTX are not recommended for diagnosis or treatment response except for assessing PDB activity in untreated patients or when ALP is normal and in presence of concomitant liver disease. A bone biopsy of affected site is seldom required for diagnosis (Ralston 2013; Ralston et al. 2019).

1.4.6 Aetiology

In spite of significant developments in last few decades, causes of PDB are still incompletely understood. It is regarded as a complex disease resulting from an interplay between genetic and environmental factors.

1.4.6.1 Environmental triggers

A reduction in prevalence of disease in some countries in recent years as well as absence or delayed appearance of symptoms in offspring of patients with *SQSTM1* mutation mediated familial PDB point to environmental triggers regulating disease occurrence and severity (Ralston & Albagha 2011).

Several environmental factors such as viral infection, dietary intake of calcium in childhood, Vitamin D deficiency, mechanical loading of the skeleton, exposure to environmental toxins, a rural lifestyle, exposure to farm animals and chronic infection with measles, respiratory syncytial or distemper virus have been suggested to play a role as well but evidence is inconclusive. Most extensively studied environmental factor is paramyxovirus (chronic measles) infection but evidence in favour of viral aetiology remains conflicting (Ralston & Layfield 2012).

Measles virus nucleocapsid gene (MVNP) expression in murine osteoclasts leads to Pagetic-like phenotype in these osteoclasts and induces bone lesions (Kurihara et al. 2011). More recently, MVNP has been associated with *IGF1* and *IL6* upregulation in osteoclasts in mouse models as well as PDB patients and also induces osteoblast differentiation in parallel thereby strongly supporting the role of MVNP in PDB pathogenesis (Teramachi et al. 2016).

1.4.6.2 Genetics and PDB

PDB has a strong genetic component. Evidence in support of this includes

- Familial clustering in classical PDB; 5-40% of cases have a positive family history. The disease, in many cases, is inherited in an autosomal dominant fashion and shows high penetrance as one approaches

seventh decade (Sofaer et al. 1983; Hocking et al. 2001; Laurin et al. 2001; Albagha & Ralston 2016).

- Ethnic differences in PDB prevalence persist after emigration (Barker 1984).
- Several candidate loci identified by genome linkage scans (Laurin et al. 2001; Hocking et al. 2001).
- Mutations in four genes identified as cause of PDB and associated syndromes (Lucas et al. 2006).

Several genes have been identified that cause classical PDB as well as rare PDB-like syndromes.

Genes that cause rare PDB-like syndromes

Several rare disorders which share some of the clinical features of PDB, have been described. They show Mendelian inheritance and early age of onset.

Mutations in *TNFRSF11B* gene which encodes OPG are responsible for Juvenile Paget's disease (JPD) (Whyte et al. 2002). JPD is inherited in an autosomal recessive manner. Clinical features include bone pain, deformity and fracture during childhood with a grossly abnormal bone turnover resulting in a mix of lytic and sclerotic enlarged bone lesions similar to PDB. OPG mutations include full deletion as well as missense change which result in complete lack of OPG or defective OPG protein not capable of binding RANKL and inhibiting osteoclastogenesis / bone resorption. These mutations are absent in classical PDB but there is some evidence which suggests that variants at this locus predispose to PDB at least in females (Ralston & Albagha 2012).

Mutations in *TNFRSF11A* gene encoding RANK result in familial expansile osteolysis (FEO) (Osterberg et al. 1988), Expansile skeletal hyperphosphatasia (ESH) (Whyte et al. 2000) and Early onset familial PDB (EoPDB) (Nakatsuka et al. 2003) all of which show autosomal dominant inheritance and overlapping clinical features such as early deafness, tooth

Table 1.1 Genes involved in rare PDB-like syndromes

Chromosome	***Gene (Protein)***	***Disease Syndrome***	***Function***
8q24	*TNFRSF11B* (OPG)	Juvenile Paget's disease of bone (Whyte et al. 2002)	Inhibits osteoclastogenesis and bone resorption by acting as RANKL's decoy receptor
9p21	*VCP* (VCP)	Inclusion body myopathy, Paget's disease of bone and Frontotemporal dementia (Watts et al. 2004)	Proteasomal degradation of IKBα
18q21	*TNFRSF11A* (RANK)	Familial expansile osteolysis (Osterberg et al. 1988), Expansile skeletal hyperphosphatasia Whyte et al. 2000) and Early onset Paget's disease of bone (Nakatsuka et al. 2003)	Osteoclast formation, function and survival
7p15.2 and 12q13.13	*hnRNPA2B1* (hnRNPA2B1) *hnRNPA1* (hnRNPA1)	Inclusion body myopathy, Paget's disease of bone and Frontotemporal dementia / Amyotrophic lateral sclerosis (Nalbandian et al. 2011, Kim et al. 2013)	RNA binding proteins involved in RNA metabolism and transport
1q21.3	*ZNF687* (C2H2 ZFP)	Paget's disease of bone / Giant cell tumour of bone (Rendina et al. 2015)	Unknown but possibly by increasing osteoclast size and nucleation (Osteoclast phenotype) thereby activity

loss and focal osteolytic expansile bone lesions that manifest in childhood or early adulthood. The causative mutations are duplications of 15-27 nucleotides in Exon1 leading to elongation of RANK signal peptide that result in its abnormal cleavage and accumulation in the golgi apparatus. This probably results in aberrant NF-kB signalling but evidence is conflicting. Although similar mutations in RANK have been excluded to cause classical PDB, common variants at this locus are strongly associated with PDB susceptibility (Albagha et al. 2010, 2011).

Inclusion body myopathy, PDB and Frontotemporal dementia (IBMPFD) is another autosomal dominant disease syndrome resulting from missense mutations in the gene *Valosin-containing protein* (*VCP*) (Watts et al. 2004). The clinical features mainly include myopathy (age of onset after 40yrs affecting 90% of the patients), PDB in 40% of cases which manifests at an earlier age (between 40 and 50 years) and dementia in 40% of cases with an average age of onset between 50 and 60 years. *VCP* encodes p97 which is involved in membrane fusion, ubiquitin mediated protein degradation and autophagy. The mechanism by which mutant *VCP* leads to IBMPFD phenotype is not fully understood but possibilities include an impairment of autophagy in presence of *VCP* mutations or abnormal activation of the NF-kB signalling along with dysregulation in IKBα protein degradation, which could contribute to the mechanism of pathogenesis in multiple tissues affected by IBMPFD especially bone (Ralston & Albagha 2011; Ralston & Albagha 2012). Mutations of *VCP* have been ruled out as a cause of classical PDB but we have recently found a novel heterozygous missense mutation in a single elderly patient with classical PDB lacking myopathy or neurological complications (Wani, Albagha and Ralston, unpublished data).

Various loss of function missense mutations have been found in heterogeneous nuclear ribonucleoproteins (*hnRNPs*) *A2B1* and *A1* genes in families affected by IBMPFD/ALS (amyotrophic lateral sclerosis) in absence of *VCP* mutations. The resulting dominantly inherited multisystem proteinopathy involves degeneration of muscle, bone, brain and motor

neurons arising due to altered RNA metabolism as a result of defective ribonucleoprotein granule assembly (Nalbandian et al. 2011; Kim et al. 2013).

Patients with PDB have increased risk of developing giant cell tumour of bone (GCT). Though PDB is associated with GCT in less than 1% of cases, these patients have increased severity of PDB and reduced life expectancy (Rendina et al. 2015). Mutations (c.2810C>G and c.725G>T) in *ZNF687* gene are not only associated with severe, early onset classical form of PDB but the mutation c.2810C>G in addition increases the likelihood of developing GCT (Divisato et al. 2016). *ZNF687*, a downstream target of NF-kB, encodes C2H2 zinc finger protein that acts as a transcriptional co-regulator of bone cell proliferation and differentiation. It is highly expressed during osteoclast and osteoblast development and significantly upregulated in tumour tissue of patients with PDB/GCT as well as peripheral blood of PDB cases irrespective of *SQSTM1* status (Divisato et al. 2016).

Based on current evidence, classical PDB appears to result more likely from a combination of rare variants (in genes such as *SQSTM1*) and more common alleles, which, in spite of their smaller effect size, when inherited together with rare high penetrance variants, are likely to increase PDB risk considerably (Ralston & Albagha 2011; Albagha et al. 2013).

Genes that cause classical PDB include:

SQSTM1:

The most important gene in relation to PDB is the *sequestosome 1* (*SQSTM1*) gene encoding p62 protein. p62 has three functional domains: an N-terminal region which is involved in kinase interactions, a hinge region and a C-terminal region containing the Ubiquitin-binding domain (UBA) (Geetha & Wooten 2002). Linkage analysis first identified the chr 5q35 locus to be associated with PDB in two independent populations (Laurin et al. 2001; Hocking et al. 2001). Mutation screening of the critical region identified a proline to leucine change at codon 392 (P392L) in the UBA of *SQSTM1* as the cause of PDB in a French-canadian population cohort (Laurin et al. 2002). Subsequent studies

identified P392L in British and several other populations including Chinese people where PDB appearance is rare (Hocking 2002; Beyens et al. 2004; Falchetti et al. 2004; Johnson-Pais et al. 2003; Gu et al. 2012). Several more mutations clustered in the UBA domain as well as few others outside the UBA of *SQSTM1* have been found to be associated with PDB in populations worldwide, P392L being the most common (Rea et al. 2013).

p62 is an adaptor protein that binds ubiquitin. It plays an important role in NF-kB signalling and osteoclast activation downstream of RANK. RANK-RANKL interaction results in polyubiquitylation of TRAF6 leading to activation of several downstream signalling pathways (Layfield & Hocking 2004) and nuclear translocation of NF-kB, AP-1 and NFATc1 ultimately leading to transcriptional activation of osteoclast specific genes such as *ACP5* (TRAcP*)* and *CTSK* (Cathepsin K). Recruitment of CYLD to the RANK-TRAF6 protein complex requires ubiquitin binding domain of p62. Deletion of this domain and/or the mutations within it result in impaired p62-CYLD binding thereby leading to increased TRAF6 ubiquitination, enhanced RANK and NF-kB signalling leading to increased osteoclast activity and bone resorption (Jin et al. 2008; Ralston & Layfield 2012).

p62 is also involved in the process of autophagy, a novel pathway which has recently being found to be dysregulated or defective in PDB (Usategui-Martín et al. 2015).

Approximately 10% of sporadic cases and 40% of familial cases of PDB show germline *SQSTM1* mutations (Laurin et al. 2002; Hocking 2002). Although presence of *SQSTM1* mutations hastens the onset of PDB and increases its severity, few patients with these mutations have a phenotype not suggestive of PDB, meaning additional mutations or exposure to environmental trigger(s) is needed for the disease to manifest and *SQSTM1* mutations are predisposing rather than causing the disease by itself. Thus, additional causal genes remain unidentified (Ralston et al. 2008; Albagha et al. 2013; Cundy et al. 2015).

Genes associated with increased susceptibility to PDB:

With the aim of identifying additional causal genes, Genome wide association studies (GWAS) were performed by our group and have identified single nucleotide polymorphisms at the seven loci on chr 1, 7, 8, 10, 14, 15 and 18 (containing *CSF1*, *NUP205, DCSTAMP, OPTN*, *RIN3, PML and TNFRSF11A* respectively*)* as significant risk factors for PDB development (Albagha et al. 2010; Albagha et al. 2011). Three of these (*CSF1, TNFRSF11A* and *DCSTAMP*) have known roles in bone metabolism whereas the remaining four had not been implicated in bone metabolism at the time GWAS were conducted. Two of these regions have now been studied in detail and found to have a functional role in bone metabolism: RIN3 encoded by the 14q locus and OPTN encoded by the 10q locus (Vallet et al. 2014; Obaid et al. 2015).

Table 1.2 Summary of most significant PDB-associated genes found by GWAS

Chromosomal locus	***Closest gene (protein)***	***Top GWAS SNP***	***Function***
1p13	*CSF1* (M-CSF)	rs10494112	Osteoclast formation and survival
7q33	*NUP205* (Nucleoporin 205)	rs4294134	Unknown role in bone metabolism
8q22	*DCSTAMP* (DCSTAMP)	rs2458413	Critical role in osteoclast precursor fusion
10p13	*OPTN* (Optineurin)	rs1561570	Negative regulation of osteoclastogenesis
14q32	*RIN3 (*Ras and Rab interactor 3)	rs10498635	Positive regulation of osteoclast function
15q24	*PML, GOLGA6A* (PML/GOLGA6A)	rs5742915	Unknown role in bone metabolism
18q21	*TNFRSF11A* (RANK)	rs3018362	Controls osteoclast differentiation and function

M-CSF, Macrophage colony stimulating factor;

DC-STAMP, Dendritic cell-specific transmembrane protein

CSF1: is located on chr 1p13 and encodes cytokine M-CSF which is involved in macrophage and osteoclast differentiation as well as osteoclast survival. The strongest association at this locus was with SNP rs484959 located 87kb upstream of *CSF1* (Albagha et al. 2010). Untreated PDB patients have raised serum CSF1 level (Neale et al. 2002) whereas loss of function mutations in *Csf1* in mice and rats cause osteopetrosis (Yoshida et al. 1990). Causal variants from *CSF1* have yet to be identified but most likely induce PDB by regulating CSF1 expression levels and activity (Ralston & Albagha 2012; Albagha & Ralston 2016).

NUP205: The strongest GWAS signal at chr7q33 was rs4294134 within intronic region of *NUP 205* which encodes the nucleoporin 205KDa, a component of the nuclear pore complex that regulates transport processes between nucleus and cytoplasm but has unknown role in bone metabolism (Albagha et al. 2011; Albagha & Ralston 2016).

DCSTAMP: is located on chr8q22 and encodes DC-STAMP which is essential for fusion of osteoclast precursors to form mature multinucleated osteoclasts (Yagi et al. 2005). RANKL upregulates DC-STAMP expression in osteoclast precursors. DC-STAMP is essential for RANKL-induced osteoclastogenesis. PDB patients show hypernuclear and larger osteoclasts compared to healthy controls. Genetic variants at this locus could therefore result in predisposition to PDB by enhancing *DCSTAMP* expression leading to increased fusion of osteoclasts (Ralston & Albagha 2012).

OPTN: located on chr 10p13 locus which encodes for Optineurin, is involved in the regulation of NF-kB signalling and autophagy (Zhu et al. 2007; Shen et al. 2011) which could explain its involvement in PDB. The strongest GWAS SNP rs1561570 was found to be an eQTL with reduced OPTN mRNA expression in PDB-predisposing high risk T-allele carriers. *Optn* knock-in (*D477N*) mutant mice (with a polyubiquitin binding defect) show increased osteoclast activation and bone turnover with low penetrance PDB-like lesions. OPTN was found to negatively regulate osteoclast differentiation by controlling IFN- β signalling and NF-kB in these mice. Thus, genetic variants

at the *OPTN* locus could be leading to reduced OPTN expression thereby predisposing to PDB by increasing osteoclast differentiation and activity. (Obaid et al. 2015). Another study, however, has shown that SNP rs1561570 leads to increased *OPTN* expression via loss of methylation site leading to a phenotype of increased osteoclast activity (Silva et al. 2018) though the sample size in this study was much smaller. A more recent study has now confirmed that complete deletion of *Optn* (using *Optn* knockout mice) results in hyperactive osteoclasts and abnormal bone remodelling leading to osteolytic lesions characteristic of PDB via altered Type 1 IFN signalling. The lesions were observed mainly in aged mice (22 months) (Wong et al. 2019).

RIN3: encoding Ras and Rab interactor 3 protein located on chr 14 was the most likely candidate gene from this locus. RIN3 interacts with Ras and Rab GTPases which play an important role in vesicular trafficking (Kajiho 2003) and osteoclast function. 14q32 locus was investigated in PDB patients and controls by deep sequencing and identified p.R279C as the most probable causal variant from this locus. p.R279C was in strong LD with the GWAS signal rs10498635. 13 rare missense variants affecting important RIN3 domains were found which when combined increased the risk of disease presentation. *RIN3* expression was tenfold higher in osteoclasts compared to osteoblasts. Thus, RIN3 could be contributing to PDB pathogenesis by positively regulating osteoclast function (Vallet et al. 2014; Alonso et al. 2017)

TNFRSF11A: located on Chr 18q21 encodes RANK involved in osteoclast differentiation and bone resorption (Li et al. 2000). This region corresponds to PDB7 locus previously identified in families by linkage analysis (Good et al. 2002). Disruption of RANK leads to osteopetrosis in mice and genetic variability in *TNFRSF11A* could increase PDB severity in those with *SQSTM1* mutations (Li et al. 2000; Gianfrancesco et al. 2012). Mechanisms involved in association of common genetic variants at this locus with PDB predisposition currently remain unclear (Alonso et al. 2017).

PML/GOLGA6A: located on the chr 15q were the most likely candidate genes from this locus though both of them have never been implicated in bone

metabolism. The strongest association was with SNP rs5742915, which results in an amino acid change at codon 645 within *PML* gene (phenylalanine to leucine: p.Phe645Leu) (Albagha et al. 2011). *PML* gene has been described in detail later in section 1.5.

Somatic mutations in PDB

PDB is a focal disease and shows asymmetric distribution. What causes this is not clear yet. It could be explained by presence of somatic mutations in *SQSTM1* and other PDB associated genes. Studies have found P392L as a somatic mutation in affected PDB bones from some patients and few Pagetic osteosarcomas whereas in others, the results were negative. The signal for mutant allele was weak and lower compared to those of P392L germline heterozygotes indicating only a minor proportion of cells affected by somatic mutations (Matthews et al. 2009; Merchant et al. 2009; Ralston & Layfield 2012). Another study (Sparks et al. 2001) found no somatic mutations in the gene *TNFRSF11A* (RANK) from affected PDB tissue and osteosarcoma cell lines. We are exploring the role of somatic mutations in focal nature of PDB using exome sequencing of DNA extracted from affected human bones and comparing it to DNA sequences obtained from peripheral blood.

Autophagy associated genes and other candidate genes for PDB

Autophagy is the process involved in degradation of cytoplasmic proteins, damaged organelles and protein aggregates. It has recently been found to be dysregulated or defective in PDB. Several PDB associated genes such as *SQSTM1*, *OPTN* and *VCP* are involved in the process of autophagy. *SQSTM1* directs ubiquitinated proteins for degradation in autophagolysosomes. Mice with the P394L *Sqstm1* mutation show enhanced autophagosome formation (consistent with increased *Sqstm1*, light chain 3 gene (*Lc3*) and autophagy-related gene 5 (*Atg5*) mRNA expression in osteoclast precursors from these mice as well as increased LC3-II protein levels) (Daroszewska et al. 2011; Ralston & Layfield 2012). Autophagy genes (*ATG5*, *ATG4B* and *ATG7*) have been shown to affect osteoclastic bone resorption and polymorphisms in *ATG* genes have been shown to increase risk of PDB (*ATG5* and *ATG16L1*) and

vice versa (*ATG10*) in a Spanish cohort of PDB cases (DeSelm et al. 2011; Usategui-Martín et al. 2015).

Nominally significant associations have been identified in some studies between PDB and polymorphisms in genes *CASR*, *ESR1* and *TNFRSF11B* whereas no association was found in genes *IL1RA, IL6, IL1B, IL8, TNFA, TNFFS11* and *VDR* (Donáth et al. 2004; Corral-Gudino et al. 2006; Beyens et al. 2007; Corral-Gudino et al. 2010). Though *TNFRSF11B* encoding OPG did not appear as a candidate locus in GWAS, current evidence suggest that variants in this gene predispose to PDB only in women and further studies are warranted (Beyens et al. 2007; Ralston & Albagha 2011).

1.4.7 Treatment

Bone pain is the main indication for treatment in PDB. The first choice of drugs are nitrogen-containing bisphosphonates with zoledronic acid most preferred of the lot in achieving a favourable pain response. These are potent anti-resorptives which preferentially target the affected skeletal sites and are highly effective in suppressing the increased bone turnover at these active PDB skeletal sites (Reid et al. 2011; Ralston 2013; Ralston et al. 2019). A research project “Pain in Paget’s disease (PiP)” under Prof. Stuart Ralston is in progress to look in detail at causes and understand mechanisms of pain to try and improve pain management in PDB patients.

Calcitonin is also effective in reducing bone pain and suppressing bone turnover but is less potent than bisphosphonates and has more adverse effects and is therefore used only in exceptional cases for short term treatment of PDB when bisphosphonates are contraindicated such as those with renal impairment. Other drugs such as anti-inflammatory, analgesics and antineuropathic agents are often used or required to manage pain. Osteoclast inhibitor Denosumab which is a monoclonal antibody inhibiting RANKL has shown promise but there is insufficient evidence to warrant its clinical use in PDB and it has therefore not yet been licensed for treating PDB (Ralston 2013; Ralston et al. 2019).

Non pharmacological agents such as acupuncture, physiotherapy and hydrotherapy have been tried for relieving pain and increase muscle strength as well as mobility but clinical evidence is lacking. Orthopaedic surgery is recommended for fracture fixation through the pagetic bone; total knee or hip replacements recommended for patients with complications such as osteoarthritis (where medical treatment is unsatisfactory) and spinal surgery may be considered for spinal stenosis/compression due to PDB (Ralston et al. 2019). Surgery may be required for those with osteosarcoma but the prognosis is often poor in these cases (Sharma et al. 2005).

PRISM (Paget's disease of bone: Randomized trial of intensive bisphosphonate treatment versus symptomatic management) study and its extension did not find any evidence of clinical benefit in treating PDB patients with intensive bisphosphonate therapy versus symptomatic management (Langston et al. 2010, Tan et al. 2017). Thus, guidelines recently published recommend treating patients with the aim of improving symptoms rather than pursue a treat-to-target treatment strategy aimed at normalising total ALP in PDB (Ralston et al. 2019). Treatment of PDB patients with altered biochemical activity and/or family history in absence of symptoms is still under debate. An international randomized clinical trial Zoledronate in the prevention of Paget's (ZiPP study, ISRCTN11616770) led by Prof. Stuart Ralston at the University of Edinburgh, UK is currently in progress to determine if Zoledronate can prevent PDB in asymptomatic individuals with family history and *SQSTM1* mutations (Alonso et al. 2017). Another study led by Prof. Ralston is also investigating contribution of genetic and microbiome markers to PDB development in asymptomatic offspring of PDB patients.

1.5 Promyelocytic Leukaemia (PML)

One of the GWAS loci was located on 15q24.1 and it contains two likely candidate genes *PML* and *GOLGA6A* both of which have unknown role(s) in bone metabolism. The association at this locus was replicated in several independent populations from UK, Australia, Spain, Italy, Belgium and the Netherlands. The strongest association was with SNP rs5742915, which results in an amino acid change at codon 645 within *PML* gene (phenylalanine to leucine: p.Phe645Leu) (Fig. 13) (Albagha et al. 2010; Albagha et al. 2011).

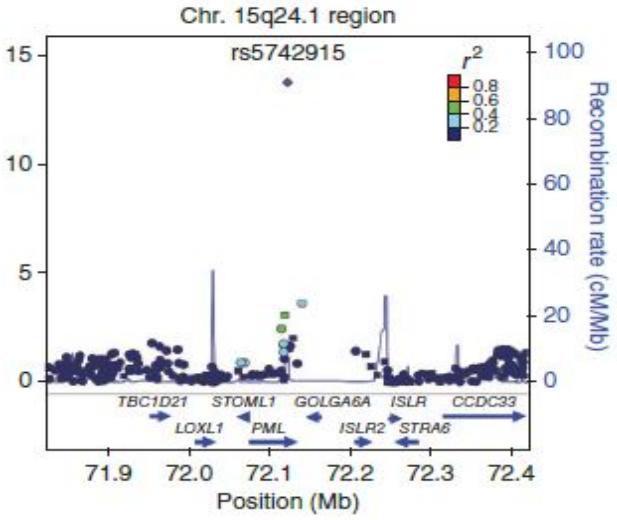

Figure 1.12
Regional association plot of 15q24.1 locus.
Shows chromosomal position of SNPs in 15q region plotted against $-\log^{10} P$ values based on NCBI hg build 36. Genotyped (squares) and imputed (circles) SNPs are colour coded according to the extent of LD with highest association SNP rs5742915. The estimated recombination rates (cM/Mb) from HapMap CEU release 22 are shown as light blue lines. The blue arrows represent known genes. (Albagha et al. 2011)

PML is a tumour suppressor gene that is disrupted in acute promyelocytic leukemia (APL) resulting in its fusion to retinoic acid receptor alpha (*RARA*) gene as a result of the chromosomal translocation t(15;17) (Nisole et al. 2013).

The *PML* gene is located on long arm of chromosome 15. The gene consists of nine exons. Alternative splicing of exons 5-9 yields a large number of isoforms. The seven main ones are experimentally validated and designated PML I-VII. PML I is the longest isoform with 882 amino acids (aa) whereas PML VII is the shortest with 435 aa. They share the N-terminal region (exon

1-3) and differ in their C-terminal regions (El Bougrini et al. 2011; Nisole et al. 2013; Guan & Kao 2015).

The GWAS hit rs5742915 lies at the start of Exon 9 in the C terminal region of *PML* and therefore exists only in isoform 1. The amino acid change associated with this SNP is predicted to be tolerated by SIFT and benign by Polyphen and is not conserved through evolution. This means there are likely to be other variants driving the association with PDB risk. The gene as a whole, is not evolutionally conserved across eukaryotes. PML protein appears to be show conservation in mammals but seems to be absent from plants and from lower eukaryotes. Thus, PML function seems to be restricted to higher eukaryotes (Borden 2002; Borden 2008).

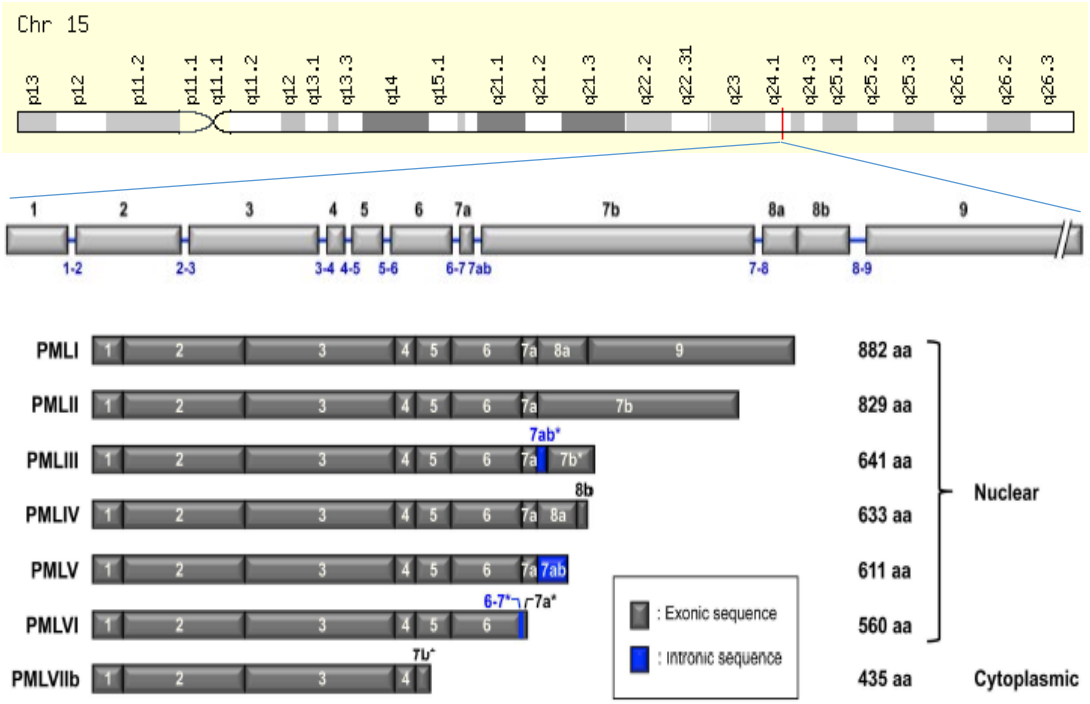

Figure 1.13. Chromosomal location and Structure of *PML* gene with seven main isoforms.

Adapted from (Nisole et al. 2013).

PML protein is ubiquitously expressed and is a member of the tripartite motif family and therefore also known as TRIM19. The N-terminal 418 aa, common to all isoforms, contains a number of well characterized zinc-binding domains.

These include a RING (really interesting new gene) finger domain, adjacent to two cysteine/histidine-rich motifs known as B-boxes (B1 and B2). The RING, B-boxes and α-helical coiled-coil domain, form a conserved motif known as TRI-partite motif (TRIM) or RBCC (El Bougrini et al. 2011; Nisole et al. 2013).

The difference in the COOH-terminal parts of the isoforms not only determines their localisation in the cell but also determines their partners, and in turn, the specific function(s) for each isoform. PML is localised to subnuclear matrix-associated structures, known as PML nuclear bodies (NBs). The RBCC domain plays an integral role in this as well as PML homodimerisation via the coiled-coil domain. Exon 6 encodes a nuclear localization sequence (NLS) which is responsible for PML nuclear localization. The nuclear export signal (NES) located on exon 9 is found only in PML I isoform, consistent with the cytoplasmic and nuclear distribution of this isoform. The SUMO interacting motif (SIM) is located on exon 7 with its hydrophobic core adjacent to specific serines that act as sites for Casein Kinase 2 (CK2) phosphorylation (El Bougrini et al. 2011; Nisole et al. 2013).

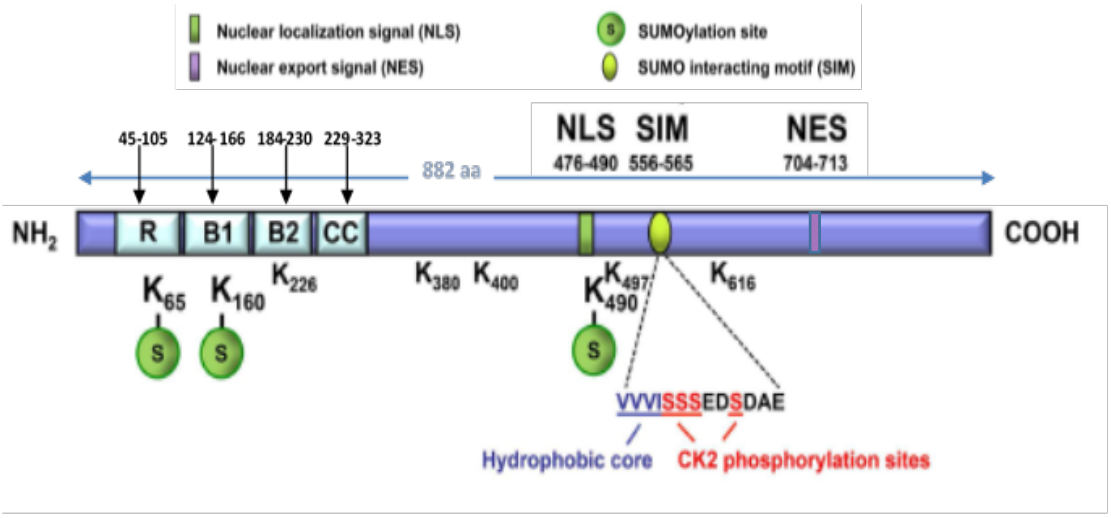

Figure 1.14. Domain organisation, motifs and Amino acid (aa) positions in the longest PML protein.

Adapted from (Nisole et al. 2013)

PML nuclear bodies range from 0.2 to 1um in size. PML is essential for the formation of these important structures since they interact with a number of

proteins, either transiently or stably and comprise chromosomal regions of high transcriptional activity. They regulate important cellular processes such as cell cycle, apoptosis and transcription, in association with their interacting partners. Modifier proteins such as deubiquitinases, phosphatases, kinases, acetyltransferases and ubiquitin/SUMO E3 ligases, as well as their substrates co-localise and interact to bring about protein modification at PML nuclear bodies (Salomoni & Pandolfi 2002; Bernardi & Pandolfi 2007; Guan & Kao 2015; Ahmed et al. 2017).

Role of PML in multiple biological processes

PML has been shown experimentally to physically interact with 120 proteins either transiently or constitutively leading to mutual regulation (http://thebiogrid.org). PML is therefore involved in multiple cellular pathways and activities such as regulation of cell growth, senescence, apoptosis, DNA repair, stem cell maintenance, protein degradation, autophagy and antiviral responses (Guan & Kao 2015).

PML senses DNA damage and organises multiple DNA repair complexes (such as Rad50/NBS1/hMre11 and BLM/Rad51/RPA) thereby maintaining genome integrity and stability and plays a crucial role in promoting alternative lengthening of telomeres (Dellaire and Bazett-Jones 2004; Chung et al. 2012).

PML is also involved in transcriptional regulation and functions mainly through nuclear bodies by interacting with cofactors to repress or activate transcription. PML disrupts DNA binding activity of Sp1 and its transactivation of epidermal growth factor promoter (Vallian et al. 1998) and interferes with Nur77 binding to its target promoter (Wu et al. 2002) as well as STAT3 DNA binding and activity (Kawasaki et al. 2003). PML represses NF-kB induced transcription of A20 (a NF-kB target gene) by competitively binding to A20 promoter (Wu et al. 2003). PML is required for transcriptional repression by tumour suppressor Mad and it achieves this by forming complexes with multiple corepressors (c-ski, N-Cor and mSin3A) (Khan et al. 2001) as well as histone deacetylase 1 (HDAC1) thereby exerting control at the epigenetic level (Wu et al. 2001).

PML also exhibits positive effects on transcription of many genes. PML stimulates AP-1 transcriptional activity (Vallian et al. 1998) and is essential for c-Jun DNA binding and activity in response to UV irradiation (Salomoni et al. 2005). PML is required for all-trans retinoic acid (ATRA)-dependant transactivation of p21 (Wang et al. 1998) and physically associates with and facilitates activity of important haematopoietic stem cell differentiation TF's GATA 1 (Wu et al. 2014) and GATA 2 (Tsuzuki et al. 2000). PML activates a subset of B-catenin responsive genes such as ARF and Siamois (Shtutman et al. 2002) and at the same time, sequesters transcriptional corepressor Daxx in PML NBs to cause transcriptional derepression of Pax3 (Lehembre et al. 2001). PML also forms transcriptional complex with NF-kB, STAT1 and CBP to activate Type I interferon (IFN-β) response (Guan & Kao 2015).

PML mediates apoptosis in response to various stimuli such γ-irradiation, Fas, IFNs (Type I and II) and TNF-α. The process requires caspase-3 activation by PML but PML can also mediate non-caspase mediated apoptosis by recruiting BAX and p27KIP1 (Wang et al. 1998; Huang et al. 2011). PML is a critical regulator of p53 tumour suppressor activity and p53 mediated cellular processes such as apoptosis, cell cycle arrest, DNA repair and senescence. PML activates p53 by sequestering Mdm2 thereby inhibiting p53 degradation and by promoting phosphorylation as well as acetylation of p53 (Bernardi et al. 2004). PML also promotes apoptosis by inhibition and sequestration of AKt/protein kinase B, inhibition of NF-kB survival pathway whereas cytoplasmic PML positively regulates TGF-β-induced apoptosis and promote its tumour suppressive activity (Guan & Kao 2015).

PML protein is upregulated in response to Ras oncogene resulting in potentiation of retinoblastoma protein (Rb) and p53 leading to premature cell senescence (Pearson et al. 2001).

Regulation of PML

PML expression is regulated by multiple factors and at multiple levels. Various cytokines such as Interferons, TNF-α and IL-6 enhance PML transcription via JAK-STAT pathway activation, STAT-1 activation and via stimulation of NF-

kB/JAK-STAT pathway respectively. Furthermore, B-catenin and plakoglobin act on PML promoter to activate its transcription. PML mRNA translation has been found to be enhanced in rodent cells by oncogenic Ras and TNF-α has been shown to stimulate the IRES site in the 5'-UTR of human PML mRNA (Guan & Kao 2015).

Post-translational modifications of PML are also known to regulate its protein levels within the cell and thereby control its functions. Arsenic trioxide, an inorganic cytotoxic compound which is used in chemotherapy of APL patients, directly binds to PML resulting in SUMOylation-dependent, ubiquitin-mediated proteasomal degradation of PML via RNF4 (Lallemand-Breitenbach et al. 2008). CK2 phosphorylation promotes PIAS-1 mediated degradation of PML (Scaglioni et al. 2006). Similarly, PML phosphorylation by ERK2, IGF1 and CDK1/2 results in PML-Pin1 interaction, protein isomerization followed by ubiquitin-mediated PML degradation (Lim et al. 2011). Protein acetyltransferase p300 acetylates PML leading to its degradation (Hayakawa et al. 2008) whereas deacetylase SIRT1 induces PML SUMOylation leading to accumulation of PML as well as increase in PML NB abundance (Guan et al. 2014).

Specific function of PML isoforms

Alternative splicing of PML gene generates several isoforms. Many studies have performed to try and understand specific function of different isoforms. PML I plays an important role in haematopoietic cell (myeloid lineage) differentiation by interacting with acute myeloid leukaemia 1. PML I interaction with HSV-1 ICP0 results in self-degradation by a SUMO-independent mechanism. PML IV, the most studied PML isoform, is involved in antiviral defence against many viruses such as Varicella-zoster virus, rabies virus and Encephalomyocarditis virus mainly via sequestration in PML NB's and also interacts with p53, PU.1, TRF1 and TIP60 to mediate their activity. In contrast, PML II interacts with Ad5-E1A-13Svirus to activate its transcription. PML III is involved in inhibition of centrosome duplication via suppression of Aurora A activation. PML V acta as a scaffold for PML NB formation and recruitment of

Daxx and Sp100 in PML NB's. PML VI lacks the SIM and thereby confers resistance to arsenic-induced PML degradation (Nisole et al. 2013).

In addition to 6 PML nuclear isoforms, a fraction of PML is also localised in the cytoplasm. The cytoplasmic isoform PML VIIb is involved in activation of TGF-β signalling and induction of target genes via interaction with SMAD 2/3 and SARA (Lin et al. 2004).

PML has, however, never been implicated directly in bone metabolism. My PhD study deals with exploring the role of chr 15q24 locus containing *PML* in bone metabolism and disorders of bone turnover such as PDB.

GOLGA6A

The *GOLGA6A* gene encodes a member of the golgin family of coiled-coil proteins. They are associated with the Golgi apparatus, and probably act as structural supports for the Golgi cisternae as well as play a role in membrane fusion (Albagha et al. 2011). The gene contains 18 exons spanning 10kb (www.omim.org/entry/610288).

The protein has a predicted molecular mass of 75KDa with a restricted pattern of expression confined mainly to testis. The role of the *GOLGA6A* gene in bone metabolism is currently unknown. However, skeletal dysplasia which is lethal (Smits et al. 2010) and a severe form of osteoporosis (Hennies et al. 2011) have been shown to result from mutations in other members of this family.

CHAPTER TWO

Project Aims

2 Project Aims and likely impact of findings

To examine the role of chromosome 15 locus in bone metabolism and development of Paget's disease of bone by:

- Fine mapping of 15q24 locus to identify functional genetic variants and susceptibility genes in relation to PDB using targeted next generation sequencing and functional analysis of any relevant variants.

- Investigate how abnormalities in *PML* regulate bone cell function thereby contributing to PDB using:

    - Expression analysis of *PML* in bone cells of murine as well as of human origin and in patients with PDB.
    - *In vitro* knockdown and overexpression assays in mouse monocyte-macrophage-like cell line – RAW 264.7 to assess and understand *PML* gene function in bone and
    - Examine phenotype of young as well as older *Pml* knockout mice and analyse relevant mechanisms and bone signalling pathways.

2.1 Impact

- Genetic factors identified at this locus could be used in conjunction with other genetic markers to assess individuals with family history as well as higher risk of developing PDB so that treatment or disease modifying strategies can be implemented early in life before permanent damage occurs.
- Better understanding of PDB pathophysiology as well as identify new molecular and bone signalling pathways and potential therapeutic targets.
- Lead to better understanding and applications for other disorders with abnormal bone turnover.

CHAPTER THREE

Materials and Methods

3 Material and Methods

3.1 Reagents/Materials

Media: Minimal Essential Medium Eagle - αMEM (Sigma), Dulbecco's Modified Eagle's medium- DMEM (Sigma), Fetal Calf Serum (Hyclone) and L-Glutamine (Invitrogen).

Antibodies: PML (sc-5621 1:500 SantaCruz Biotechnology), Rabbit Anti-Actin 1:1000 (AA20-33) IgG (Sigma), Rabbit alpha-tubulin mAb 1:1000 (2125 Cell Signalling)

Cytokines: Murine M-CSF (Prospec Tech.) and human recombinant RANK-L (gift from Dr. Patrick Mollat-Proskelia SASU and R&D Systems), IFN-γ (Lifetech, gift from Elaine Nimmo, IGMM).

Buffers, chemicals and other reagents: Cell dissociation buffer (Gibco), RNAlater solution (Sigma-Thermoscientific), Penicillin (Invitrogen), Streptomycin (Invitrogen), Genticin (Neomycin analogue-G418 LifeTech), jetPEI-Macrophage (Polyplus) and Alamar Blue reagent (Invitrogen). Please see appendices 1, 5 and 6 for further details.

Kits: GenElute Mammalian Total RNA kit (Sigma), RNeasy kit and DNeasy blood and tissue kit (Qiagen), qScript cDNA SuperMix kit (QuantaBioscience), SensiFAST Probe No-ROX kit (Bioline), Ambion Ribopure Blood RNA isolation kit;

Cell lines: RAW 264.7 (ATCC)

3.2 Targeted Next generation DNA sequencing

3.2.1 Study population

138 cases (negative for *SQSTM1* mutations and age at diagnosis of PDB <65 years) and 50 controls (unaffected individuals) were selected, DNA prepared and samples sent to Oxford Genomics for Targeted capture and sequencing.

3.2.2 Sequencing

15q24 locus was investigated by target capture of a 200 kb region surrounding the GWAS SNP rs5742915 using Haloplex target enrichment kit from Agilent. This region included six genes (*LOXL1*, *PML, STOML1, GOLGA6A, ISLR, ISLR2*).

Libraries were prepared, labelled with barcodes and sequenced on the Illumina HiSeq2000 platform. Sequencing analysis was performed by my supervisor Dr. Albagha and data was provided after QC, variant calling and annotation for further analysis. Burrows-Wheeler Alignment tool (BWA) package was used to map the sequenced reads (Fastq) to the reference human genome (hg19/b37). Picard version 1.89 was used to remove duplicate reads. Local re-alignment of the mapped reads around potential indel sites was done using Genome Analysis Toolkit ver 1.6 (GATK; http://www.broadinstitute.org/gsa/wiki/index.php/Home_Page). GATK was also used to recalibrate base quality (Phred Scale) scores and GATK unified genotyper used to call SNPs and indel variants.

3.2.3 Data analysis

PLINKSeq was used to analyse the genetic variation data. Publicly available databases such as ENSEMBL, 1000 genomes, NHLBI and ENCODE were used for annotation and/or filtering the variants. Variants passing quality control measures were filtered to include missense variants, 3' or 5' UTR variants and functional variants as predicted by ENCODE.

Publicly available bioinformatics tools such as SIFT and PolyPhen-2 were used to predict the functional effect of identified SNPs. Other tools such as

Mutation taster, I-mutant 2.0, SNIPA browser (Germany) and Regulation spotter were also used to assess SNP effects. Association testing of common variants was done by chi-square allelic test and rare variants were subjected to Fisher's exact test.

3.3 Mice

PML knockout (KO) mice (*Pml*$^{-/-}$) on a C57/B16 background were obtained from National Cancer Institute, USA. *PML* was disrupted in the mouse germ line and knockout generated by deleting part of exon 2 (94 bp) which encodes the RING finger domain (Wang et al. 1998). Wild type (WT) C57/B16 mice were used as controls.

Ethics Committee at the University of Edinburgh approved all animal protocols and procedures and they were conducted in accordance with the UK Home Office regulations (Personal licence number IBF9C1299, Project licence number 70/7964)

3.3.1 Mouse genotyping

Genomic DNA was extracted from mouse earsnips using the Qiagen DNeasy Blood and Tissue Kit according to manufacturer's protocol. DNA extracted was amplified by PCR in a 25ul reaction volume using Qiagen Taq polymerase kit, run on a 2% agarose gel and band size determined using a reference 100 bp Ladder from NEB.

Primers used:

Y317: 5'-TTT CAG TTT CTG CGC TGC C -3'
Y318: 5'-CGA CCA CCA AGC GAA ACA -3'
Y319: 5'-TTG GAC TTG CGC GTA CTG TC -3'

Table 3.1 Primers used for genotyping *Pml*$^{-/-}$ mice.

Primer combination	Band Size	Genotype
Y317/Y319	450 bp	WT
Y318/Y319	650 bp	KO

Table 3.2 PCR reagents and thermocycler conditions used for genotyping *Pml*$^{-/-}$ mice.

PCR reaction (25ul)	
Reagents	**Volume (ul)**
Qiagen 10x Buffer	2.5
dNTPs (10mM)	2
Qiagen Q-Solution (5X)	5
Y317 Primer (10uM)	1
Y318 Primer (10uM)	1
Y319 Primer (10uM)	1
Distilled Water	7.3
Qiagen Taq Polymerase (U/ul)	0.2
DNA (10ng/ul)	5

Thermocycler conditions		
Step	**Temperature(**°C)	**Duration**
Initial Denaturation	94	4min
Denature Template	94	30sec
Annealing	60	1min
Extension	72	1min
Number of cycles		35
Final Extension	72	10min
Hold	4	Forever

3.4 Cell culture

All tissue culture work was carried out in designated areas, under a laminar flow hood or a class II biological safety cabinet and was performed under sterile conditions with pre-sterilised or autoclaved reagents and consumables. All cultures were maintained in an incubator with standard conditions of 37°C, 5% CO_2 in a humidified atmosphere. Cell counting was done using a haemocytometer and cultures visualised using an inverted light microscope.

3.4.1 Alamar blue viability assay

This assay was used to quantitatively measure cell viability in culture. Healthy viable cells maintain a reducing environment within the cytoplasm. Alamar blue reagent resazurin, the active ingredient of alamarBlue reagent, is a cell

permeable, non-toxic compound that is blue in colour and non-fluorescent. Once it enters the cell, resazurin is reduced to resorufin which is red in colour and fluorescent. The colour change is directly proportional to the number of viable, metabolically active cells. Alamar blue was added as 10% of total volume in each well and left for 2.5 hours at 37^0C. The resulting fluorescence was measured by the plate reader (BIO-Tek Synergy HT) using excitation wavelength of 540nm and an emission wavelength of 590nm. Control wells containing only media were used to correct the data for background fluorescence.

3.4.2 Osteoclast culture

This was done using primary mouse bone marrow cells as well as RAW 264.7 cell line. It is a mouse monocyte-macrophage-like cell line established from the ascites of a tumour which was induced in a male mouse by intraperitoneal injection of Abselon leukaemia virus (A-MuLV) and forms osteoclasts in response to RANKL treatment (Raschke et al. 1978; Vincent et al. 2009).

Bone marrow cells were isolated from the long bones (tibia and femur) of 3-4 month old mice. The mice were culled by cervical dislocation, lower limbs carefully dissected to remove any soft tissue and bones collected in sterile PBS. This was followed by isolation of bone marrow under a flow hood. The epiphyses of long bones were cut, bone marrow flushed with αMEM using a plastic 5ml syringe and 25 gauge needle into a 10cm petri dish and homogenized with a broader 21 gauge needle. This was centrifuged at 300g for 3 mins, supernatant discarded, cell pellet resuspended in αMEM and cultured in 10 cm petri dish in the presence of M-CSF (100ng/ml) for 48 hrs to generate bone marrow derived macrophages (BMDMs). Adherent cells were gently scraped with a rubber scraper after removal of the medium and incubation with 5ml cell dissociation buffer for 5 mins at 37°C to lift the cells. Fresh medium was added to dissociated cells, all contents of petri dish collected in 15 ml falcon tube, centrifuged, supernatant discarded and the cell pellet resuspended in 1ml supplemented medium for counting. The cells were then plated (seeding density: 10,000 BMDMs per 96 well and 100,000

BMDMs per 12 well) and stimulated with M-CSF (at a concentration of 25ng/ml) and RANKL (100ng/ml), medium replaced on 3rd day and culture continued until osteoclasts were formed (usually 4-5 days post RANKL stimulation). Multinucleated osteoclasts (≥ 3 nuclei and ≥ 10 nuclei) were visualised using TRAcP staining (as described later in section 3.4.7). The medium used was αMEM supplemented with 10% foetal calf serum (FCS), 2mM L-glutamine, 100µg/ml streptomycin and 100 U/ml penicillin.

For IFN-γ experiments, BMDMs were treated with IFN-γ (5ng/ml) for 24 hrs followed by treatment with MCSF and RANKL as above to generate osteoclasts.

RAW 264.7 cell line with early passage number was grown in T75 flask. When 70-80% confluent, the cells were scraped, centrifuged, pellet resuspended, counted and cultured (Seeding density: 10,000 per 96 well and 100,000 per 12 well) in DMEM (supplemented as above with 10% foetal calf serum (FCS), 2mM L-glutamine, 100µg/ml streptomycin and 100U/ml penicillin) for 4 days with RANKL (100ng/ml) until osteoclasts were formed.

Protein and RNA were isolated (described in section 3.7.1 and 3.8 respectively) and collected on the following days during osteoclast development: Day 0 (no RANKL), Day 2/3 (intermediate stage) and Day 4/5 (Final stage of osteoclast).

3.4.3 Bone resorption assay (Osteoassay)

The bone resorption activity of osteoclasts was determined using osteoassay surface multi well plate. BMDMs were plated (50,000 cells/well in 500ul/well supplemented αMEM) and osteoclasts obtained (as described above in osteoclast culture) on Osteo Assay Surface 24 well plates. Following this, cells were removed from wells using a 2% sodium hypochlorite solution for 5 minutes, washed with distilled water and air-dried. For modified Von-Kossa staining, plates were treated away from light, with 250 µl/well of a 5% (w/v) silver nitrate solution for 30 minutes at room temperature. Supernatants were aspirated and rinsed for 5 minutes with distilled water. Supernatants were

aspirated again, and incubated in 250 µl/well of a 5% (w/v) sodium carbonate in formalin solution for 5 minutes at room temperature. Plates were then washed twice with distilled water followed by drying them in a 50°C incubator for an hour. Plates were then imaged with a Zeiss inverted microscope and resorption areas analysed using ImageJ software (NIH).

The wells in these plates have a thin film of calcium-phosphate (hydroxyapatite) coated at the bottom which acts as a substrate for osteoclasts. Osteoclasts grow over the surface and resorb the hydroxyapatite layer via their activity and this in turn can be measured by looking at areas of clearance under a light microscope. The technique is simple, easy to perform, widely reported in literature (Jeganathan et al. 2014; Wong et al. 2019) and gives a good direct quantitative measurement of bone resorbing activity of osteoclasts in an *in vitro* setting compared to osteoclast culture on dentine slices which are not easy to source, require processing/optimization as well as pH adjustments and resorption quantification on dentine is challenging. However, the osteoassay method is limited due to the fact that it is less physiologically similar to bone compared to dentine and needs support from additional biochemical markers of osteoclast activity to validate the findings.

3.4.4 Osteoclast survival

Osteoclasts were generated from BMDMs (as described in section 3.4.2) in 96 well plates. RANKL was then withdrawn from culture medium while retaining all other reagents. Plates were fixed at the following time points post RANKL withdrawal (0 hrs, 16 hrs, 24 hrs and 48 hrs), stained with TRAcP and osteoclasts counted.

3.4.5 Overexpression of Pml *in vitro*

This was done using RAW 264.7 cell line. A GFP expressing plasmid (PEGFP, Clontech) was initially used to evaluate the jetPEI-Macrophage reagent for transfection efficiency in RAW cells. RAW cells (50-60% confluent) were seeded at relevant densities 4 hours before transfection. Various combinations were tested as described in Table 3.3.

Table 3.3 Transfection optimisation for *Pml* overexpression

Culture Vessel	Number of cells	Total amount of DNA (µg)	Volume of NaCl added to dilute DNA (µl)	Volume of jetPEI Macrophage added (µl)	Volume of NaCl added to dilute jetPEI Macrophage (µl)	Total volume of complexes added per well (ul)
96 well	15,000	0.2	10	0.7	10	20
96 well	15,000	0.5	10	1.6	10	20
24 well	100,000	2	50	6.4	50	100
T25	1.5 million	6	100	19.2	100	200

Post-transfection, half the medium was replaced at 3 hrs and in full after 24 hours. jetPEI alone was used as a negative control to test its toxicity on RAW cells. GFP reporter activity was analysed 4 hrs and 24 hrs after transfection.

Based on the best combination and downstream cell requirement, RAW cells were seeded and transfected with GenEZ Mouse *Pml* ORF expression plasmid DNA (OMu22116-Genscript) or empty vector DNA (pcDNA3.1) using jetPEI according to the table above and manufacturer protocol (details on next page). The vector map is as shown in Figure 3.1. Cells were transiently selected for 3-4 days using 500ug/ml neomycin. Overexpression was confirmed by qRT-PCR. Cells overexpressing *Pml* or control cells were seeded in 96 well plate (10,000/well) in supplemented DMEM (150ul/well) and stimulated with RANKL (100ng/ml) for 4 days. Cells were then fixed, TRAcP stained and TRAcP positive multinucleated cells were counted.

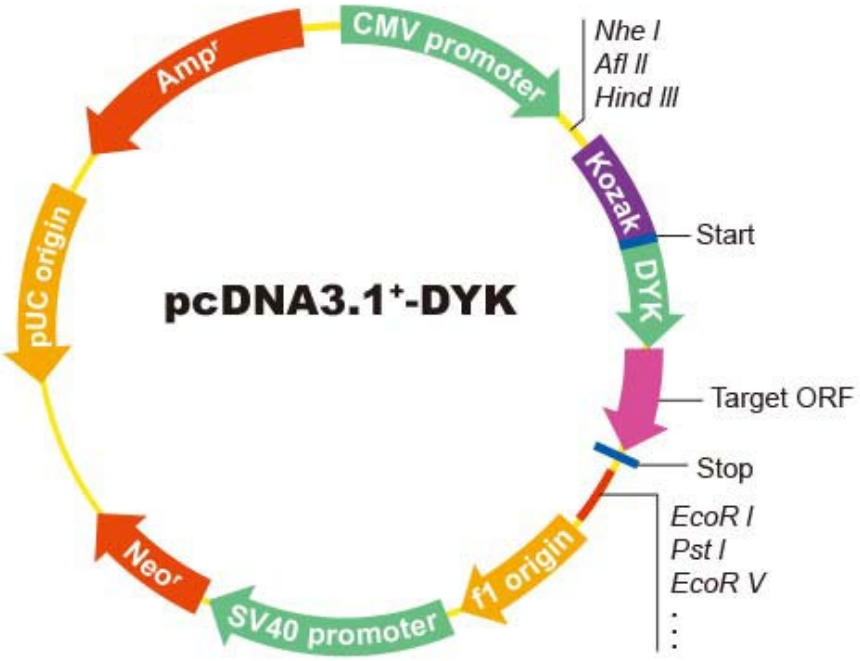

Figure 3.1 pcDNA3.1+-DYK vector map.

The figure above shows different components of the plasmid vector (GenEZ) with the inserted ORF (mouse *Pml*) for expression in mammalian cells (RAW 264.7).

JetPEI-Macrophage protocol

The protocol below describes the transfection procedure in a T25 flask with 1.5 million RAW cells:

6 µg of DNA was diluted into 100 µl of 150 mM NaCl, vortexed gently and spun down briefly. In a separate tube, 19.2 µl of jetPEI®-Macrophage was diluted in 100 µl of 150 mM NaCl, vortexed gently and spun down briefly. 100 µl jetPEI®-Macrophage solution was added to the 100 µl DNA solution at once (avoiding the reverse order). The solution was vortex-mixed immediately and spun down briefly followed by incubation for 15 to 30 minutes at room temperature. 200 µl of jetPEI®-Macrophage/DNA complexes was added to each T25 culture flask and homogenized by gently swirling the flask and the flask returned to the cell culture incubator.

3.4.6 *Pml* knockdown *in vitro*

This was achieved using arsenic trioxide, an inorganic compound that degrades PML and is used in the treatment of acute promyelocytic leukaemia. RAW 264.7 were cultured in 12 well plates (as mentioned in 3.4.2) and treated with arsenic trioxide for 24 hrs at various concentrations prior to stimulation for 4 days with RANKL (100ng/ml) until osteoclasts were formed and effect on osteoclast development was assessed.

Arsenic trioxide was tried at a concentration of 1um, 5um and 25um. *Pml* knockdown was achieved at 25um.

3.4.7 TRAcP staining

Tartrate resistant acid phosphatase (TRAcP) is a bone marker secreted by osteoclasts and helps in their visualization post-staining. After osteoclasts formed, media was removed, washed with PBS and cells fixed in 4% formaldehyde (v/v) for 10min followed by a PBS wash. TRAcP stain (65ul per well of a 96 well) whose preparation is described in Appendix 1 was then applied for 35-45 minutes at 37°C until osteoclasts develop a red colour corresponding to expression of TRAcP. The wells were washed with PBS and stored in 70% EtOH at 4°C. Osteoclast count was performed using a Zeiss inverted light microscope at 10x resolution.

3.4.8 Osteoblast culture

3.4.8.1 Osteoblast culture and bone nodule assay

Osteoblasts were isolated from the calvariae of 2-4 day old mice (pups) by sequential collagenase/EDTA digestion (Details below in section 3.4.8.2) and cultured in T75 flask containing αMEM supplemented with 10% fetal calf serum, 5% glutamine, 100 µg/ml streptomycin and 100 U/ml penicillin.

The medium was refreshed 24 hrs later to remove non-adherent cells and on reaching confluence (1-2 days later), cells were detached with trypsin, counted and re-plated in 12-well plates at a density of 1×10^5 cells/well. Cells were cultured in osteogenic medium (αMEM supplemented as above with 3

mM β-glycerol phosphate (βGP) and 50 µg/ml Vitamin C (Vit.C). Medium was replaced carefully three times per week and cultures continued for up to 18 days until mineralisation. RNA and protein were collected at various timepoints during osteoblast development.

3.4.8.2 Collagenase/EDTA digestion of Mouse calvariae for osteoblast isolation

Mouse calvariae were dissected from pup heads using a pair of forceps and scissors. They were washed thoroughly in Hank's balanced salt solution (HBSS) and transferred individually to a sterile 15 ml falcon tube containing 2ml of collagenase type 1 (1mg/ml) in HBSS and incubated in a shaking water bath for 10 minutes at 37^{o}C. Supernatant was discarded and each calvaria in 15ml falcon tube was incubated for 30 minutes in 4ml of collagenase type 1 (1mg/ml) in HBSS. Cell suspension was removed, collected in a fresh 50ml falcon (labelled "Tube Osteoblast") and mixed with 6ml of standard αMEM. The remaining tissue in 15ml falcon tube was washed in 2ml PBS, PBS wash transferred to original 50ml falcon tube labelled "Tube Osteoblast" and remaining tissue in 15ml falcon tube treated for 10 minutes with 4ml of ethylenediaminetetraacetic acid (EDTA 5mM) 1:100 in PBS. Cell suspension was removed, transferred to original tube labelled "Tube Osteoblast" and mixed with further 6ml of standard αMEM. The remaining tissues in 15ml falcon tube were incubated for 20 minutes in 4ml of collagenase type 1 (1mg/ml) in HBSS. Cell suspension was removed, transferred to original tube labelled "Tube Osteoblast" and mixed with final 6ml of standard αMEM. Cell suspensions thus pooled (in 50ml falcon tube labelled "Tube Osteoblast") were centrifuged at 300g for 3 minutes. Supernatant was discarded and cell pellets were resuspended in supplemented αMEM.

Mineralized nodules formed after 21 days of calvarial osteoblasts in culture were detected for calcium using Alizarin Red staining (details below in section 3.4.8.3), and bone nodule formation was quantified by destaining the cultures overnight in 10% (w/v) cetylpyridinium chloride and dissolving the stain in 10 mM sodium phosphate (pH 7.0). The absorbance of the extracted stain was

then measured at 562 nm in a BIO-Tek Synergy HT plate reader and compared to an Alizarin Red standard curve (Standards at 0, 0.05, 0.1, 0.25, 0.5, 1, 1.5, 2.5, 5, 7.5, 10mM). Alizarin red values were corrected for viable cell count as determined by the Alamar Blue viability assay (section 3.4.1).

3.4.8.3 Alizarin red staining of osteoblast derived mineralised nodules

Osteoblasts in 12 well plates were washed with pre warmed PBS and fixed in 70% ethanol. The plates were stored at 4°C overnight. The following day, fixed cells were washed with distilled water and stained with 1ml/well of 40mM Alizarin red (adjust pH to 4.1-4.3 with ammonium hydroxide (10% v/v)) for 20mins on a rocker, washed four times with distilled water (dH_2O) for 5 mins each time and then left to air-dry followed by imaging the plate on an Epson scanner. This was followed by destaining of Alizarin red and quantification as described in section 3.4.8.2 above.

Alizarin red staining is the traditional gold standard method for detection and quantification of osteoblast mineralisation and used as a readout of osteoblast differentiation efficiency. The method is simple, inexpensive and widely accepted but time-consuming, cumbersome and requires fixing and termination of cultures thereby preventing further examination or manipulation of cultures. Alternative methods exist with advantages but also have their limitations. Von Kossa is an alternative staining method but also needs cell fixation prior to staining and exhibits non-specificity for calcium. Alkaline phosphatase detection is more suited to detect matrix maturation as opposed to mineralisation. Calcein dye is a fluorescent, non-cell permeable agent which can be used to monitor mineralisation without affecting cell physiology and background intracellular fluorescence. It provides a suitable alternative to alizarin red allowing real-time monitoring of mineral deposition in live cells when combined with advanced automatic time-lapse imaging such as IncuCyte ZOOM, thereby providing convenience and increased accuracy, but at an additional cost. Electron microscopy and infrared spectroscopy are good alternatives but not always available or feasible and need expertise.

3.5 Microcomputed tomography

3.5.1 Scanning

Micro CT (μCT) was performed using an *ex vivo* Skyscan 1172 system (Bruker, Belgium). Mice were originally sacrificed by CO_2 inhalation. Lower limbs, lumbar spine, skull, liver, spleen and kidney were dissected, isolated and fixed in 4% formaldehyde in PBS for a day. They were then removed and placed for long term storage in 70% ethanol. The lower limb (usually left femur and tibia) of 4-month and 14-month old animals was dissected free of most soft tissue, and scanned *ex vivo* at a resolution of 5μm. Briefly, the leg was wrapped in parafilm, placed in the sample holder and mounted upright on the stage of μCT. The scanner was warmed initially for 15 mins before starting the scanning process. Radiation was set to 60KV and 167μA. Medium camera was used with pixel size set to 4.9um with Aluminium filter at 0.5mm and rotation step 0.6°. Set oversize and multiple scan was used to get a scout scan of the sample and to select the boundaries of the scan (usually 3 segments spanning from top to bottom: the distal femoral diaphysis, femoral metaphysis, knee joint, proximal tibial metaphysis and diaphysis). Each segment took around 50 minutes to scan and once finished, the leg was returned to 70% ethanol and remaining scans performed. Raw images were generated as TIF files. Image reconstruction was performed using the Skyscan NRecon package (parameters in Appendix 2) and reconstructed images obtained as bmp files.

3.5.2 μCT analysis

Skyscan dataviewer software was used to load the reconstructed image stack in 3D (transverse, sagittal and coronal axes of the femur and tibia), and to rotate and fix the orientation of the bone.

Trabecular and cortical bone measurements were done using Skyscan CTAn software Trabecular and cortical bone analysis was done on the proximal tibial metaphysis and diaphysis respectively of all mice (Fig. 3.2 left). The reference level used was the end of growth plate (Fig. 3.2 right). The region of interest

(ROI) for trabecular analysis was a selection of 200 slices distal to the reference level and for cortical analysis, a selection of 100 slices located 500 slices distal to reference level (Fig. 3.2 left).

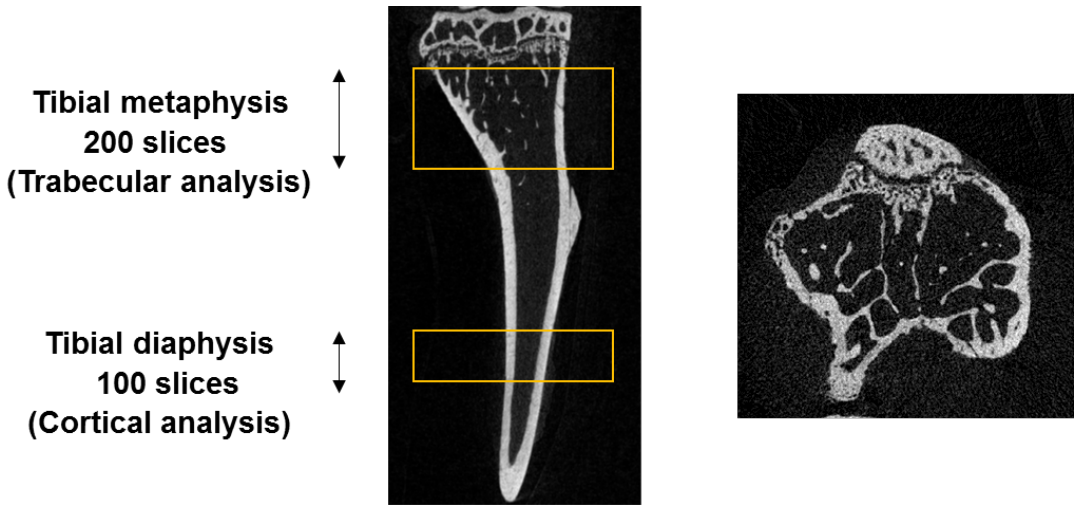

Figure 3.2 Images from Skyscan dataviewer software.

On the left, top yellow box i.e proximal tibial metaphysis represents region of interest (ROI) selected for trabecular analysis and the yellow box at the bottom in the tibial diaphysis region is the ROI for cortical analysis. The image on right represents the reference level used for trabecular and cortical analysis (end of growth plate).

CTAn allows manual tracing of the ROI in a transaxial view of the 3D reconstructed slices. Trabecular bone was chosen by selecting the trabeculae and excluding the endosteal surface whereas cortical bone includes all the cortex (Fig. 3.3left). The software then calculates the following bone parameters (Table 3.4) using a series of task lists relevant for trabecular and cortical bone which separates soft tissue from bone as well as amelioration of ROI such as reduction of background noise, removal of speckles and closing of pores (Main parameters for CTAn listed in Appendix 3).

Table 3.4 Parameters analysed and output given by CTAn software.

Parameter	Abbreviation (Unit)
Trabecular bone volume	BV/TV (%)
Trabecular number	Tr. N. (1/mm)
Trabecular thickness	Tr. Th. (um)
Trabecular separation	Tr. Sp. (um)
Cortical thickness	Ct. Th. (um)

The output is in the form of an excel sheet. Additionally, CTAn generates a 3D model of the trabecular and cortical bone that allows visualisation of the bone morphology in detail using Skyscan CT Vol software (Fig. 3.3right).

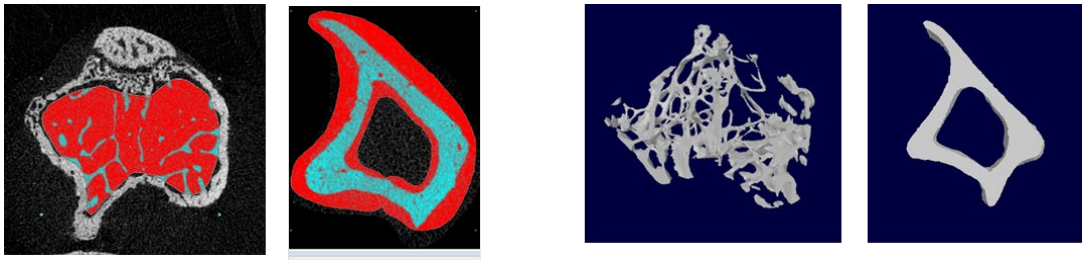

Figure 3.3 Images from CTAn and CTVol software.

On the left are representative images from CTAn software showing manual tracing of ROI for trabecular bone and cortex. On the right are 3D model images of trabecular and cortical bone using CTVol software.

3.6 Immunohistochemistry

PML expression was detected in human osteoclasts by Immunohistochemistry (IHC) of Formalin-fixed paraffin embedded (FFPE) sections from healthy controls with unaffected bone as well as bone sections from patients with PDB and giant cell tumour of bone (positive control).

Sections from normal and pathological human bone tissue were subjected to Immunohistochemistry using Envision Immuno protocol (described in Appendix 4).

3.7 Immunoblotting

3.7.1 Isolation of protein

Plated cells had their medium removed, washed with cold PBS followed by lysis using RIPA buffer (described in Appendix 5). The plates were placed on ice for 10-15 mins followed by storage at -20°C. After thawing, the culture wells were scraped with a pipette tip or a syringe plunger, collected in an eppendorf tube and centrifuged at 12000g for 10 mins at 4°C and the protein (cell extract supernatant) stored for downstream experiments at -20°C.

3.7.2 Measurement of protein concentration

The concentration was measured using Pierce protein assay. The working solution was prepared by mixing bicinchoninic acid solution with copper II sulfate pentahydrate 4% solution with in a ratio of 50:1. Ready-made bovine serum albumin protein standards were added along with protein samples (diluted 1:5 with sterile water) in duplicate in a 96 well plate (10ul of standard or diluted query sample + 200ul of working solution per well), plate sealed and incubated at 37°C for 15-20 mins. The colorimetric detection of intense purple colour developed was then measured at 562 nm in a BIO-Tek Synergy HT plate reader and compared to linear BSA standard curve.

3.7.3 Gel electrophoresis and Transfer

Protein samples (20-30ug in total) were mixed with sample loading buffer (Appendix 5) in a ratio of 1:5, denatured for 5 mins at 95°C, cooled,

centrifuged and subjected to Mini Protean TGX Precast gel (4-20%) electrophoresis in a BioRad Tetra cell tank filled with running buffer (Appendix 5). A ladder (mix of 6ul each of Kaleidoscope and Magic mark) is run in parallel to determine molecular weight of the protein. The gel was run for 45 mins at 200V. Once the dye front disappears at the bottom of the gel, current was stopped, the gel was removed from the cassette and electroblotted onto Biorad Mini PVDF membranes using Transblot Turbo transfer system. The transfer was accomplished in 10 minutes at a constant current of 2.5A and 25V. Gel transfer assembly is as shown in Fig. 3.4

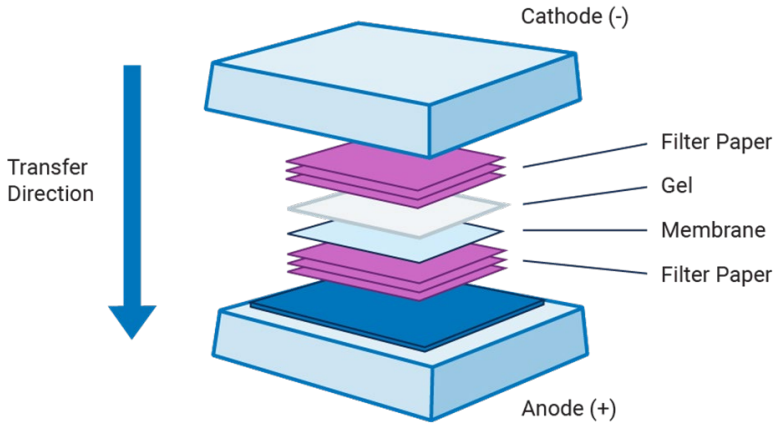

Figure 3.4 Gel transfer setup (Image obtained from www.licor.com)

3.7.4 Antibody treatment and Immunostaining

Membranes were blocked with 5%(w/v) non-fat milk in Tris buffered saline with TBS-tween (TBST) (150 mM NaCl, 50 mM Tris, 0.1% [v/v] Tween-20) for 1 hr at room temperature and probed with relevant primary antibody (Ab). The primary Ab was prepared at the recommended dilutions (1:500 or 1:1000) using 3% BSA in TBST. The membrane was incubated with the primary Ab (raised in rabbit) overnight with shaking at 4°C. After washing with TBST (3 washes at 15 minutes each), membranes were incubated with anti-rabbit horseradish peroxidise conjugated secondary antibody (1:5000, Cell Signalling), washed 3 times for 15 mins each with a final wash in TBS for 10mins and visualized using Clarity Western ECL kit (BioRad) on a Licor Odyssey imager. Intensities of bands were quantified using Image Studio Lite

Ver 3.1 software. The target protein was corrected for loading as well as target protein normalised by probing the membranes with housekeeping stably expressed genes such as Beta Actin and Alpha Tubulin.

For re-probing with a new antibody, when necessary, the membrane was treated with Stripping buffer (Appendix 5) in 50ul DTT and placed in a water bath for 10 min at 55°C with constant gentle shaking. The membrane was visualised as mentioned above to ensure complete stripping followed by blocking and other steps of antibody detection and Immunostaining.

3.8 Quantitative Real-Time PCR (qRT-PCR)

Cells in culture had their medium removed and lysis buffer added for 3 minutes. The lysis buffer was prepared by adding 10ul of β-mercaptoethanol to 1ml of lysis buffer from RNA isolation kit (Sigma). After removing the medium from the wells, 250ul of this mix was added to each well of a 12 well plate, plate tapped from side to side, and left at room temperature for 3 minutes and lysate collected. The resulting lysate was stored at -70°C until RNA isolation. Total RNA was isolated using GenElute Mammalian Total RNA Kit (Spin column protocol involving filtering, washing and elution) and/or Qiagen RNeasy Mini Isolation kit and RNA was quantified using the Nanodrop ND-8000 Spectrophotometer.

Blood samples from Pagetic cases were stored in RNAlater solution at -20°C prior to isolating total RNA using Ambion Ribopure Blood RNA isolation kit, RNA quantified using Nanodrop ND-8000 (Thermoscientific) and subjected to reverse transcriptase-PCR to generate cDNA.

The Complementary DNA (cDNA) was generated by reverse transcriptase-PCR using the Quanta qScript cDNA SuperMix kit following the manufacturer's instructions (details on next page).

Quanta reverse transcriptase PCR

All RNA samples to be reverse transcribed were equated to similar starting concentration (100ng-1ug) using DEPC treated water. This was used as the template for reverse transcriptase-PCR. All reagents were kept on ice including PCR 8 well strip or 96 well plate preparation. PCR reaction and conditions were as follows:

Table 3.5 PCR reaction and cycling conditions for reverse transcriptase-PCR

PCR reaction	
Reagents	**Volume (ul)**
qScript super mix (5X)	4
DEPC water	Variable
RNA (100ng-1ug)	Variable
Total	20

Thermocycler conditions		
Step	**Temperature**	**Duration**
1 cycle	22°C	5min
1 cycle	42°C	30min
1 cycle	85°C	5min
Hold	4°C	Forever

cDNA synthesized by reverse transcriptase-PCR was diluted 1:5 or 1:10 with DEPC water for qRT-PCR.

Primers and labelled probes were designed using Primer 3 and the Universal ProbeLibrary System Assay Design Center application on Roche Diagnostics website: (https://lifescience.roche.com/en_gb/brands/universal-probe-library.html#assay-design-center). The probe label was FAM for all the targets (genes) of interest. Table 3.6 describes primer sequences and other details for target genes analysed by qPCR.

Table 3.6 qPCR primers and other details.

Target Gene	Primers (5' - 3') (F:Forward; R:Reverse)	Probe Number	Amplicon (bp)	Species
PML	F: ccgagacccctctgaag R: cgcagaaactggaactcctc	26	91	Human
Pml	F: tgtcgacaacaggactctgc R: cctcctgtatggcttgctct	6	112	Mouse
Nfatc1	F: tccaaagtcattttcgtgga R: tttgcttccatctcccagac	50	62	Mouse
Dcstamp	F: tgggggacttatgtgtttcc R: agactcccaaatgctggatg	20	64	Mouse
Ctsk	F: cgaaaagagcctagcgaaca R: tgggtagcagcagaaacttg	18	67	Mouse
Alpl	F: cggatcctgaccaaaaacc R: tcatgatgtccgtggtcaat	31	74	Mouse

Real-time PCR was performed using SensiFAST Probe No-ROX kit on a Chromo 4TM Detector or Bio RAD CFX Connect system and analysed using the Opticon MonitorTM software version 3.1 or Bio RAD CFX Manager V1.0. Reagents and cycling conditions are shown in Table 3.6. Amplification curves were generated (fluorescence plotted against number of cycles) and Ct values determined by the software. Ct value represents the cycle number at which the fluorescence of PCR product exceeds the background signal and reaction enters exponential phase.

Samples were normalized to 18s rRNA expression. 18s cDNA was amplified with the predesigned VIC-labelled probe-primer combination from Applied Biosystems (4319413E) allowing two channel detection of one cDNA.

Table 3.7 Reagents, concentrations and thermocycler conditions for qRT-PCR.

PCR reaction (20ul)	
Reagents	**Volume (ul)**
Sensifast 2x Mix	10
10uM Forward Primer	0.8
10uM Reverse Primer	0.8
10uM Universal Probe	0.2
DEPC treated Water	4.2
Total	16
cDNA template	4

Thermocycler conditions		
Step	**Temperature(°C)**	**Duration**
Initial Denaturation	95	10min
Denature Template	95	15sec
Annealing	60	30 sec
Extension	72	15sec
Number of cycles		39
Hold	4	Forever

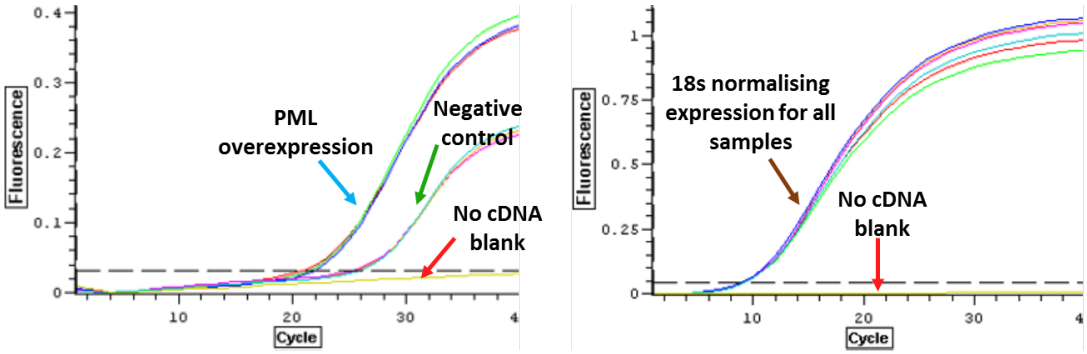

Figure 3.5 Example of quantification curves from Opticon Monitor 3.1 software.

Cycle threshold (Ct) is shown as dotted line in both curves. The left image shows FAM labelled target gene (*PML*) expression in an overexpressed sample run in triplicate (blue arrow with lower Ct values) compared to negative empty vector control (green arrow with higher Ct values). The image on right shows VIC labelled normalising control gene expression (18s in this case) for

both overexpressed and negative control samples with similar Ct values. The red arrows indicate no cDNA control blanks (Ct below threshold).

3.9 Cloning and digestion of plasmid DNA

3.9.1 Transformation of plasmids into DH5-α cells

10ml liquid broth (Luria broth LB) without antibiotic was put in a universal and heated to 37ºC in a waterbath. Competent cells (DH5-α) from the -80ºC freezer were distributed into 50ul aliquots (in 2ml Eppendorf tubes). DH5-α cells were thawed on ice. 2µl of appropriate pre-prepared plasmid (at a concentration of 50ng/µl) was added to appropriately labelled DH5-α cell 50µl aliquot, mixed gently by tapping and incubated on ice for 30 minutes. Cells were given a heat shock at 42ºC for 20 seconds and then placed on ice for 2 minutes. 950µl of pre-warmed LB broth without antibiotic was added to each tube and tubes incubated at 37º for 1 hour in shaking incubator at 225rpm. In a clean environment with the Bunsen flame on, 50µl of transformation reaction was spread onto appropriately labelled agar plate using a sterile spreader and covering all the plate. Two plates were done for each transformation and the plates placed at 37ºC in the incubator overnight.

A starter culture was made by adding a colony selected from a streaked plate to an appropriately labelled universal containing 5ml of liquid broth with antibiotic carbenicllin (100ug/ml final concentration). This procedure was done near a Bunsen flame and using a sterile loop. The universal(s) were placed in shaking incubator at 37ºC overnight. Next morning, 2ml of the culture medium was centrifuged in a 2ml eppendorf tube at 13000g for 1 minute, supernatant discarded and a further 2ml of culture medium added to the pellet and spun at 13000g for 1 minute (remainder of culture mix was kept in fridge). Supernatant was discarded. Qiagen Miniprep kit protocol was performed on the pelleted cells as per the manufacturer protocol. The extracted plasmid DNA was subjected to restriction enzyme digest (described in next section) and sequence verified by PCR-Sanger DNA sequencing as detailed in chapter 5.

3.9.2 Restriction digest (double digestion) of plasmid DNA

Pml ORF expression plasmid DNA was double digested with HindIII and EcoRV, the product run on a 1.2% agarose gel (Figure 8.1)

Table 3.8 Restriction digest of *Pml* overexpression plasmid.

Restriction digest reaction (20ul)	
Reagents	**Volume (ul)**
NEB buffer 2	2
10U/ul Hind III	1
10U/ul EcoRV	1
BSA	0.2
Distilled Water	10.8
Total	15
Miniprep product	5

Thermocycler conditions		
Step	**Temperature**	**Duration**
1	37°C	3 hours
Hold	4°C	Forever

Similarly empty vector pcDNA3.1 was double digested with XhoI and MluI with similar thermocycler conditions and the product run on a 1.2% agarose gel (Figure 8.1)

Table 3.8 Restriction digest of pcDNA3.1 empty vector plasmid.

Restriction digest reaction (20ul)	
Reagents	**Volume (ul)**
NEB buffer 3	2
10U/ul XhoI	1
10U/ul MluI	1
BSA	0.2
Distilled Water	10.8
Total	15
Miniprep product	5

3.10 Disease severity score

A composite disease severity score was computed and tested to see if *PML* expression levels correlated with disease severity scores. The score was computed by taking into account various clinical features and complications of PDB. Briefly, one point was assigned for each bone affected and additional points were assigned as follows: previous orthopaedic surgery for PDB (0=no; 1=yes); previous fractures through Pagetic bone (0=no; 1=yes); history of osteosarcoma (0=no; 1=yes); bisphosphonate treatment in the previous 12 months (0=no; 1=yes); bisphosphonate treatment >12 months ago (0=no; 1=yes); bone deformity (0=no deformity; 1=mild or moderate deformity; 2=severe deformity, for each bone affected by PDB); age at diagnosis (1= ≥70 years; 2=60–69 years; 3=40–59 years; 4=<40 years) and use of a hearing aid in patient with PDB of the skull (excluding mandible and maxilla) (0=no; 1=yes) (Albagha et al. 2013). Regression model-ANOVA in SPSS 22 was used to determine the correlation between *PML* expression and PDB severity.

3.11 Statistical analyses

Analysis was performed using IBM SPSS 22 and Microsoft Excel software. Values in the graphs indicate group means ± standard deviation (SD) or standard error of mean (SEM), as indicated in the figure legends. Two-tailed *t*-test was performed for comparisons between groups. *P value* ≤ 0.05 was considered to indicate statistical significance. Experiments were performed as independent replicates and data presented as indicated in figure legends.

CHAPTER FOUR

Targeted DNA sequencing of chr15 locus

4 Targeted DNA sequencing of chr15 locus

4.1 Summary

One of the seven PDB susceptibility loci identified using GWAS on chr 15 was subjected to targeted DNA sequencing. The targeted region spanning 200kb surrounding the most significant GWAS SNP rs5742915 from this locus was investigated in a cohort of 138 PDB cases and 50 unaffected controls and included six genes (*LOXL1*, *PML, STOML1, GOLGA6A, ISLR, ISLR2*). A total of 39 protein coding and 33 regulatory variants were found. However, only 3 missense variants (including top SNP rs5742915) and a couple of regulatory variants were associated with PDB; all located within *PML* at the 15q24 locus. Thus, *PML* seems to be the most likely susceptibility gene for PDB from this locus warranting further investigation by its expression and functional analysis.

4.2 Introduction

PDB has a strong genetic component. However, mutations in only one gene *SQSTM1* have been found in approximately 10% of sporadic cases and 40% of familial cases but additional causal genes remain unidentified (Laurin et al. 2002; Hocking 2002). Genome wide association studies have identified seven genome wide significant loci that predispose to PDB (Albagha et al. 2010; Albagha et al. 2011).

One of these loci was located on 15q24.1 and it contains likely candidate genes *PML* and *GOLGA6A* both of which have unknown role(s) in bone metabolism. The association at this locus was replicated in several independent populations from UK, Australia, Spain, Italy, Belgium and the Netherlands (Albagha et al. 2011). The strongest association was with SNP rs5742915, which results in an amino acid change (phenylalanine to leucine: p.Phe645Leu) at codon 645 within *PML* (Albagha et al. 2011).

Therefore, 15q24 locus was investigated by target capture and sequencing of a 200 kb region surrounding the top GWAS SNP rs5742915 in 138 PDB cases

(negative for *SQSTM1* mutations and earlier age at diagnosis of PDB <65 years) and 50 controls (unaffected individuals). This region included six genes (*LOXL1*, *PML, STOML1, GOLGA6A, ISLR, ISLR2*).

4.3 Results

Targeted DNA sequencing of the chr15q24 locus was performed on DNA extracted from PDB cases and unaffected controls as described in section 3.1. My supervisor Dr. Albagha did the initial QC, variant calling and annotation and provided me with this data for further analysis. The mean coverage of target was 47X, and 98.45% of aligned bases had quality scores >20.

A total of 39 protein-coding variants (summarised in Appendix 7) and 33 potential regulatory variants (summarised in Appendix 8) were found at this locus. These included three novel protein coding variants (two in *LOXL1* and one in *PML)* and seven novel potential regulatory variants. 22 missense variants were found (5 in *LOXL1*, 13 in *PML*, 3 in *ISLR* and 1 in *ISLR2*).

Association testing of common variants was done by chi-square allelic test and rare variants were subjected to Fisher's exact test.

The top SNP rs5742915 showed highest association (P=0.004) with PDB as expected. Three other protein coding SNPs (rs34353835 in *STOML1*, rs743580 and rs743581 in *PML*) also showed significant association (P<0.05). SNPs rs5742915, rs743580 and rs743581 are missense SNPs and code for a different amino acid and therefore likely to be of functional significance. However, rs34353835 in *STOML1* is a synonymous change coding for the same amino acid and more likely to be not damaging.

Low scores in phyloP, phastCons and GERP++ (information from SNIPA browser: https://snipa.helmholtz-muenchen.de/snipa3/) indicated that all four SNPs were lowly conserved and not evolving rapidly.

Table 4.1 Three missense variants in *PML* found on Targeted sequencing with allele frequencies (AF) and predicted function.

Variant	Gene	Gene region	Type (protein variant)	AF Cases (%)	AF Controls (%)	P value	Function Prediction (SIFT/Polyphen)
rs5742915	*PML*	Exonic	Missense (F→L)	59	43	0.004	Tolerated/Benign
rs743581	*PML*	Exonic	Missense (G→V)	26	40	0.01	Benign
rs743580	*PML*	Exonic	Missense (S→G)	36	48	0.04	Benign

F(Phenylalanine), L(Leucine), G(Glycine), S(Serine) and V(Valine).

In silico analysis of the three significantly associated coding variants

All 3 missense variants were classed as tolerated and benign by SIFT and polyphen respectively. Mutation taster determined them to be probably harmless polymorphisms. All 3 SNPs were also not found to be deleterious substitutions based on information from SNIPA browser.

I-mutant (v2.0) which predicts protein stability changes based on protein sequence changes resulting from mutations, found that rs5742915 decreases protein stability with a Reliability index (RI) of 5. rs743580 too, decreases protein stability with a Reliability index (RI) of 5 whereas rs743581 increases stability but with a Reliability index (RI) of 0. Higher the RI, higher is the confidence of software in predicting protein stability.

Two SNPs in the *PML* promoter (rs79233608 and rs5742914) also showed significant association with PDB.

Table 4.2 Two regulatory variants in *PML* found on Targeted sequencing with allele frequencies (AF) and predicted function

Variant	Gene	Gene region	AF Cases (%)	AF Controls (%)	P value	Regulatory site	Regulator
rs79233608	*PML*	Promoter	8	1	0.003	Promoter Loss	GATA2
rs5742914	*PML*	Promoter/ 5'UTR	8	17	0.009	Promoter Loss/ Encode TFBS	IRF1, STAT1, SP1, SP2, STAT2

These are in the regulatory region and are predicted to result in promoter loss and/or alter transcription factor (TF) binding site. rs79233608 is associated with binding of TF GATA2 which plays an important role in haematopoietic cell differentiation whereas SNP rs5742914 is associated with binding of TF IRF1 and STAT1 both of which play an important role in bone metabolism as negative regulators of osteoclastogenesis and osteoblastogenesis (Salem et al. 2014).

Regulation spotter software classed rs5742914 as a harmless polymorphism whereas rs79233608 was determined to be functional (with much evidence) by the same software.

However, none of the SNPs was an eQTL for *PML* gene expression using publicly available expression quantitative trait loci (eQTL) data. *https://genenetwork.nl/bloodeqtlbrowser* (Zeller et al. 2010 and Westra et al. 2013) in peripheral blood as well as other tissues (*http://eqtl.uchicago.edu/cgi-bin/gbrowse/eqtl/?name=Sequence:NM_033238*)

Figure 4.1 Updated Linkage Disequilibrium (LD) plot of the 15q24.1 locus with extent of LD between the SNP rs5742915 and other SNPs in this region which were genotyped as part of 1000 Genomes Project (SNAP, Broad Institute).

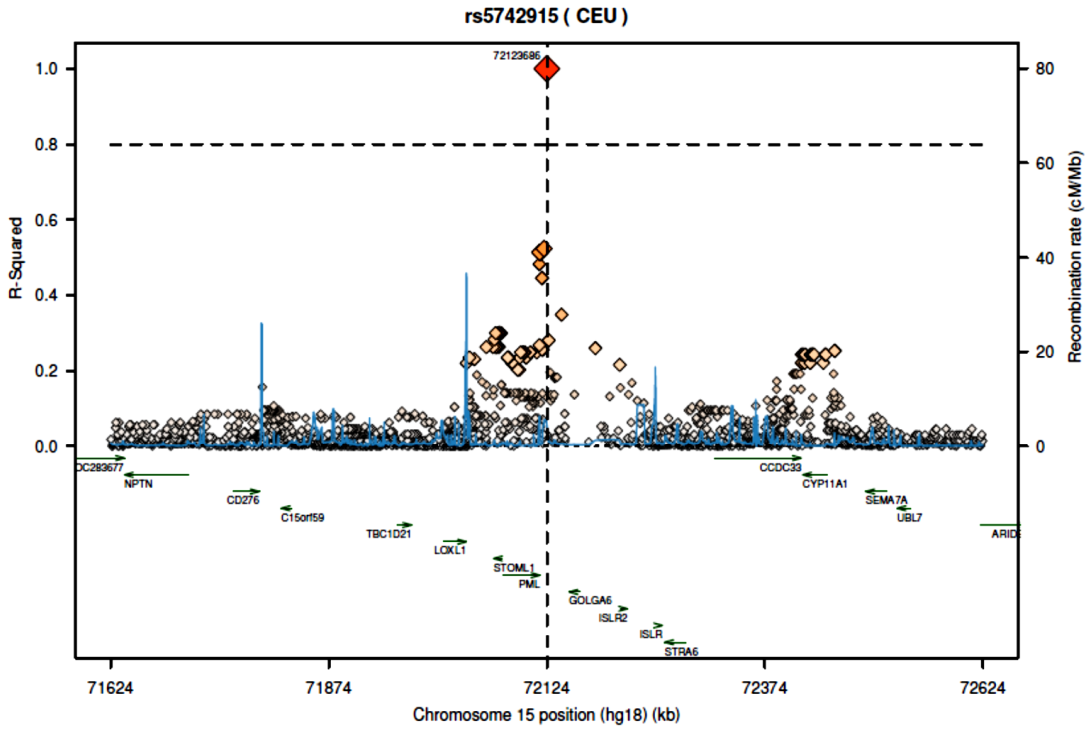

The SNP rs5742915 is in moderate LD with one of the protein coding (missense) SNP rs743580 as well as four other intronic SNPs (rs876383, rs7183908, rs752004 and rs9479) found on Targeted Sequencing. The presence of a strong recombination hotspot around 100 kb upstream of rs5742915 means the association with PDB is unlikely to extend upstream of *LOXL1*.

Thus, Targeted Sequencing analysis identified 3 missense variants (including top SNP rs5742915) and a couple of regulatory variants associated with PDB; all located within *PML* at the 15q24 locus.

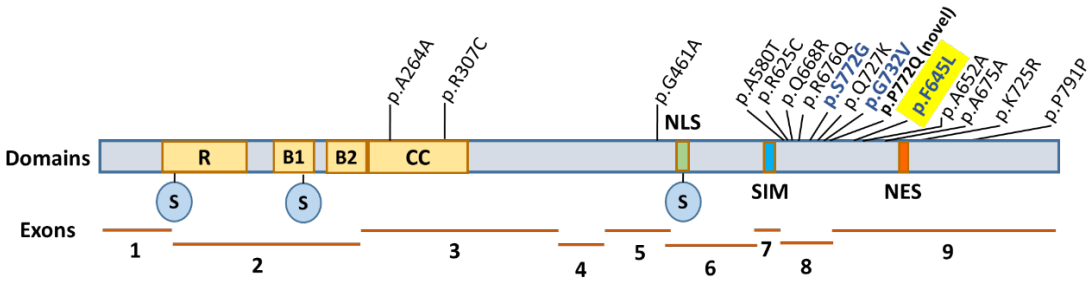

Figure 4.2 Schematic representation of coding variants found within PML on Targeted DNA sequencing in relation to various domains of PML protein.

R: RING finger; S: SUMOylation site; B1B2: B-boxes; CC: Coiled coil; NLS: Nuclear localisation signal; SIM: SUMO interacting motif; NES: Nuclear export signal.

The variants are clustered mainly in the variable C-terminal region of PML protein. The three missense variants associated with PDB are shown in blue with the most significant GWAS SNP rs5742915 (p.F645L) (which also shows highest association on targeted sequencing) is highlighted in yellow. The novel SNP (p.P772Q) is only present in controls at a very low frequency, is neither associated with PDB nor in LD with top SNP rs5742915.

The two regulatory variants rs5742914 and rs79233608 (and their possible functional role as described in this section before) are located around 120 bp and 2kb respectively upstream of exon 1 of PML within the PML promoter. DNA sequence of the promoter region surrounding the two SNPs are shown and the nucleotide change(s) associated with the two SNPs are highlighted in figure 4.3.

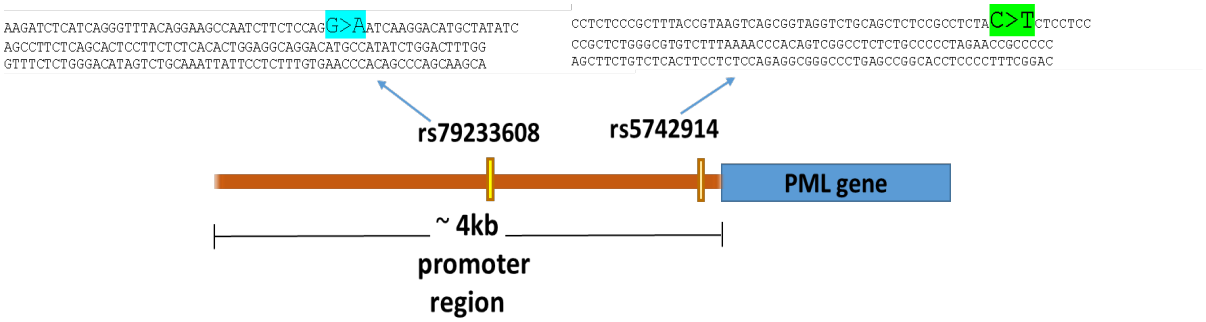

Figure 4.3 Schematic representation of two most significant PDB associated regulatory variants found within PML on Targeted DNA sequencing in relation to PML promoter.

4.4 Discussion

In genetic studies of complex disease, GWAS have resulted in identification of a number of loci associated with many diseases, however, the most significant variants that come up are common in the populations tested with mild or moderate effect size and tend to miss rare variants with larger effect size (Dickson et al. 2010; Auer & Lettre 2015). With the exception of SNP rs1561570 (*OPTN* locus) and SNP rs2458415 (*TM7SF4* locus) which were found to be strong eQTL's in peripheral blood monocytes (Zeller et al. 2010), the seven top PDB associated SNPs showed no evidence of functional significance based on bioinformatics analysis and were likely marking for other unknown true functional genetic variants (information from SNIPA browser: https://snipa.helmholtz-muenchen.de/snipa3/).

With the aim of identifying these functional genetic variants, fine mapping of one of the loci on the chr15 PDB susceptibility region resulted in identification of three nonsynonymous protein coding SNPs in the *PML* gene and two regulatory SNPs in the *PML* promoter that were associated with the disease. Thus, *PML* seems to be the most likely susceptibility gene for PDB from this locus.

PML has never been implicated directly in bone metabolism and may have a role in bone biology by regulating myeloid cell differentiation, proliferation and osteogenic differentiation of human mesenchymal stem cells, p62/autophagy and/or through its involvement in bone related pathways such as IFN-γ, NF-kB, TGF-β, and Wnt- β-catenin signalling (Wu et al. 2003; Shtutman et al. 2002; Lin et al. 2004; El Bougrini et al. 2011; Ahmed et al. 2017).

PML may indirectly influence bone metabolism since it regulates IFN-γ signalling which in turn is involved in regulating osteoclastogenesis (Choi et al. 2006; El Bougrini et al. 2011). *PML* gene itself is an Interferon responsive gene (ISG) with IFN-γ activated site (GAS) and Interferon stimulated response element (ISRE) in its promoter that mediate induction by type I and II IFNs (Chen et al. 2015). IFNs induce transcription of *PML* through activation of Janus kinase / signal transducer and activator of transcription (JAK/STAT) pathway (Guan & Kao 2015).

PML induces apoptosis through repression of the NF-kB survival pathway (Fig 4.2a), an essential pathway in osteoclast biology (Wu et al. 2003). PML sequesters NF-kB subunit RelA/p65 and suppresses NF-kB -mediated A20 transcription by preventing it from binding to the promoter of *A20*, a NF-kB target gene (Wu et al. 2002). Depletion or lack of PML may result in abnormal activation of NF-kB signalling resulting in its nuclear translocation and activation of osteoclast specific genes. This in turn shall lead to increased osteoclast differentiation and activity thereby predisposing to PDB. Apoptosis is known to be defective in osteoclasts associated with PDB, another mechanism by which PML could potentially contribute to PDB (Chamoux et al. 2009; Ralston & Layfield 2012). A more recent study found that PML promotes NF-kB activity by increased phosphorylation of NF-kB p-65 and increased NF-kB DNA binding (Ahmed et al. 2017). So it will be interesting to see how PML interacts with NF-kB in the context of bone.

Cytoplasmic PML (Isoform *PML VIIb*) is essential for TGF-β function; PML positively regulates TGF-β–signalling leading to induction of TGF-β target

genes (Lin et al. 2004) via phosphorylation and nuclear translocation of the TGF-β signalling proteins Smad2 and Smad3 (Fig 4.2b).

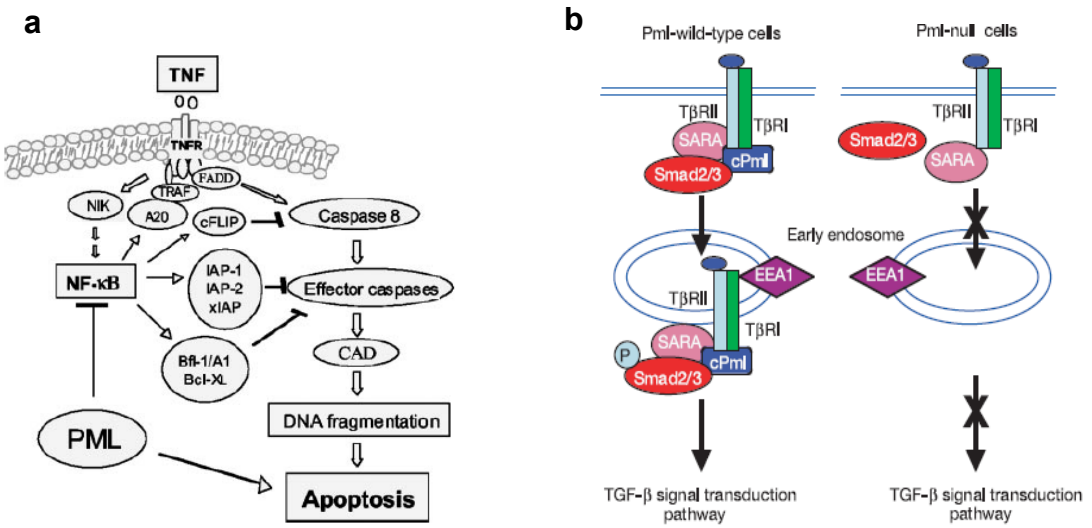

Figure 4.4 a) Schematic illustration of PML induced apoptosis by inhibition of NF-kB (Wu et al. 2003) and b) Role of PML in TGF-β Signalling (Lin et al. 2004)

Since TGF-β is known to play a role in the regulating bone remodelling (Wu et al. 2016), it is possible that TGF-β signalling might be mediating the association between PML and PDB.

PML knockout mice (*Pml*$^{-/-}$) showed a significant reduction of monocytes in peripheral blood as well as bone marrow suggesting an impairment in terminal maturation of these cells (Wang et al. 1998) possibly leading to increase in progenitor cells. Osteoclasts and their precursors are derived from cells of monocyte-macrophage lineage including precursors and alterations in *PML* may affect their development.

PML was also found to be stably expressed in human mesenchymal stem cells (hMSCs) which are the precursors of osteoblasts and its expression increased as cell osteogenic differentiation progressed. PML was found to regulate hMSCs by inhibiting their proliferation but promoting their osteogenic differentiation. *PML* overexpression resulted in increased mineralised matrix

production, ALP activity and upregulation of bone matrix gene integrin-binding sialoprotein (IBSP) (Huang 2013).

PML gene can also function as a target of WNT–β-catenin signalling pathway which in turn regulates osteogenesis of hMSCs in a complex manner (Shtutman et al. 2002). Activation of WNT–β-catenin signalling results in increased bone due to excess bone formation whereas its impairment leads to reduced bone mass as a result of bone resorption exceeding bone formation (Baron & Kneissel 2013). β-catenin induces PML expression and both proteins have been shown to colocalise in the nucleus (Shtutman et al. 2002).

IRF-8 is essential for PML induction in myeloid cells and an obligatory regulator of the *PML* gene in activated macrophages (Dror, Rave-Harel, et al. 2007). IRF8 regulates bone metabolism by suppressing osteoclastogenesis via inhibition of function and expression of nuclear factor of activated cells 1 (NFATc1), the master transcription factor for osteoclastogenesis (Zhao et al. 2009). Thus, PML may mediate the effects of IRF8 in bone metabolism.

PML is also involved in the regulation of autophagy, a novel pathway which has recently being found to be dysregulated or defective in PDB. (Pankiv et al. 2010). Pagetic osteoclasts are characterised by nuclear inclusions and these have recently been proposed to be abnormal protein aggregates in autophagy-defective osteoclasts. These osteoclasts also show abnormalities in bone resorption as a result of defect in ruffled border formation (De Selm et al. 2011). PDB is associated with genetic variants in genes such as *SQSTM1*, *OPTN* and *VCP*, all of which are involved in autophagic process. Mice with P394L *SQSTM1* mutation which develop PDB-like lesions show features associated with impaired autophagy in osteoclast precursors (Daroszewska et al. 2011). Mutations in ubiquitin binding domain of *SQSTM1*/p62, the same domain which is also involved in autophagy regulation, are associated with PDB. PML represses autophagy by inhibiting autophagosome formation. MEFs from *Pml* knockout mice showed increased LC3-II levels as well as liver and skeletal muscle of adult $Pml^{-/-}$ mice showed similar increase of LC3-II and

autophagosome biogenesis (Missiroli et al. 2017). PML is a known repressor of autophagy whereas p62 is degraded by autophagy (Pankiv et al. 2010; Missiroli et al. 2017). p62 also localises to PML nuclear bodies. p62 is responsible for the accumulation of polyubiquitinated nuclear proteins in PML nuclear bodies upon inhibition of nuclear protein export. Hein et al. 2015 have also found evidence of physical interaction between PML and p62 using Affinity-capture MS/quantitative BAC-GFP interactomics (source BIOGRID). Studies have also found p62 expression to be upregulated in Pagetic osteoclasts (Chamoux et al. 2009). As mentioned before in Chapter 1, p62 plays an important role in NF-kB signalling.

Thus, alteration in PML levels and its interaction with p62 may affect bone function by not only altering autophagy but also indirectly by influencing NF-kB signalling and osteoclast activity thereby contributing to PDB. Thus, PML may influence bone metabolism in multiple ways.

The variants identified to be significantly associated with PDB were clustered in and around *PML* but were not predicted to be deleterious or pathogenic by *in silico* methods. Nonetheless, they could still be functional since the SNP in the *SQSTM1* gene encoding p62 (leading to P392L change which is the most common change associated with classical PDB), though predicted to be benign by *in silico* tools, has been shown to be important for p62 function and equivalent mutation ($P394L^{+/+}$) in mice results in PDB-like lesions (Daroszewska et al. 2011). In the broader context, these genetic variants may serve as useful additional markers thereby improving the disease risk prediction and facilitate early diagnosis and intervention in susceptible individuals. Since the sample size for the initial study is relatively small, it will be replicated in a larger cohort of 2500 cases and results awaited to reveal the true association.

In the meantime, PML will be subjected to further investigation by expression analysis in bone cells as well as functional analysis of top GWAS SNP from the chr15 locus (rs5742915), and functional studies in cell line and animal models.

CHAPTER FIVE

PML expression during development and differentiation of bone cells

5 PML expression during development and differentiation of bone cells

5.1 Summary

Targeted DNA sequencing identified *PML* as the most likely susceptibility gene from chr 15 locus. Expression analysis of PML in two most important bone cell lineages: osteoclast and osteoblast was done from mouse as well as human tissue. PML was found to be expressed in primary bone cells (osteoblasts and osteoclasts) as well as RAW 264.7 cell line and its expression varies during the development and differentiation of these cells suggesting a possible role in bone biology. PML expression was mainly confined to nuclei in bone sections from human tissue. *PML* was downregulated in patients with PDB but the levels did not correlate with disease severity. Though the sample size was small, it does raise the possibility that reduction in *PML* expression due to genetic variation could be associated with susceptibility to PDB and lack of correlation with disease severity indicates that additional factors (both genetic and environmental) need to be present for the disease to become fully penetrant and to manifest clinically.

5.2 Introduction

PML is known to be expressed ubiquitously within the human body (Alcalay et al. 1998). Genetic variations could influence bone metabolism by altering *PML* expression levels. Therefore, PML expression was evaluated in bone cells such as osteoclasts and osteoblasts in mouse as well as human tissue. In this chapter, the expression profile of PML was investigated in Formalin-fixed paraffin embedded (FFPE) sections from human bone tissue affected by PDB and compared them with unaffected non-pagetic bone tissue. Finally, *PML* expression was studied in peripheral blood samples from PDB cases and compared to healthy controls. The cases were randomly selected and recruited from a cohort of PDB patients attending local clinic at Western general hospital, Edinburgh under Prof. Stuart Ralston's care. Controls were healthy individuals (either spouse or relative) of Paget's patients. Blood was taken from consented individuals, PBMCs isolated, RNA extracted, converted to cDNA and PML expression analysed using qPCR.

5.3 Results

5.3.1 PML is expressed in bone cells from mouse as well as human tissue

5.3.1.1 PML is expressed during osteoclast development in mouse tissue

Bone marrow cells isolated from wild type C57Bl6 mice were cultured in presence of M-CSF and RANKL until osteoclasts were formed as described in section 3. RAW 264.7 cells were treated with RANKL until osteoclasts were formed. PML expression was determined using western blot analysis.

PML was expressed in mouse monocyte-macrophage cell line RAW 264.7 as well as primary bone marrow derived macrophages (BMDM) and at all stages during their differentiation to osteoclasts following stimulation with RANKL. PML expression was found to increase during osteoclast formation (Fig. 5.1 a,b and 5.2 a,b)

a

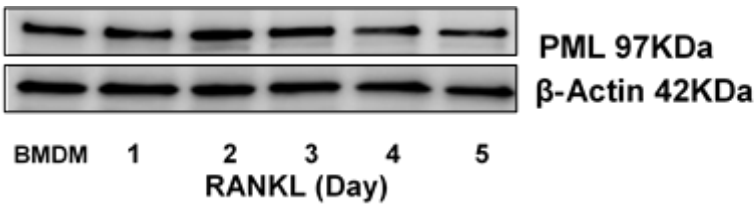

b

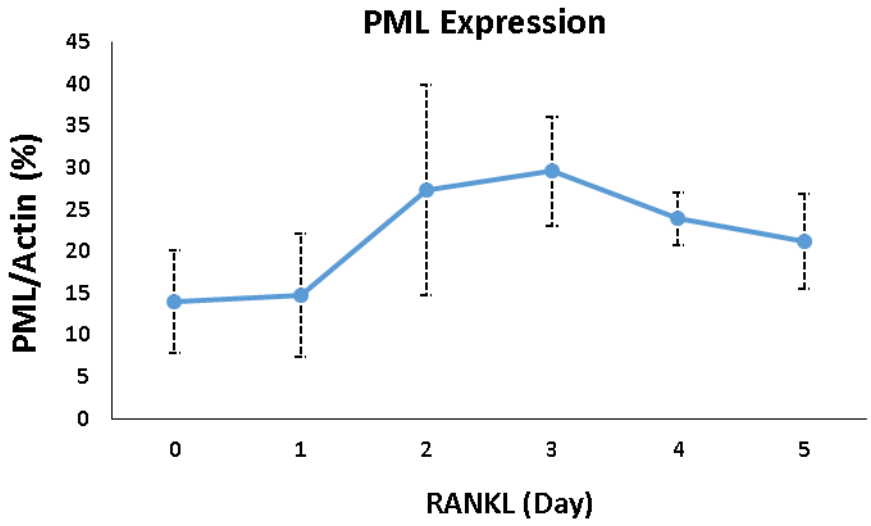

Figure 5.1 PML protein expression during osteoclast differentiation in mouse BMDMs.

a: Immunoblot showing Pml and β-actin protein expression from BMDMs before and after treatment with RANKL (Day1-5), b: PML levels expressed as a ratio of PML/β-actin. Values are means ± SEM (combined data) from three independent experiments (biological replicates).

a

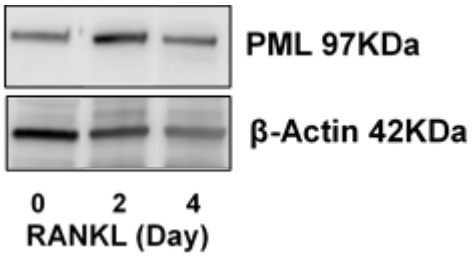

b

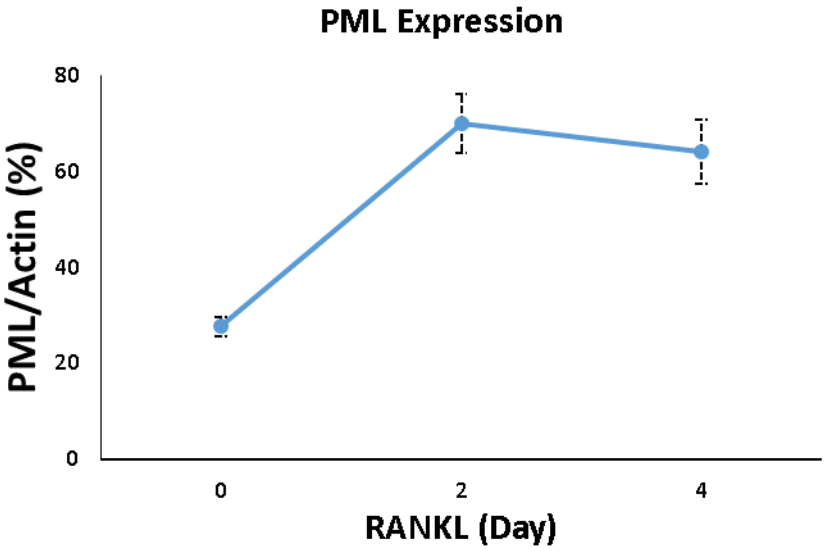

Figure 5.2 PML protein expression during osteoclast differentiation in RAW cell line.

a: Immunoblot showing Pml and β-actin protein expression from RAW cells before and after treatment with RANKL (Day 2 and 4), b: PML levels expressed as a ratio of PML/β-actin. Values are means ± SEM (combined data) from two independent experiments. PML expression increased during osteoclast formation.

5.3.1.2 PML protein is expressed during osteoblast development in mouse tissue

Osteoblasts grown from calvaria of 2-4 day old wild type C57Bl6 mice were cultured for up to 18 days in osteogenic medium until mineralisation. PML expression increased during the first week of osteoblast differentiation in calvarial osteoblasts and stabilises to basal levels soon after until bone nodule formation (Fig. 5.3 a,b).

a

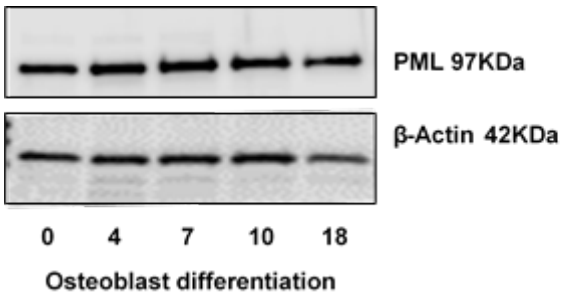

b

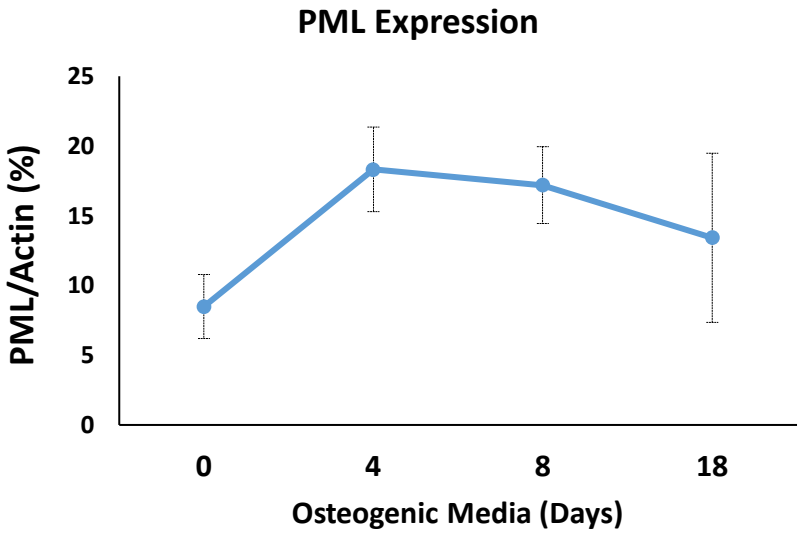

Figure 5.3 PML protein expression during osteoblast development.
a: Immunoblot showing PML and β-actin protein expression from murine osteoblasts b: PML levels expressed as a ratio of PML/β-actin. Values are means ± SEM (combined data) from three independent experiments. PML

expression increased during the first week of osteoblast differentiation in calvarial osteoblasts.

5.3.1.3 PML is expressed in bone cells of human origin

Formalin-fixed paraffin embedded (FFPE) sections from unaffected and pathological human bone tissue were subjected to Immunohistochemistry (IHC) using standard protocol (as described in Appendix 4).

Initial optimisation of PML immunostaining was done on Tissue microarray (TMA) using different concentrations of the sc-5621 (H-238) PML antibody. Since PML is ubiquitously expressed, negative controls were performed by omitting addition of PML primary antibody during IHC. The optimised antibody concentration of 1:200 was then used for staining human bone tissue sections. Positive control used for osteoclast staining was Giant cell tumour of bone or osteoclastoma and negative control comprised bone sections with non-addition of primary antibody. PML was detected in human osteoclasts as well as osteoblasts.

Panel A in Fig. 5.4 shows negative and positive PML immunostaining at low and high power magnification (10X and 20X respectively) and includes negative (no primary antibody) and positive PML immunostaining (from TMA as well as benign bone tumour osteoclastoma). Panel B in Fig. 5.4 shows 40X magnification images (negative and positive PML immunostaining) in osteoclasts from bone sections (unaffected as well as pathological bone tissue).

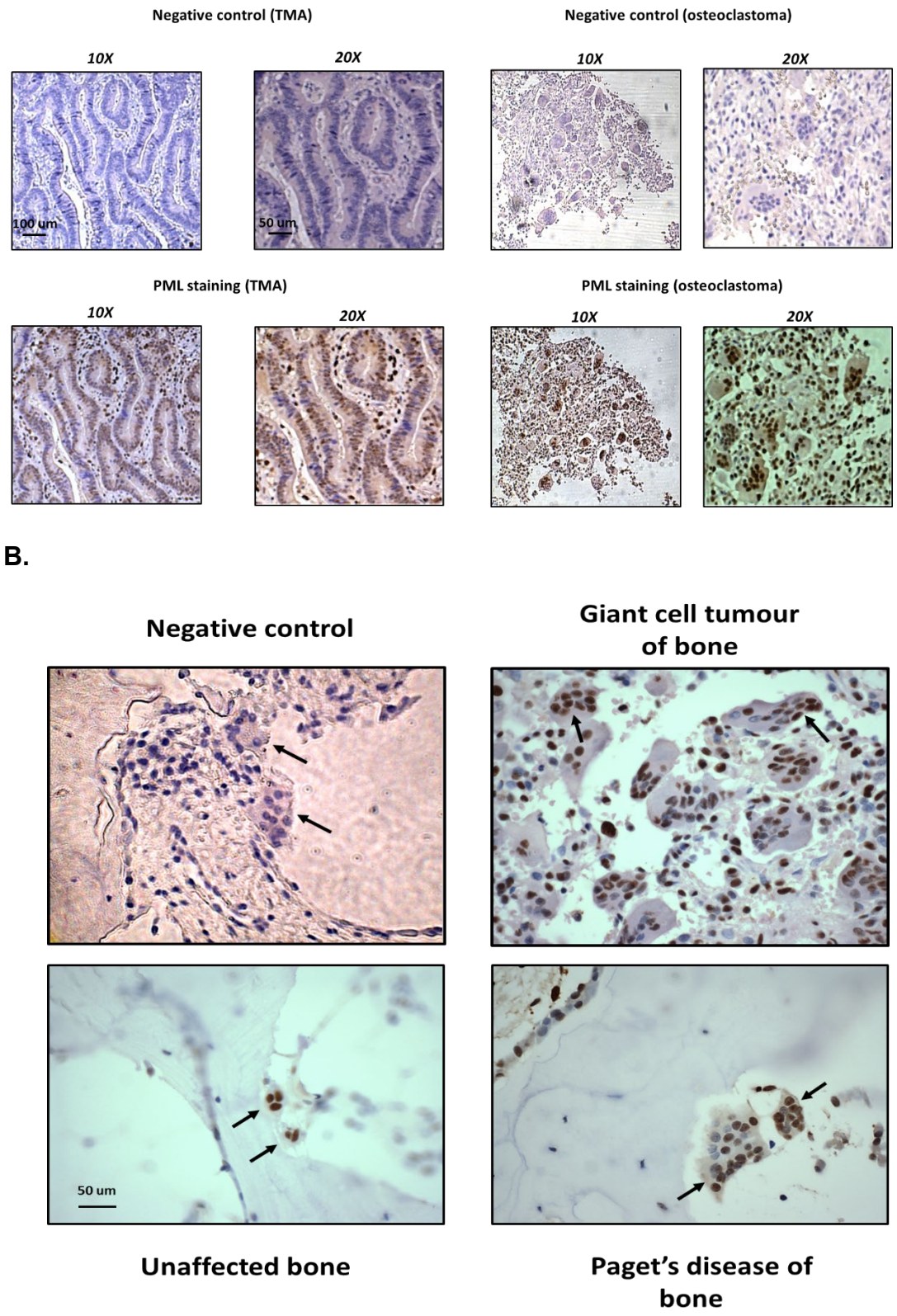

Figure 5.4 Detection of Pml in tissue sections using Immunohistochemistry.

A. Low and high magnification images of negative (no antibody added) and positive PML antibody (brown colour) immunostaining in TMA and FFPE sections of osteoclastoma.

B. Negative control (No antibody added) and positive nuclear immunostaining (brown colour) for PML in human osteoclasts from FFPE bone sections.

It can be seen in the figure 5.4 that the PML expression (brown staining) is mainly nuclear with variability in intensity of staining. In panel B, some osteoclasts (nuclei) are positive whereas others are negative for staining. It is also clear that osteoclast size is smaller and number fewer in unaffected bone compared to those in PDB and GCT.
These analyses show that PML is expressed in bone cells and its expression varies during the development and differentiation of these cells.

5.3.1.4 *PML* expression is downregulated in PDB patients

Next, we investigated *PML* expression in mRNA derived from peripheral blood samples of PDB patients (n=18) compared to healthy controls (n=7).

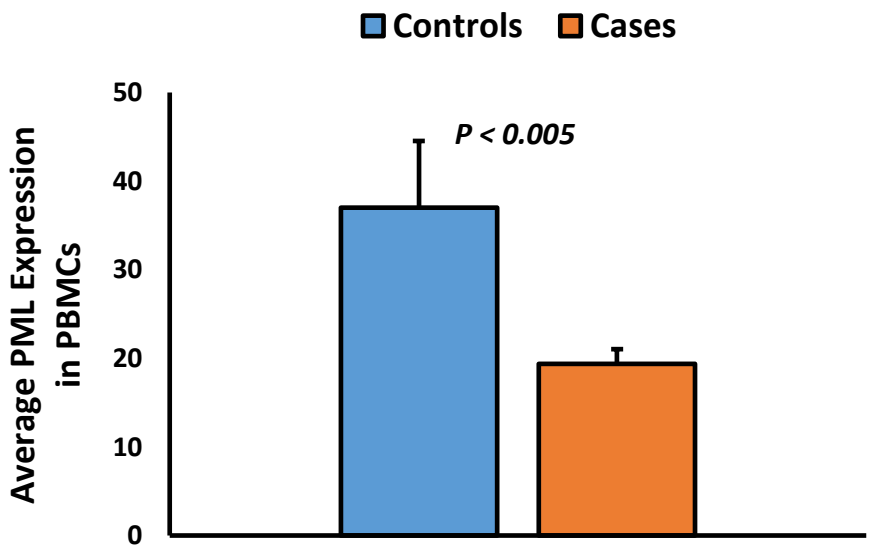

Figure 5.5 *PML* expression in PDB patients is significantly lower compared to unaffected controls.

Data are shown as mean ± SEM. RNA from blood (PBMC's) stored in RNA later was extracted and converted to cDNA. mRNA levels were assayed by qRT-PCR and normalised for 18S rRNA.

qPCR analysis found that the *PML* expression in PDB cases was 48% lower compared to unaffected controls (P = 0.003) (Fig. 5.5).

Next, a composite disease severity score was computed and tested to see if PML expression levels correlated with disease severity scores. Clinical data was incomplete or not available for a couple of cases. However, no correlation was found (P = 0.229) as shown in Figure 5.6. The score was computed by taking into account various clinical features and complications of the disease such as previous fractures through Pagetic bone, previous orthopaedic surgery for PDB, history of osteosarcoma, use of a hearing aid in patient with PDB of the skull, bone deformity, bisphosphonate treatment in the previous 12 months, bisphosphonate treatment >12 months ago, and age at PDB diagnosis.

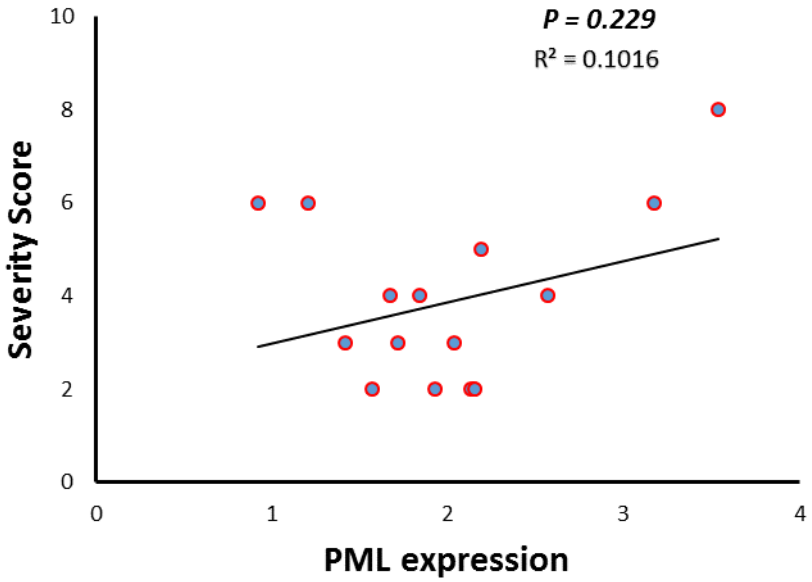

Figure 5.6 Scatter plot showing correlation between PML expression and disease severity score.

5.4 Discussion

PML was found to be expressed in mouse primary bone cells (osteoblasts and osteoclasts) as well as RAW 264.7 cell line. PML expression increased during osteoclast differentiation in both RAW cell line and primary BMDMs and was highest in the intermediate stages of development (Day 2-3). Though the increase is not so evident in BMDMs due to high error bars when data was combined from three biological replicates, individual replicates did show the trend for increased expression as osteoclast differentiation progressed. Indeed, RNA-sequencing analysis of primary BMDMs also shows the same pattern of Pml expression when differentiated into osteoclasts in response to RANKL in three independent biological mouse replicates (data not shown).

PML is subjected to alternative splicing in its C-terminal region leading to a number of isoforms. Expression analysis in cells of the monocyte-macrophage lineage (i.e. RAW 264.7 which is a mouse monocyte-macrophage like cell line and primary osteoclasts derived from macrophage-monocyte precursors), however, revealed only a single 97 KDa protein corresponding to PML-I isoform. This is consistent with findings from Condemine et al. 2006 who showed that PML-I is the most abundant isoform in macrophages and isoform specific sequences of PML-I and PML-V are highly conserved between human and mouse. Dror et al. 2007 subsequently confirmed these findings and found PML-I to be the major splice variant in activated macrophages and their study pointed to an interaction of PML-I (in response to IRF-8) with AML-1 resulting in differentiation of myeloid progenitor cells to monocytes.

In calvarial osteoblasts, PML expression increased during the first week of differentiation and then decreased to basal levels when bone nodules formed. Thus, PML expression varies during the development and differentiation of these bone cells pointing to a possible role in bone metabolism.

This is consistent with the previous findings that PML is expressed during osteogenic differentiation of hMSCs into osteoblasts and subsequent mineralisation (Huang 2013). Moreover, changes in PML expression alter the

differentiation potential of osteoblasts and in the case of monocytes, a reduction in their number (Wang et al. 1998).

In FFPE samples, PML expression was mainly restricted to nuclei in osteoclasts. The intensity of nuclear staining showed variability within the osteoclast. This could be attributed to the different stages in the life cycle of the osteoclast. It could also result from differences in age and level of activity of osteoclasts as well as their proximity to the eroding bone surface. However, it is difficult to verify or confirm this unless we analyse a lot of samples and also possibly due to the heterogeneity of the tissue within a pagetic bone as well as artefacts resulting from processing of bone tissue.

PML expression was found to be downregulated in patients with PDB. This raises the possibility that genetically determined reduction in *PML* expression could be associated with susceptibility to PDB. It is possible that the reduced expression of *PML* in PDB patients results in increased osteoclast formation and size which is one of the pathological characteristics of PDB. However, there was no correlation between *PML* expression levels and PDB severity. This indicates that additional factors (genetic as well as environmental) need to be present for the disease to become fully penetrant and to manifest clinically. However, the lack of correlation could also result from the fact that our sample size was small and increasing the size of the cohort may make the correlation stronger. It will also be interesting to test individual features (both clinical as well as disease complications) for correlation with *PML* expression levels in a larger cohort.

CHAPTER SIX

Effect of PML on osteoclast function *in vitro*

6 Effect of PML on osteoclast function *in vitro*

6.1 Summary

PML was found to be expressed in osteoclasts, the main bone cell type affected in PDB and its expression varies during the development and differentiation of these cells. The effect of altered *Pml* expression on osteoclast function *in vitro* was tested using overexpression and knockdown experiments in RAW 264.7 cell line. Also, functional analysis of top GWAS SNP rs5742915 which was also found to be the most significant PDB associated protein coding variant by targeted DNA sequencing analysis, was performed by overexpressing it and assessing osteoclast development in RAW 264.7 cell line.

Pml overexpression inhibited osteoclast formation and fusion whereas downregulation by arsenic trioxide promoted osteoclast formation and fusion pointing to a negative regulatory role of PML in osteoclast differentiation. Arsenic is used in chemotherapy of APL and though it has some degree of toxicity against other cell proteins, its action on PML leading to degradation confirmed the suppressive role of PML in osteoclast differentiation.

Overexpression of SNP rs5742915 in RAW 264.7 cell line resulted in a more marked reduction in osteoclast formation and fusion compared with WT and empty vector control. Thus, contrary to expectation, it appears to suppress osteoclast differentiation and inhibit bone resorption rather than facilitate the disease progression. This phenotype could be due to various factors and may not necessarily mimic the physiological conditions possibly due to testing of SNP in isolation, high level of artificial overexpression achieved *in vitro* as well as influence of polygenic/environmental factors in an *in vivo* setting. Nonetheless, rs5742915 is a functional variant in the context of PDB.

6.2 Introduction

Fine mapping revealed a few protein coding and regulatory variants within *PML* to be associated with PDB at the chr15 locus. This led to *PML* being the most likely gene predisposing to PDB at this locus. Next, *PML* was found to be expressed in primary bone cells (osteoblasts and osteoclasts) as well as RAW 264.7 cell line and its expression varied during the development and differentiation of these cells. Notably, *PML* was found to be downregulated in patients with PDB leading to the hypothesis that genetically determined reduction in *PML* expression could result in alteration to bone metabolism or turnover leading to increased susceptibility for PDB. Osteoclast is known to be the main cell type involved in PDB pathogenesis. This chapter therefore focusses on studies to assess the effect of altered PML expression on osteoclast function *in vitro* using overexpression and knockdown experiments in RAW 264.7 cell line.

In addition, the effect of p.Phe645Leu resulting from rs5742915 was assessed in murine tissue during osteoclast development by functional assay. rs5742915 lies at the start of Exon 9 in the C terminal region of *PML* and therefore exists only in *PML* isoform 1. It was the only protein coding SNP among the seven top GWAS PDB associated hits and was also the most highly associated SNP from chr 15 locus in the Targeted sequencing cohort resulting in a missense amino acid change from phenylalanine to leucine at codon 645 (p.Phe645Leu).

6.3 Results

6.3.1 Plasmid preparation, verification and transfection optimisation of *Pml* overexpression plasmids

RAW cells (a mouse monocyte-macrophage-like cell line that differentiates into osteoclasts on RANKL treatment) were transfected with GenEZ PML ORF expression plasmid or empty vector.

Transfection optimisation was done as described in section 3.4.5.

In all combinations tested, GFP was not expressed at 4hrs post transfection but significantly increased at 24 hrs post transfection (Fig 6.1).

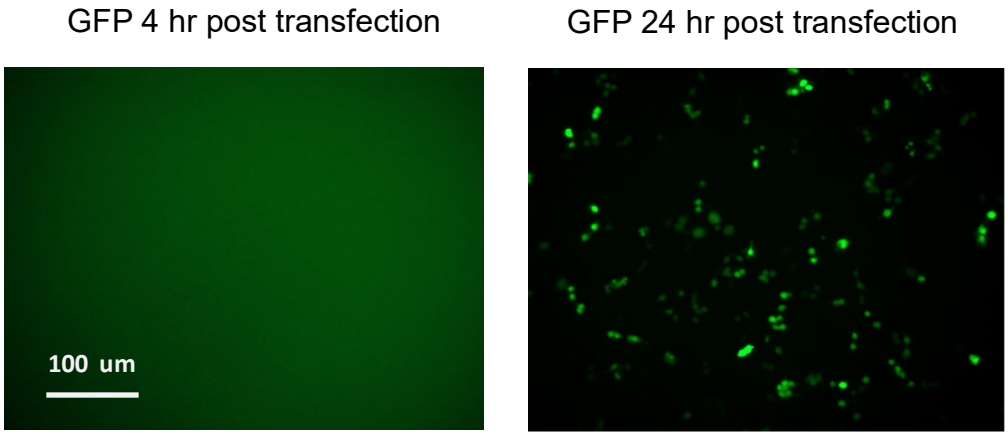

Figure 6.1 EGFP fluorescence 4 hr and 24 hr post transfection with jetPEI reagent in RAW cells.

GenEZ PML Open reading frame (ORF) expression plasmid DNA from Mouse: OMu22116 (WT as well as carrying the GWAS single base change T to C) and empty vector DNA (pcDNA3.1) were obtained from Genscript, transformed into DH5 alpha E. coli cells (details in Methods section 3.9.1) and colony minipreps done to obtain plasmid DNA followed by restriction digest (details in Methods section 3.9.2). Sanger sequencing was also performed to confirm presence of PML ORF WT as well as the missense change associated with SNP rs5742915 (T to C).

Sanger sequencing revealed the WT sequence as well as expected nucleotide change (T>C) in the ORF plasmid corresponding to rs5742915. Part of PML ORF sequence from Genscript clone WT OMu22116 with nucleotide change highlighted in red and primers for PCR-sanger sequencing highlighted in blue are shown below.

TGACAATGAA**ACCCAGAAAATTAGCCAGCTG**GCCGCGGTGAACCGGGAAAGCAAGTTCCGTGTGC

TCATCCAGCCCGAGGCC**T>C**TCAGTGTCTACTCCAAAGCTGTCTCCCTGGAGGCGGGGCT

CCGGCACTTCCTCAGCTTCCTCACCAC**CATGCACCGTCCCATCTTG**GCGTGTTCTAGGCTGTGGG

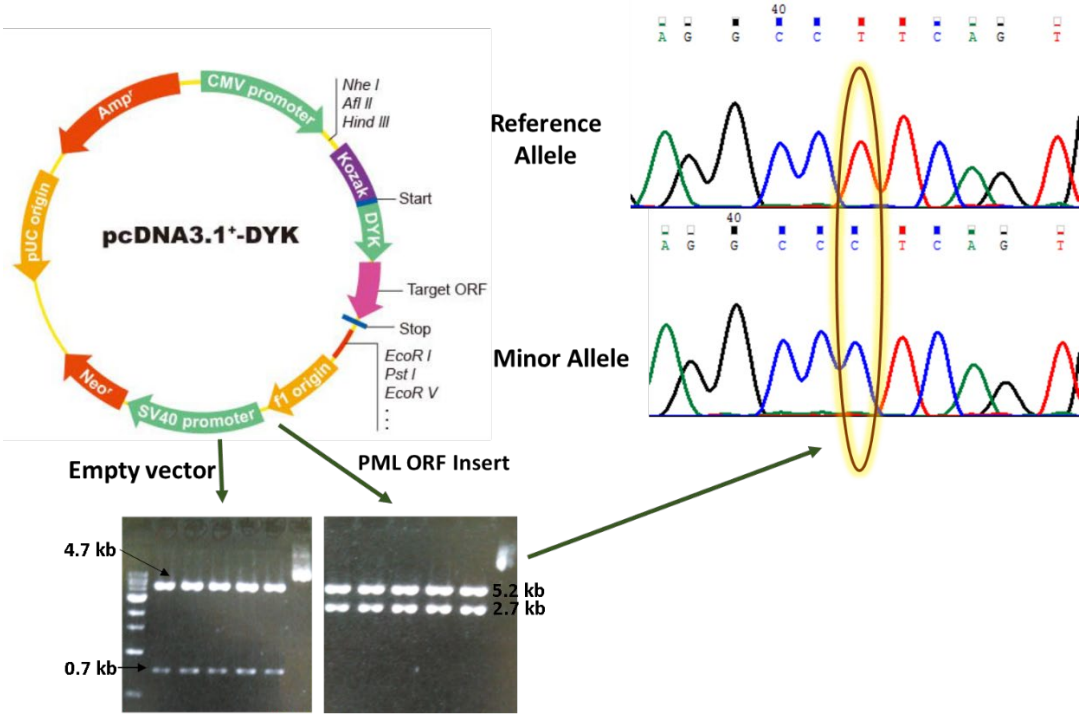

Figure 6.2 Schematic representation of PML ORF verification by restriction enzyme digest and Sanger sequencing.

PML ORF plasmid double digest gave band sizes of 2.7kb and 5.2Kb whereas empty vector double digest gave band sizes of 4.7kb and 0.7kb.

6.3.2 Effect of *Pml* WT overexpression on osteoclast development in RAW 264.7 cell line

The last combination from Table 3.3 in Methods section was chosen since it gave good GFP expression post transfection during optimisation and also satisfied the downstream cell requirements. Accordingly, RAW cells were seeded at a density of 1.5 million cells per T25 flask and transfected with 6ug of GenEZ PML ORF expression plasmid DNA (OMu22116-Genscript) or empty vector DNA (pcDNA3.1) using jetPEI. Cells were transiently selected with neomycin (500ug/ml) for 4 days and stimulated with RANKL (100 ng/ml) for 4 days to generate osteoclasts. Cells were TRAcP stained and TRAcP positive multinucleated cells (TRAcP + MNC) were counted and numbers were compared to the WT control after correction for cell viability.

Pml WT overexpression was verified by qPCR as well as western blot (Fig. 6.3 b,a).

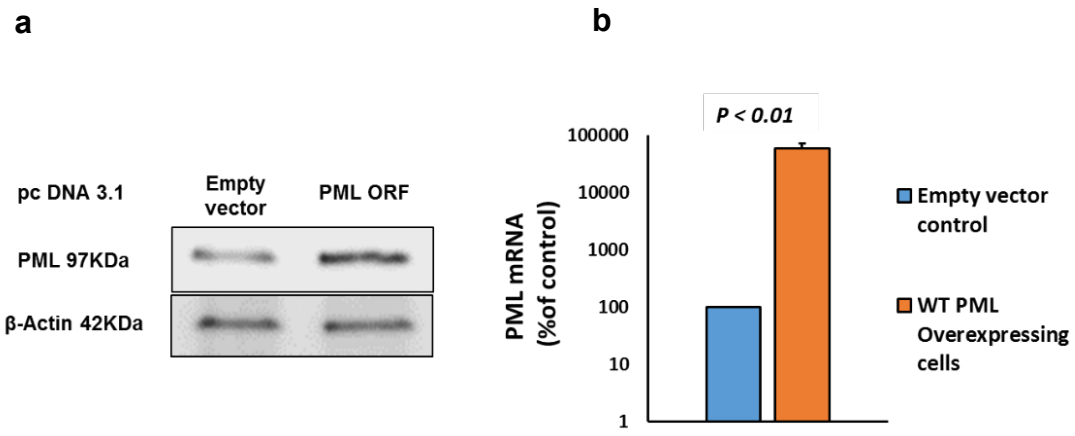

WT *Pml* overexpression in RAW cells resulted in a significant reduction in number and size of osteoclasts compared to empty vector control (Fig. 6.3 c,d)

c

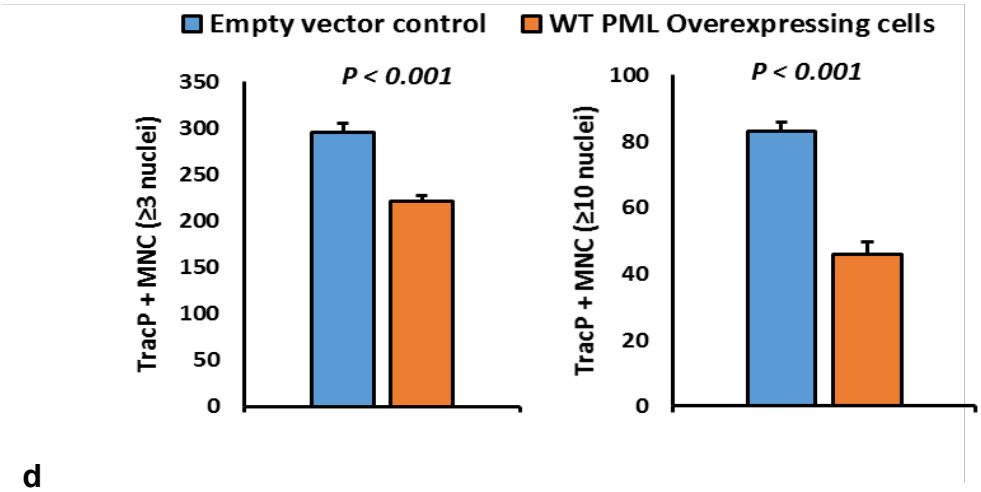

d

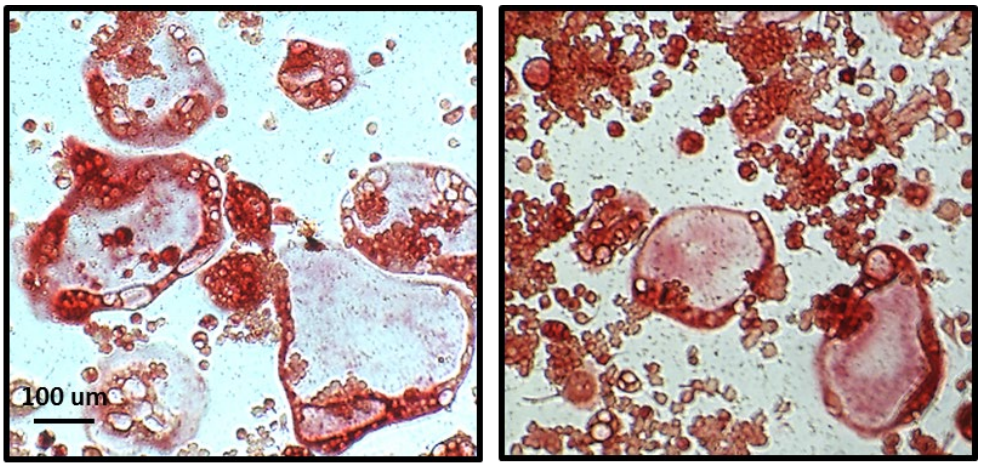

Figure 6.3 Overexpression of WT *Pml* in RAW cells reduces their ability to form TRAcP+ multinucleated (MNC) cells upon stimulation with RANKL.

a. Immunoblot showing expression of *Pml* and β-actin in cell lysates from RAW cells transfected with PML ORF expression plasmid compared with Empty vector.

b. *PML* mRNA expression in cells overexpressing *Pml* (orange bar) compared to control cells (blue bar). mRNA levels were assayed by qRT-PCR and normalised for 18S rRNA and presented as % of control cells. Values are

means ± SEM (data presented from one biological replicate) representative of three independent experiments.

c. Decreased number of TRAcP+ MNC - osteoclasts (≥3 nuclei) or hypernucleated MNC (≥10 nuclei) generated from RAW cells overexpressing *Pml* compared to control cells. Values are means ± SEM (data presented from one biological replicate) representative of three independent experiments. Minimum 6 wells were counted for each biological replicate.

d. TRAcP staining showing reduction in size and number of osteoclasts in *Pml* overexpressing cells compared to control cells.

6.3.3 Effect of *Pml* knockdown on osteoclast development in RAW 264.7 cell line

Arsenic trioxide is an inorganic compound that degrades PML and is used in the treatment of acute promyelocytic leukaemia (APL), a disorder caused by disruption of tumour suppressor PML. Arsenic is known to downregulate *Pml* (Zhu et al. 1997; Lallemand-Breitenbach et al. 2008). Accordingly, RAW cells were treated with arsenic trioxide for 24 hrs at various concentrations prior to starting RANKL and effect on osteoclast development was assessed.

Pml downregulation was achieved at 25um arsenic concentration as verified by Western blot (Fig. 6.4) and resulted in a significant increase in number and size of osteoclasts compared to vehicle PBS (Fig. 6.5 a,b).

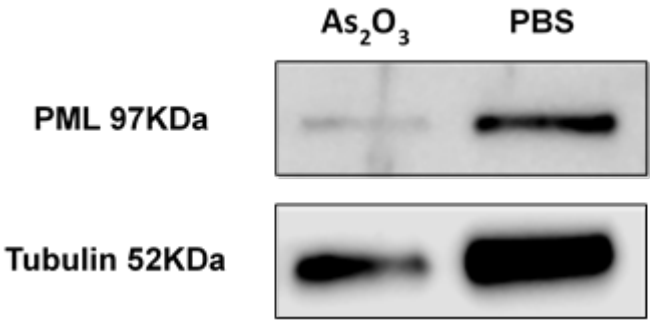

Figure 6.4 PML protein degradation was achieved with arsenic trioxide (As2O3) at 25um concentration as shown using Western blot.

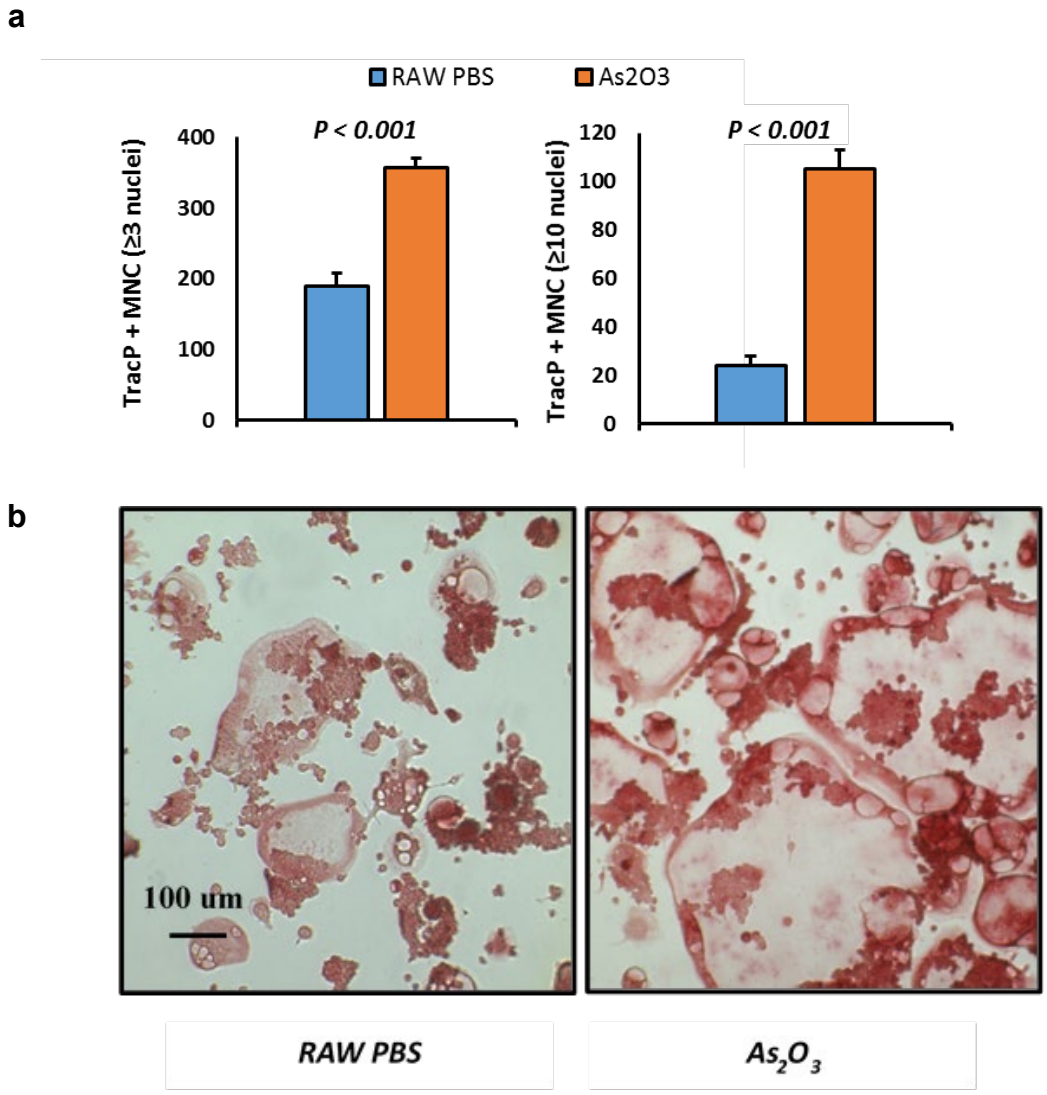

Figure 6.5 Pml downregulation in arsenic treated RAW cells enhances osteoclast formation and fusion.

a. Increased number of TRAcP+ MNC - osteoclasts (≥3 nuclei) or hypernucleated MNC (≥10 nuclei) generated from arsenic treated RAW cells compared to control cells. Values are means ± SEM (data presented from one biological replicate) representative of three independent experiments. Minimum 6 wells were counted for each biological replicate.

b. TRAcP staining showing increase in size and number of osteoclasts in arsenic treated RAW cells compared to control cells.

Cellular fusion is essential for osteoclasts to effectively resorb bone. DC-STAMP plays a key role in this fusion. Expression analysis of *Dcstamp* in arsenic treated RAW cells revealed a significant increase especially on Day 4 following RANKL treatment compared to WT RAW control (Fig. 6.6).

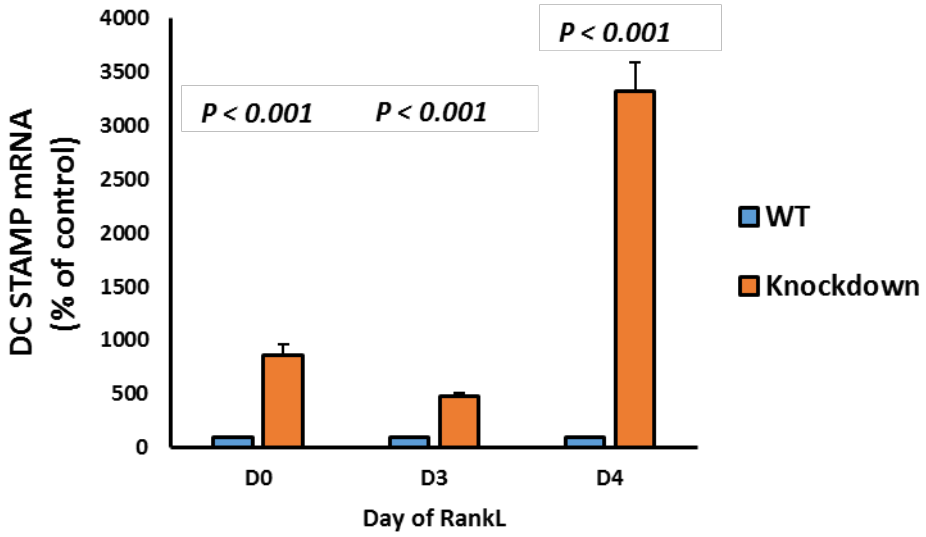

Figure 6.6 Expression analysis of *Dcstamp* mRNA by qPCR during osteoclast development in Arsenic treated RAW cells.

Reveals a significant increase especially on Day 4 following RANKL treatment compared to WT control. Values are means ± SEM (data presented from one biological replicate) representative of two independent replicates presented as % of WT.

6.3.4 Effect of SNP rs5742915 overexpression on osteoclast development in RAW 264.7 cell line

Similar to WT PML ORF, RAW 264.7 cells were transfected with GenEZ PML ORF expression plasmid (carrying the GWAS single base change T to C) or empty vector (pcDNA3.1) and transiently selected for 3-4 days with 500ug/ml neomycin and stimulated with RANKL (100 ng/ml) for 4 days. Cells were TRAcP stained and TRAcP positive multinucleated cells (TRAcP + MNC) were counted.

Pml overexpression was determined using qPCR (Fig. 6.7).

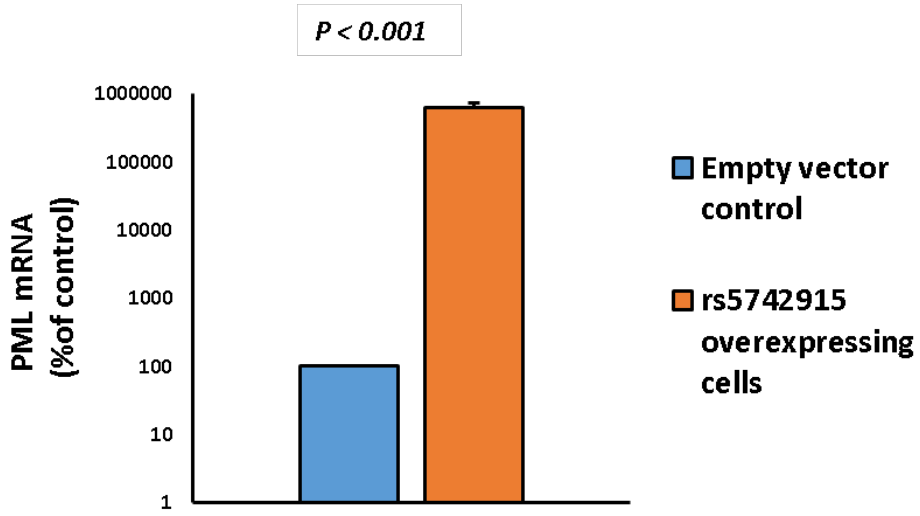

Figure 6.7 PML mRNA expression in cells overexpressing *PML* GWAS SNP (orange bar) compared to control cells (blue bar).

mRNA levels were assayed by qRT-PCR and normalised for 18S rRNA and presented as % of control cells. Values are means ± SEM (data presented from one biological replicate) representative of three independent experiments.

Overexpression of GWAS SNP resulted in a more marked reduction in osteoclast formation and fusion compared to WT PML ORF (Fig 6.8 a,b).

a

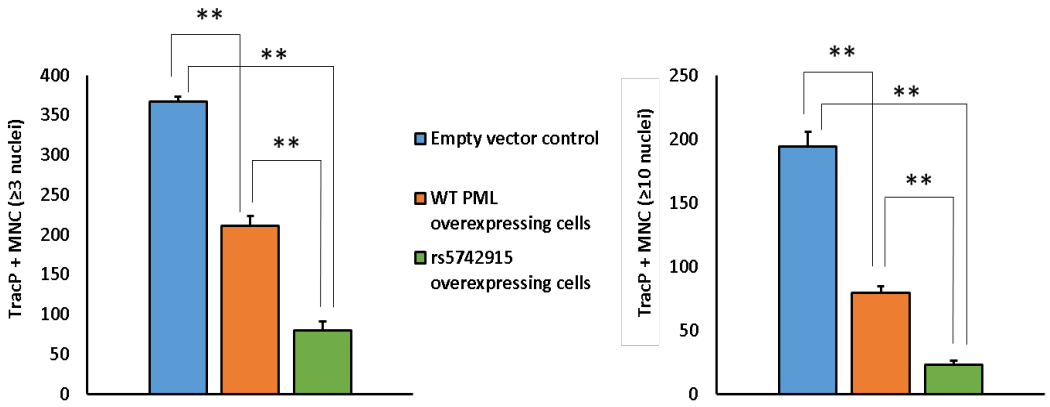

b

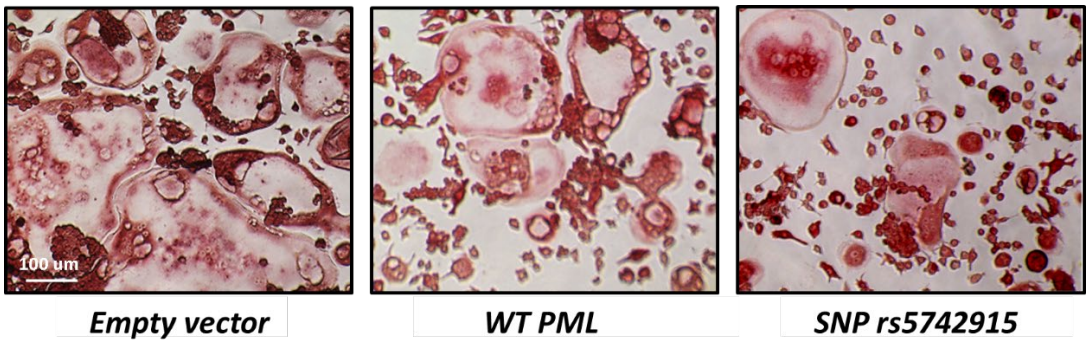

Figure 6.8 Overexpression of SNP rs5742915 in RAW cells reduces their ability to form TRAcP+ multinucleated (MNC) cells upon stimulation with RANKL.

a. Decreased number of TRAcP+ MNC - osteoclasts (≥3 nuclei) or hypernucleated MNC (≥10 nuclei) generated from RAW cells overexpressing SNP rs5742915 (green bar) compared to WT *Pml* (Orange bar) and empty vector control (blue bar) cells. Values are means ± SEM (data presented from one biological replicate) representative of three independent experiments. **p<0.0001. Minimum 6 wells were counted for each biological replicate.

b. TRAcP staining showing reduction in size and number of osteoclasts in *Pml* SNP rs5742915 overexpressing cells compared to WT and empty vector control cells.

6.4 Discussion

PML expression was evident in bone cells and downregulation of this gene was found in PDB patients compared to controls. This led to examining the effect of altered PML expression on the development and function of osteoclast, the main bone cell type involved in PDB. The experiments were performed by modifying *Pml* expression levels in RAW 264.7 cell line *in vitro* and noting its effect on osteoclast differentiation and development.

Pml overexpression *in vitro* in RAW 264.7 cell line inhibited osteoclast formation and fusion whereas downregulation by arsenic trioxide promoted osteoclast formation and fusion. These findings indicate that PML plays a role in bone metabolism as a negative regulator of osteoclast differentiation.

It is known that arsenic is a toxic compound and has non-specific effects on other proteins. This was evident from the degradation of tubulin in the western blot (Figure 6.4). It is known to alter the function of steroid receptors e.g. estrogen receptor as well as affects several interleukins and cytokines either turning them off or on leading to alterations in osteoclast differentiation and activity. Its effects are, however, known to be more pronounced in human cells compared to animal cells of non-bone origin (Lever 2002). The dose of arsenic trioxide that was needed to achieve knockdown of PML *in vitro* was much higher than that used in a clinical setting for APL treatment and was probably because RAW cells (monocyte-macrophage-like cell line) were resistant to lower doses of arsenic. Interestingly, arsenic as a pesticide in imported cotton has been suggested to be an environmental risk factor for PDB development in high prevalence area of cotton mill towns in Lancashire in 1970's (Lever 2002). More importantly, however, arsenic is also known to degrade PML (Zhu et al. 1997; Lallemand-Breitenbach et al. 2008) and is therefore also used in chemotherapy of APL. The degradation of PML was verified in my downregulation experiment and arsenic was found to promote osteoclast differentiation.

This downregulation was achieved by chemical means via proteasomal degradation of PML. Also, arsenic at higher doses is known to affect cell viability and induce apoptosis in various cell types. Other methods of downregulation such as lentiviral shRNA mediated gene knockdown or CRISPR mediated gene editing would be less toxic and more specific but need more optimisation and are costly as well as more labour-intensive and would have been counterintuitive since arsenic mediated downregulation along with wt Pml overexpression data had given adequate information needed to justify getting a full PML knockout mouse model for *in vivo* assessment of PML depletion on bone metabolism.

p.Phe645Leu change associated with the SNP rs5742915 is predicted to be tolerated by SIFT and benign by Polyphen and is not highly conserved through evolution (Fig 6.9).

This means there could be other variants driving the association with PDB risk and the SNP rs5742915 is simply tagging for these or in LD with the causal SNP(s). Nonetheless, it could still be a risk associated variant since bioinformatics tools do not always provide correct functional prediction. As mentioned before, the *SQSTM1* P392L mutation, which is known to cause PDB in humans, is predicted by bioinformatics tools to be benign but functional studies have showed this variant to be pathogenic and cause PDB-like disorder in mice ($P394L^{+/+}$) (Daroszewska et al. 2011).

Though the *PML* SNP rs5742915 is not highly conserved, this may not be so relevant in context of PDB which is a late onset disorder and does not affect reproduction. Thus, rs5742915 may still affect osteoclast though not highly conserved. Moreover, rs5742915 was one of the 697 variants which achieved genome-wide significance in relation to polygenic trait of adult human height in large scale GWAS studies. (Lango et al. 2011; Wood et al. 2014), indicating a possible effect on bone growth.

Figure 6.9 Conservation of rs5742915 across various species using Ensembl phylogenetic information.

Overexpression of *Pml* carrying the GWAS SNP rs5742915 risk allele (C) resulted in a more marked reduction in osteoclast formation and fusion compared with cells overexpressing the WT PML (reference allele T) and control empty vector cells. Thus, rs5742915 is a functional variant in context of PDB. The C allele is present at a higher frequency in cases compared to controls in the initial targeted sequencing cohort. Interestingly, however, it appears to protect against PDB rather than facilitate the disease progression by inhibiting osteoclast development.

This could be due to various factors. The SNP on its own may be functional in murine cell line with a protective phenotype but the function in a physiological setting may be influenced/altered by presence of surrounding SNPs (haplotype). Moreover, the overexpression levels achieved in such experiments may not accurately reflect the levels in a physiological setting and the control of gene expression and its effects could be more subtle than achieved in these *in vitro* studies.

Also, the net effect on PDB development or susceptibility may be modified by presence of other risk alleles involving multiple genes in an individual as well

as influenced by environmental factors highlighting once again the incomplete penetrance and the complex interplay between genetic and environmental triggers in complex disease evolution such as PDB.

The *in vitro* studies have therefore acted as a proof of concept or pilot experiment to confirm the osteoclast phenotype in relation to PML prior to investing more time and effort in sourcing *Pml* knockout mice to confirm and explore the initial findings in RAW cells. Studies in *Pml* knockout mice will throw further insights into the role of PML in bone metabolism and is discussed in detail in next chapter.

CHAPTER SEVEN

Explore role of PML in bone metabolism using knockout mouse model of PML

7 Explore role of PML in bone metabolism using knockout mouse model of PML

7.1 Summary

The role of PML in bone remodelling *in vivo* was investigated by using a mouse knockout model of PML. *Pml* $^{-/-}$ mice not only exhibited increased osteoclast formation and fusion similar to *in vitro* findings, but also showed increased activity and survival compared to WT *ex vivo*. Osteoclast related genes such as *Ctsk* encoding cathepsin K and *Dcstamp* were found to be upregulated during the differentiation of osteoclasts in these mice. Calvarial osteoblasts from *Pml*$^{-/-}$ mice showed increased mineralized calcium deposition compared to WT *ex vivo*. The above findings further confirm the role of PML in bone metabolism.

Assessment of bone micro-architecture by μCT in 4 month and 14 month old mice revealed no significant differences in bone structure between *Pml* $^{-/-}$ mice and WT controls. There was also no evidence of bone lesions associated with PDB. Thus, increase in osteoblast mineralization seems to counteract increased bone resorption by osteoclasts thereby leading to a normal skeletal phenotype even with advancing age. *Pml* $^{-/-}$ mice are being aged to 22 months of age and will be assessed for bone structure and evidence of lesions to see if they exhibit late onset penetrance and adverse bone phenotype.

7.2 Introduction

Pml overexpression in RAW 264.7 cell line led to a decrease in osteoclast number and size whereas chemical downregulation by arsenic trioxide reversed this phenotype pointing to a negative regulatory role of PML in osteoclast development and differentiation.

As a result, a mouse knockout of PML was obtained to confirm the *in vitro* findings as well as use *ex vivo* osteoclast and osteoblast cultures from these mice to further explore the role of PML in bone biology. This chapter focusses on studies to assess the effect of altered *Pml* expression on osteoclast and osteoblast function and in addition, phenotyping analysis of these mice using micro-CT scanning at different ages.

7.3 Results

7.3.1 Osteoclast development, survival and activity in *Pml* knockout mice

The role of PML in bone remodelling *in vivo* was investigated by using a mouse knockout model of PML. C57Bl6 PML knockout mice (*Pml* $^{-/-}$) were obtained from National Cancer Institute, USA. *PML* was disrupted in the mouse germ line and knockout generated by deleting part of exon 2 which encodes the RING finger domain.

PML mice were genotyped to verify the identity of homozygous (-/-), WT (+/+) and heterozygous (+/-) mice as described in section 3.3.1.

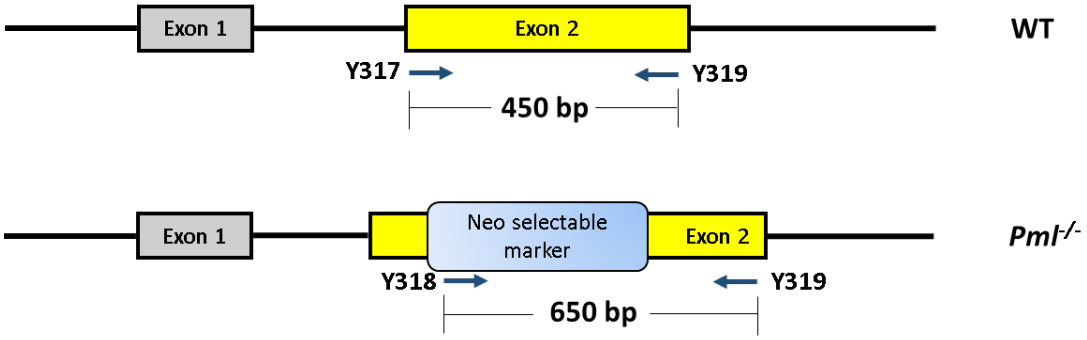

Figure 7.1 Schematic representation of genomic DNA from WT and *Pml* $^{-/-}$ mice.

It shows the partially deleted region from exon 2 which was replaced by a neomycin selection marker cassette as well as details of primers used for genotyping. Gel electrophoresis results are as shown in Figure 7.2.

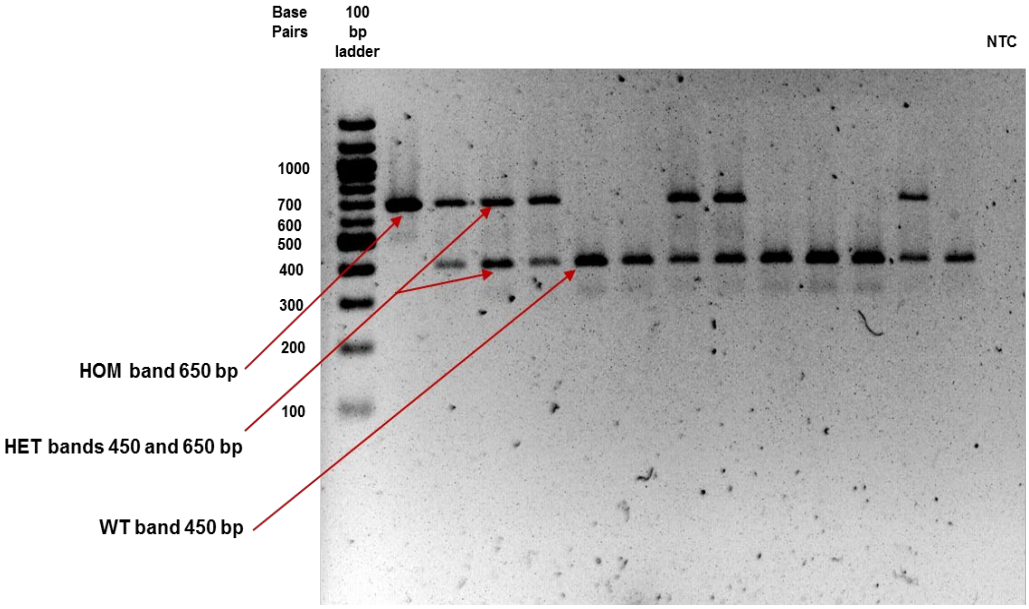

Figure 7.2 Mouse genotyping using PCR and agarose gel electrophoresis.

WT-Wild Type; HET- Heterozygote, HOM-Homozygote, NTC-No DNA template control for PCR.

Bone marrow cells from WT and *Pml* $^{-/-}$ mice were isolated and cultured in presence of M-CSF and RANKL until osteoclasts were formed. TRAcP positive multinucleated osteoclasts (≥3 nuclei) were counted and numbers

were compared to the WT control. The cells were also cultured on Osteoassay plates to assess osteoclast activity and bone resorption.

Osteoclasts formed from *Pml* $^{-/-}$ mice were significantly higher in number and larger compared to WT and showed higher activity (resorption) on osteoassay (Fig.7.3 a,b,c,d)

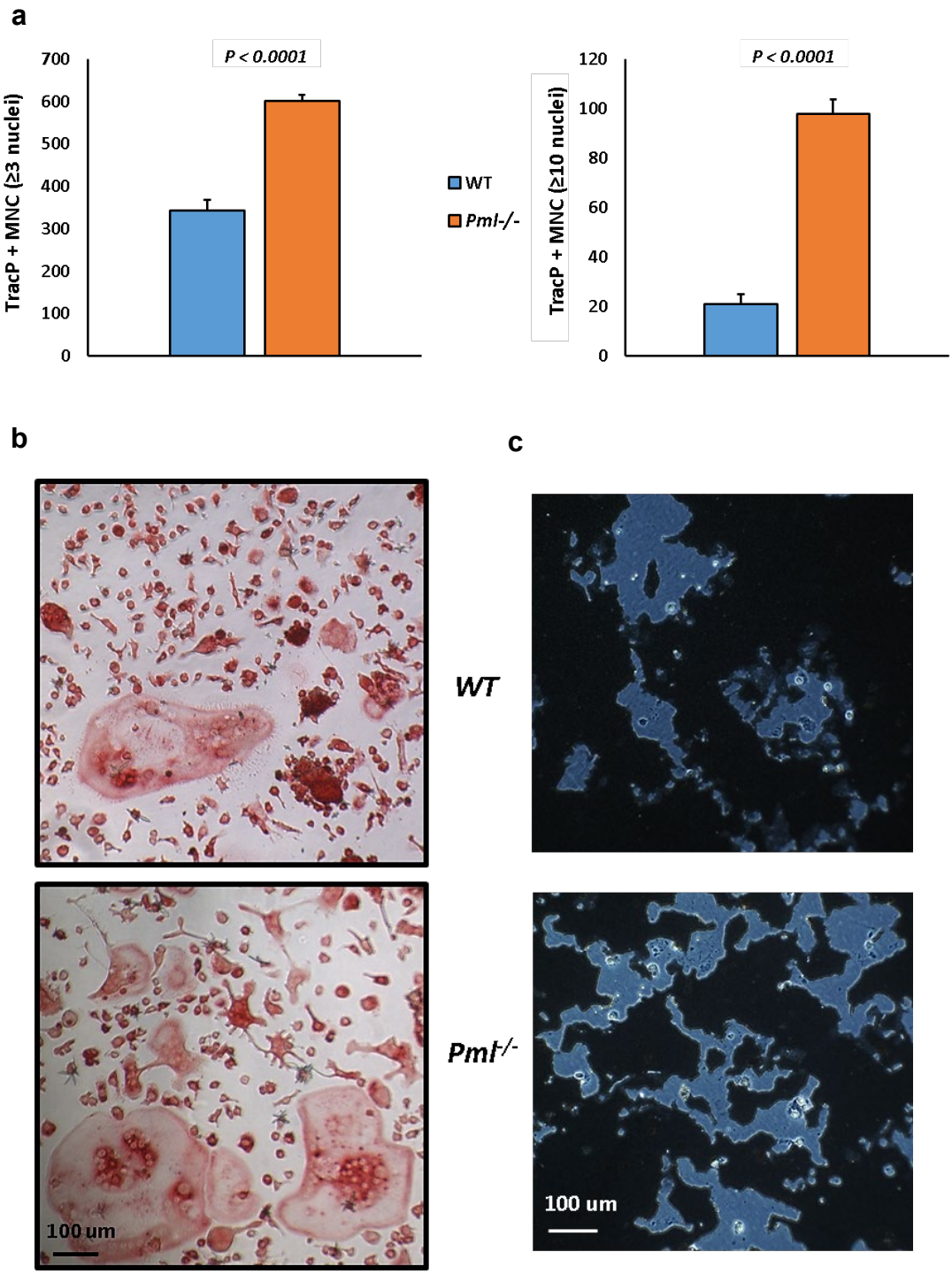

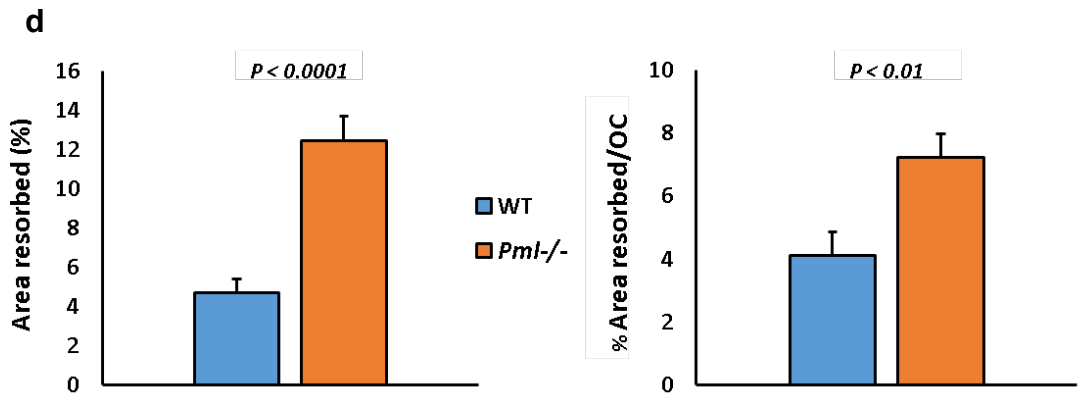

Figure 7.3 Loss of PML in BMDMs enhances osteoclast formation, fusion and activity

a. Increased number of TRAcP+ MNC - osteoclasts (≥3 nuclei) or hypernucleated MNC (≥10 nuclei) generated from *Pml* $^{-/-}$ mice compared to WT. Values are means ± SEM (data presented from one biological replicate) representative of three independent experiments. Minimum 6 wells were counted for each biological replicate.

b. TRAcP staining showing increase in size and number of osteoclasts in *Pml* $^{-/-}$ mice compared to WT.

c. Modified Von-Kossa staining on osteoassay plate shows higher activity and resorption in *Pml* $^{-/-}$ mice compared to WT.

d. Image J analysis of resorbed areas on osteoassay plate. Area resorbed expressed as % as well as area resorbed per osteoclast was much higher in *Pml* $^{-/-}$ mice compared to WT. Values are means ± SEM (combined data) representative of two independent replicates.

Effect of PML loss on osteoclast marker genes in *Pml* $^{-/-}$ mice:

Osteoclast marker gene such as *Ctsk* (Cathepsin K) was upregulated in *Pml* $^{-/-}$ mice as well as WT in response to RANKL but showed enhanced expression in *Pml*$^{-/-}$ mice compared to WT until the intermediate-late (Day3) stage of osteoclast development (Fig. 7.4).

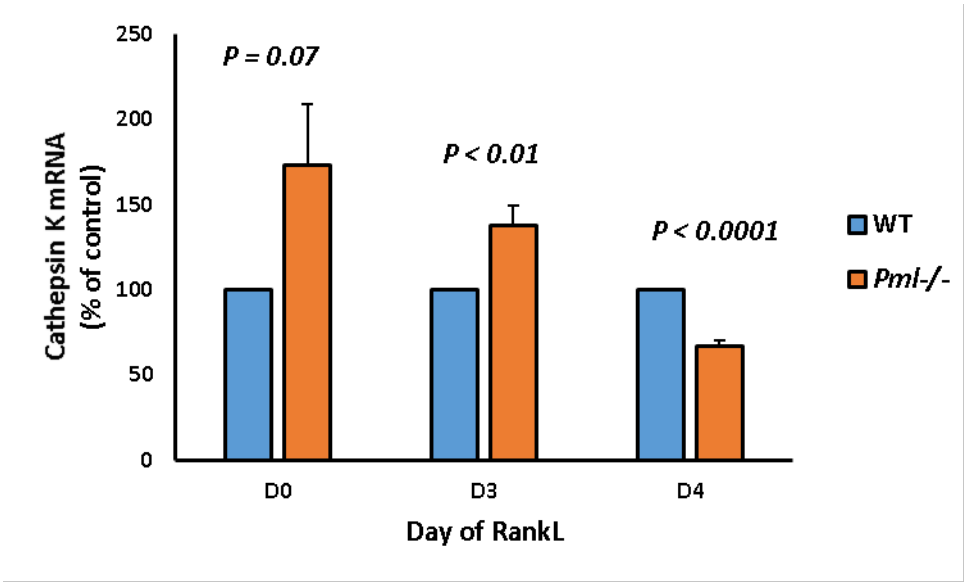

Figure 7.4 Expression analysis of *Cathepsin K* mRNA by qPCR in *Pml*$^{-/-}$ and WT mice during osteoclast development.

Cathepsin K mRNA expression was significantly higher in *Pml*$^{-/-}$ mice compared to WT in the intermediate stage (Day3) of osteoclast development. Values are means ± SEM (combined data) from two independent replicates presented as % of WT.

Expression analysis of osteoclast fusion gene *Dcstamp* in *Pml* $^{-/-}$ mice (where fusion was higher) revealed a significant increase following RANKL treatment compared to WT (Fig. 7.5)

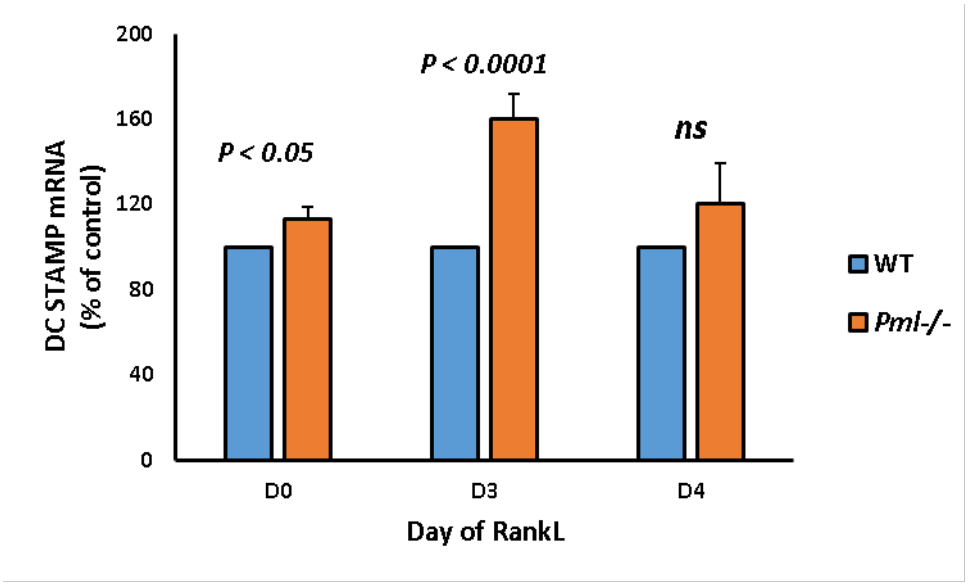

Figure 7.5 Expression analysis of *Dcstamp* mRNA by qPCR in *Pml* $^{-/-}$ mice

Reveals a significant increase following RANKL treatment compared to WT control. Values are means ± SEM (combined data) from three independent replicates presented as % of WT. ns = not significant

Thus, PML loss results in a substantial increase in osteoclast formation, fusion and activity.

Osteoclasts from *Pml* $^{-/-}$ mice showed significantly higher survival compared to WT at 16 hours (hrs) and 24 hrs post RANKL withdrawal. Osteoclast numbers were also higher at 48 hrs but not significant (Fig. 7.6).

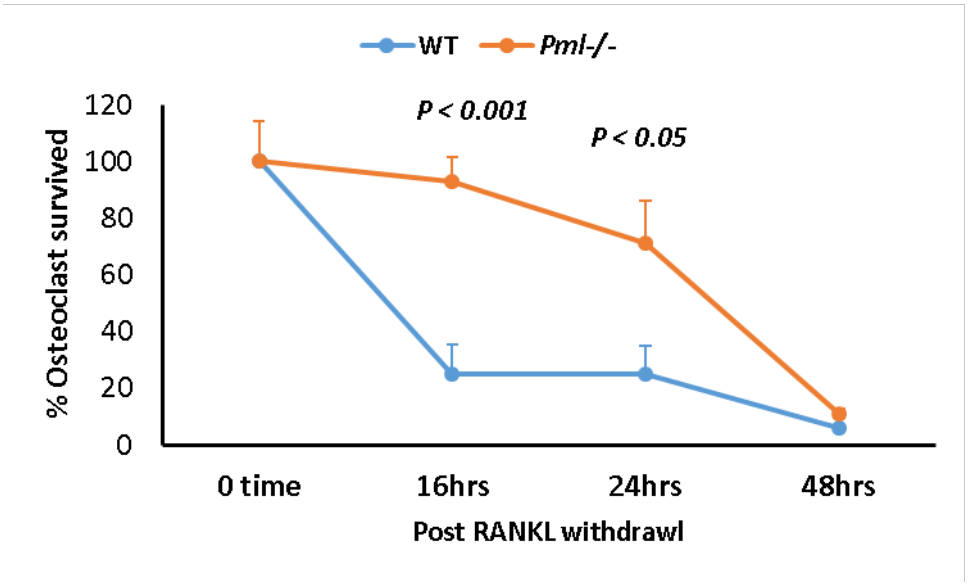

Fig. 7.6 Osteoclast survival post RANKL withdrawal.

Osteoclast survival was significantly higher in *Pml* $^{-/-}$ mice compared to WT at 16hrs (73%) and 24hrs (64%) post RANKL withdrawal. Osteoclast numbers were also higher at 48hrs but not significant. Values are means ± SEM representative of one biological replicate from four independent replicates. Minimum of 6 wells were counted per replicate.

7.3.2 Effect of PML deficiency on calvarial osteoblast mineralisation

Mouse neonatal calvarial osteoblasts were differentiated from *Pml*$^{-/-}$ mice and compared with those from WT. Calvarial osteoblasts were cultured for 18 days in osteogenic medium until mineralized bone nodules were formed. The mineralized calcium deposits were visualized using Alizarin red staining and the content quantified by destaining followed by measuring the absorbance of the extracted stain. Osteoblast mineralization was found to be significantly higher in knockout mice compared to WT. (Fig.7.7).

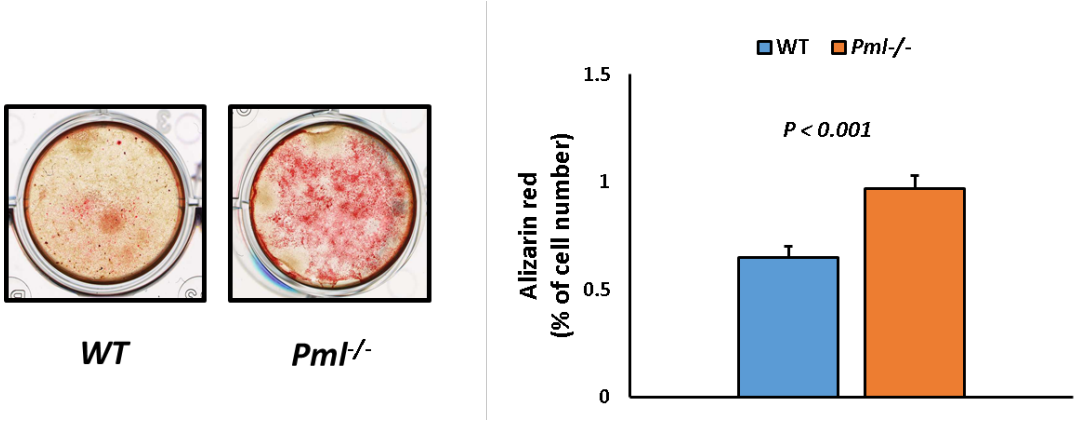

Figure 7.7 Alizarin red staining in calvarial osteoblasts from *Pml*$^{-/-}$ and WT mice to assess bone nodule formation.

Photograph of mineralized nodules stained with Alizarin red dye. Alizarin red (left) and Quantification of the stain (right). Values were corrected for viable cell number as determined by the Alamar Blue assay and presented as means ± SEM representative of one biological replicate from three independent experiments.

Mineralisation determined using Alizarin red was significantly higher in knockout mice compared to WT.

Next, the levels of alkaline phosphatase (ALP), an enzyme involved in bone mineralisation were assessed during osteoblast development. ALP mRNA was significantly higher at basal levels in calvarial osteoblasts from *Pml*$^{-/-}$ mice and upregulated during the initial week of osteoblast development (Day7).

The levels then fell significantly below WT in the second week (Day11) but recovered to higher levels compared to WT during final stages of mineralization (Day20). (Fig. 7.8).

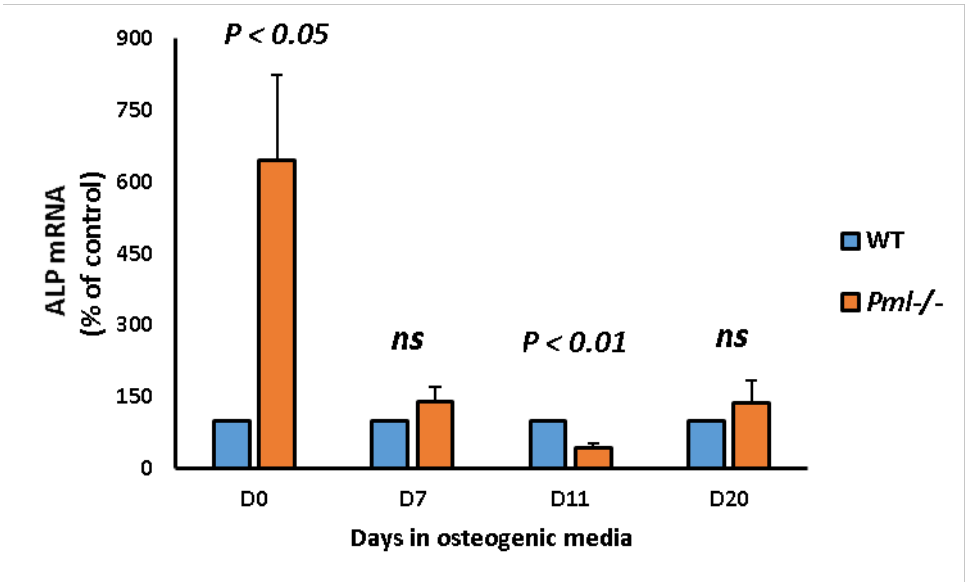

Figure 7.8 Expression analysis of Alkaline phosphatase (ALP) mRNA by qPCR in *Pml*$^{-/-}$ and wt mice during osteoblast development.

ALP mRNA level was significantly higher at basal levels in calvarial osteoblasts from *Pml* $^{-/-}$ mice compared to WT. Values are means ± SEM (combined data) from three independent replicates presented as % of WT. ns = not significant

7.3.3 Effect of PML deficiency on skeletal phenotype in young (4 month old) mice

Micro-CT (µCT) analysis of lower limbs was used to assess bone mass and structure as well as presence of osteolytic lesions in younger WT as well as *Pml*$^{-/-}$ mice. The following were measured (Bone Volume/Total Volume, Trabecular number, separation and thickness as well as Cortical thickness).

µCT analysis revealed no significant differences in trabecular and cortical bone parameters between the two genotypes (Fig.7.9 a,b). There was no evidence of any focal osteolytic lesions characteristic of PDB at the age of 4 months.

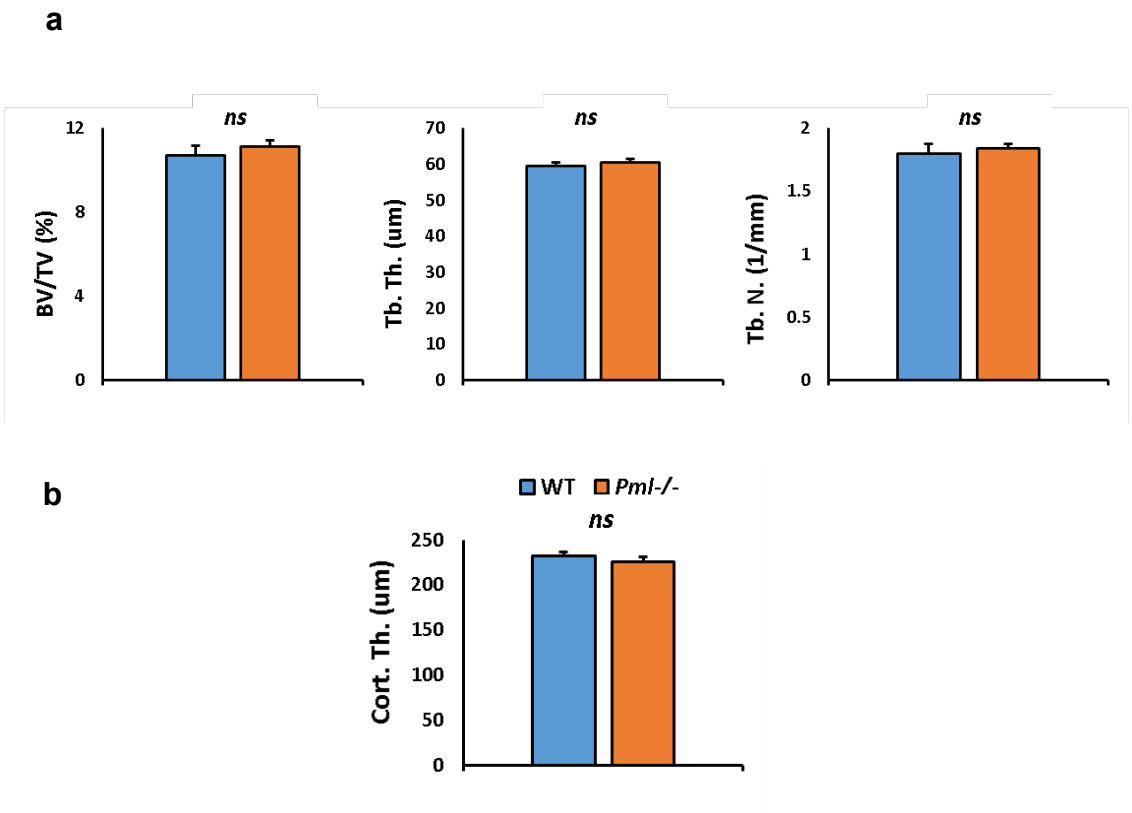

Figure 7.9 Analysis of Bone Structure in *Pml*$^{-/-}$ and WT mice by MicroCT

(a) Comparison of bone volume/total volume (BV/TV); trabecular thickness (Tb.Th) and trabecular number (Tb.N) between WT and *Pml*$^{-/-}$ female mice using uCT of trabecular bone from the tibial metaphysis.

(b) Comparison of cortical thickness (Cort. Th.) using uCT of cortical bone from the tibial diaphysis between WT and *Pml*$^{-/-}$ female mice.

Values are means ± SEM from nine *Pml*$^{-/-}$ and eight WT mice aged 4 months. ns=not significant. None of the parameters analysed showed significant differences between the two genotypes. uCT resolution was 4.9um.

a

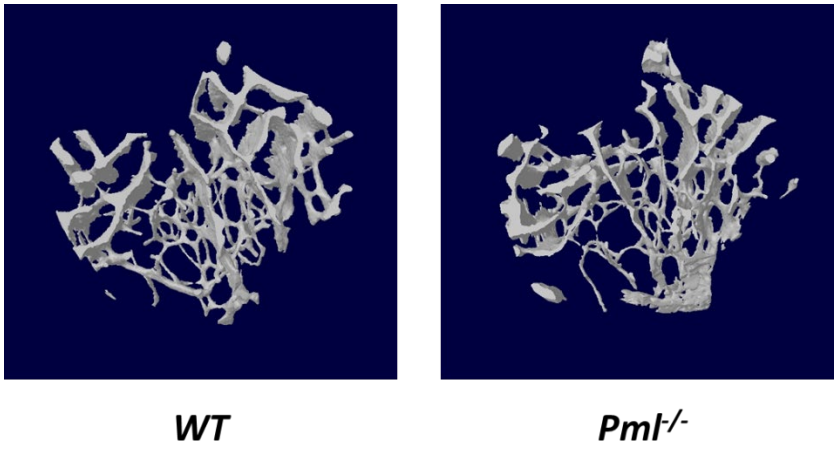

b

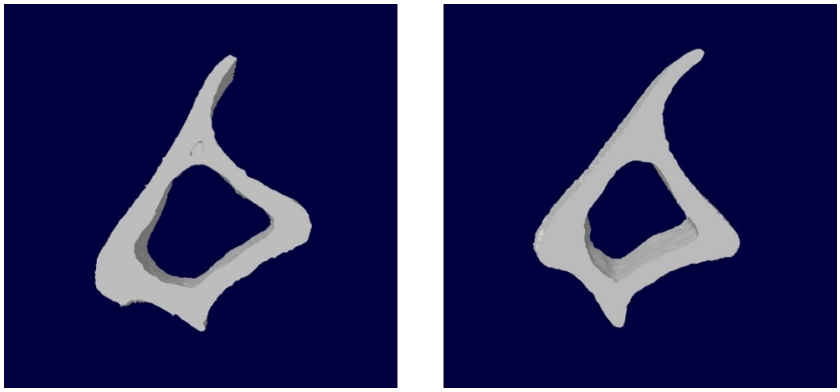

Figure 7.10 Representative CTVol generated 3D model images of (a) trabecular bone from tibial metaphysis and (b) cortical bone from tibial diaphysis in WT and *Pml*$^{-/-}$ mice by MicroCT.

7.3.4 Effect of PML deficiency on skeletal phenotype in older (14 month old) mice

Pml$^{-/-}$ mice were aged and assessed for bone structure and evidence of lesions at 14 months of age to determine how lack of PML affects the bone remodeling process with age. MicroCT analysis (done similar to that described in younger 4 month old mice), however, revealed no significant differences in cortical bone structure between *Pml* $^{-/-}$ and WT mice (Fig 7.11).

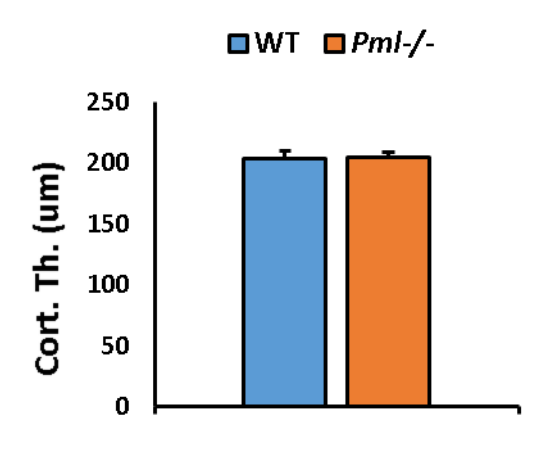

Figure 7.11 Analysis of cortical thickness in 14 month old *Pml* $^{-/-}$ and WT mice by MicroCT. Difference between two genotypes was not significant in *Pml* $^{-/-}$ and WT female mice (n=8 each). Values are means ± SEM. ns=not significant.

uCT resolution was 4.9um. None of the mice analysed had any focal osteolytic lesions characteristic of PDB at the age of 14 months.

Table 7.1 Female mice (WT and *Pml*$^{-/-}$) screened for presence of focal PDB-like lesions by MicroCT.

Mouse Model	**PML knockout**			
Age group	**4 months**		**14 months**	
Genotype	**WT**	***Pml*$^{-/-}$**	**WT**	***Pml*$^{-/-}$**
Total (n)	**8**	**9**	**8**	**8**
Total with lesion (n)	**0**	**0**	**0**	**0**

7.4 Discussion

PML was found to be expressed in bone cells and lower levels of this gene were found in PDB patients compared to controls. *In vitro* studies in RAW 264.7 cell line found that *Pml* overexpression inhibited osteoclast formation and fusion whereas downregulation by arsenic trioxide promoted osteoclast formation and fusion pointing to a negative regulatory role in osteoclast differentiation.

Further studies in *PML* knockout mice using *ex vivo* primary mouse derived cultures corroborated these findings and osteoclasts from these mice not only exhibited increased osteoclast formation and fusion but also showed increased activity and survival compared to WT. Osteoclast related genes such as *Ctsk* encoding Cathepsin K and *Dcstamp* were found to be upregulated during the differentiation of osteoclast precursors into mature osteoclasts in primary BMDMs from these mice.

Osteoclast is the primary cell type affected in PDB. Osteoclasts from pagetic patients show increased number, size and nuclei as well as increased activity and prolonged survival compared to normal subjects (Roodman et al. 2005, Seitz et al. 2009, Chamoux et al. 2009). Findings from this chapter showed that PML loss resulted in a substantial increase in osteoclast formation, fusion, survival and activity. The findings therefore clearly point to a potential role of PML in PDB pathogenesis.

Osteoblast was also investigated using PML knockout mice. Calvarial osteoblasts from *Pml*$^{-/-}$ mice showed increased mineralized calcium deposition compared to WT *ex vivo*. This is likely due to a direct primary effect of PML deficiency on osteoblast.

Assessment of bone micro-architecture by μCT in young mice at age of 4 months revealed no significant differences in bone structure between *Pml*$^{-/-}$ mice and WT controls. Thus, increase in osteoblast mineralization seems to counteract increased bone resorption by osteoclasts thereby leading to a normal skeletal phenotype. Moreover, the levels of Alkaline phosphatase

(ALP) mRNA were also found to be significantly higher at basal levels (early stages of osteoblast differentiation) in osteoblasts from *Pml*$^{-/-}$ mice compared to WT and do not show a sustained increase like they do in WT as osteoblast differentiation proceeds. This could mean that osteoblasts, in absence of PML, are already exposed to high levels of ALP at basal levels and during initial stages of their differentiation leading to their higher activity and subsequent mineralization to neutralize the effects of increased bone resorption by osteoclasts.

It is also worth noting that PDB is a late-onset disease characterized by focal osteolytic lesions generally affecting older people. So the bone remodeling changes in *Pml*$^{-/-}$ mice may actually manifest at a later age than the younger age of 4 months when we assessed these mice. Hence, *Pml*$^{-/-}$ mice were aged and assessed for bone structure and evidence of lesions at 14 months of age. MicroCT analysis, however, revealed no significant differences in cortical bone structure between *Pml*$^{-/-}$ mice and WT controls. There was also no evidence of bone lesions. Thus, bone remodeling changes mediated by osteoclast and osteoblast seem to balance each other out even with advancing age.

Interestingly, however, a recent study (Wong et al. 2019) found evidence of PDB associated bone lesions with 100% penetrance only once the mice reached 22 months of age. The mice in question were deficient in another PDB susceptibility gene *OPTN*, which is also known to be a negative regulator of osteoclastogenesis. Therefore, *Pml*$^{-/-}$ mice are being aged to 22 months of age and will be assessed for bone structure and evidence of lesions to see if they develop late onset phenotype similar to that observed in *Optn* deficient mice.

In addition to μCT, additional assessment of phenotype in *Pml*$^{-/-}$ mice and WT controls which would strengthen the current findings include measurement of bone turnover markers in serum and quantitative assessment of bone structure and remodelling by bone histology as well as bone histomorphometry analysis using bone sections from these mice.

Bone turnover markers commonly used for assessing bone resorptive activity as well as bone formation include C-terminal telopeptide of Type 1 collagen (CTX) and N-terminal propeptide of Type 1 procollagen (PINP) respectively. Abnormalities in bone remodelling including PDB shall be reflected in abnormal levels of these markers. The CTX ELISA assay quantitatively determines CTX, a collagen breakdown product which is released in circulation post bone resorption and in turn determines the level of osteoclast / bone resorptive activity. Similarly, PINP assay measures PINP, a marker of bone formation which is released in circulation during collagen biosynthesis. It is important to take into consideration that though these markers provide good indication of aberrant bone turnover or remodelling, they are subject to random individual as well as biological variation (less so with PINP) such as age, gender, body mass index, fasting/food intake status and circadian variations. Also, they provide only a snapshot of the bone turnover status at a single time point when the serum is collected. In addition, levels of matrix protein osteocalcin and osteoblast derived bone specific ALP (BSAP) in serum can be used as markers of bone formation and serum or urinary N-terminal telopeptide of Type I collagen (NTX) as a bone resorption marker along with osteoclastic enzymes Cathepsin K and TracP.

Though µCT is much more sensitive technique due to its high resolution and broader coverage in 3D compared to bone histomorphometry, performing the latter would reveal further information on bone microarchitecture (structure as well as remodelling) in these mice. For example. TracP staining of bone tissue sections with aniline blue counterstain followed by histomorphometric analysis would not only allow visualisation of osteoclasts *in situ* but also give quantitative output of bone resorption indices (like osteoclast number and surface). Similarly, Von Kossa staining with Van Gieson counterstain would enable osteoid analysis and provide quantitative output of bone formation indices (such as osteoid surface and volume). Calcein double labelling on the other hand will enable dynamic assessment of bone formation and remodelling by measuring parameters such as mineral apposition rate and bone formation rate.

CHAPTER EIGHT

Effect of PML on signalling in osteoclast

8 Effect of PML on signalling in osteoclast

8.1 Summary

Studies in RAW cells and *Pml* $^{-/-}$ mice pointed to a negative regulatory role of PML on osteoclast differentiation. PML is associated with various pathways which play an important role in osteoclastogenesis. PML positively regulates Interferon gamma (IFN-γ) signalling and Interferon regulatory factor 8 (IRF-8) is a known regulator of *PML* gene in response to IFN-γ activation. IRF-8 is known to suppress osteoclast development by inhibiting NFATc1 whereas IFN-γ inhibits osteoclastogenesis by interfering with RANK-RANKL signalling and Cathepsin K expression.

Hence, effect of IFN-γ stimulation on *Pml* $^{-/-}$ mice was explored during RANKL mediated osteoclastogenesis. It was found that IFN-γ stimulation inhibited osteoclastogenesis in WT mice but the effect was not so pronounced on osteoclasts in *Pml* $^{-/-}$ mice. Also, osteoclast related gene's (*Nfatc1*) expression was much higher in *Pml* $^{-/-}$ mice compared to WT in the initial stages of osteoclast development. PML deficiency may therefore result in IFN-γ and/or IRF-8 ineffective in suppressing osteoclastogenesis. In other words, actions of IRF-8 and/or IFN-γ in regulating osteoclastogenesis may be mediated via PML.

8.2 Introduction

PML is associated with various pathways which play an important role in bone metabolism.

IFN-γ inhibits both osteoclast formation at an early stage by interfering with RANK-RANKL signalling pathway (Takayanagi et al. 2000) and osteoclast gene expression (*Cathepsin K*) in preosteoclastic cells (Pang et al. 2005) as well as mature osteoclasts (Kamolmatyakul et al. 2001). IFN-γ is also known to induce IRF-8 and PML in mouse peritoneal macrophages (Dror et al. 2007). *PML* gene is a target gene regulated by IRF-8 in response to IFN-γ activation (Khalfin-Rabinovich et al. 2011). IRF-8 and IFN-γ both have binding sites in the *PML* promoter (Stadler et al. 1995; Dror et al. 2007).

IRF-8 is a transcription factor expressed in haematopoietic cells particularly monocytes, macrophages and dendritic cells and plays an integral role in their development (Tamura et al. 2015). IRF-8 is known to be downregulated in RANKL mediated osteoclastogenesis whereas *Irf8*$^{-/-}$ mice show enhanced osteoclastogenesis and subsequently develop osteoporosis (Zhao et al. 2009).

IRF-8 is essential for PML induction in myeloid cells and an obligatory regulator of the *PML* gene in activated macrophages (Dror et al. 2007). Moreover, IRF-8 has also been found to inhibit the expression and function of nuclear factor of activated cells 1 (NFATc1) (Zhao et al. 2009), the master transcription factor for osteoclastogenesis.

Thus, effects of IRF-8 and IFN-γ in osteoclast may be mediated via PML. Hence, we investigated the effect of IFN-γ stimulation on *Pml* $^{-/-}$ mice during RANKL mediated osteoclastogenesis.

8.3 Results

IFN-γ stimulation inhibited osteoclastogenesis in WT mice but the effect was not so substantial on osteoclasts in *Pml* $^{-/-}$ mice (Fig. 8.1 a).

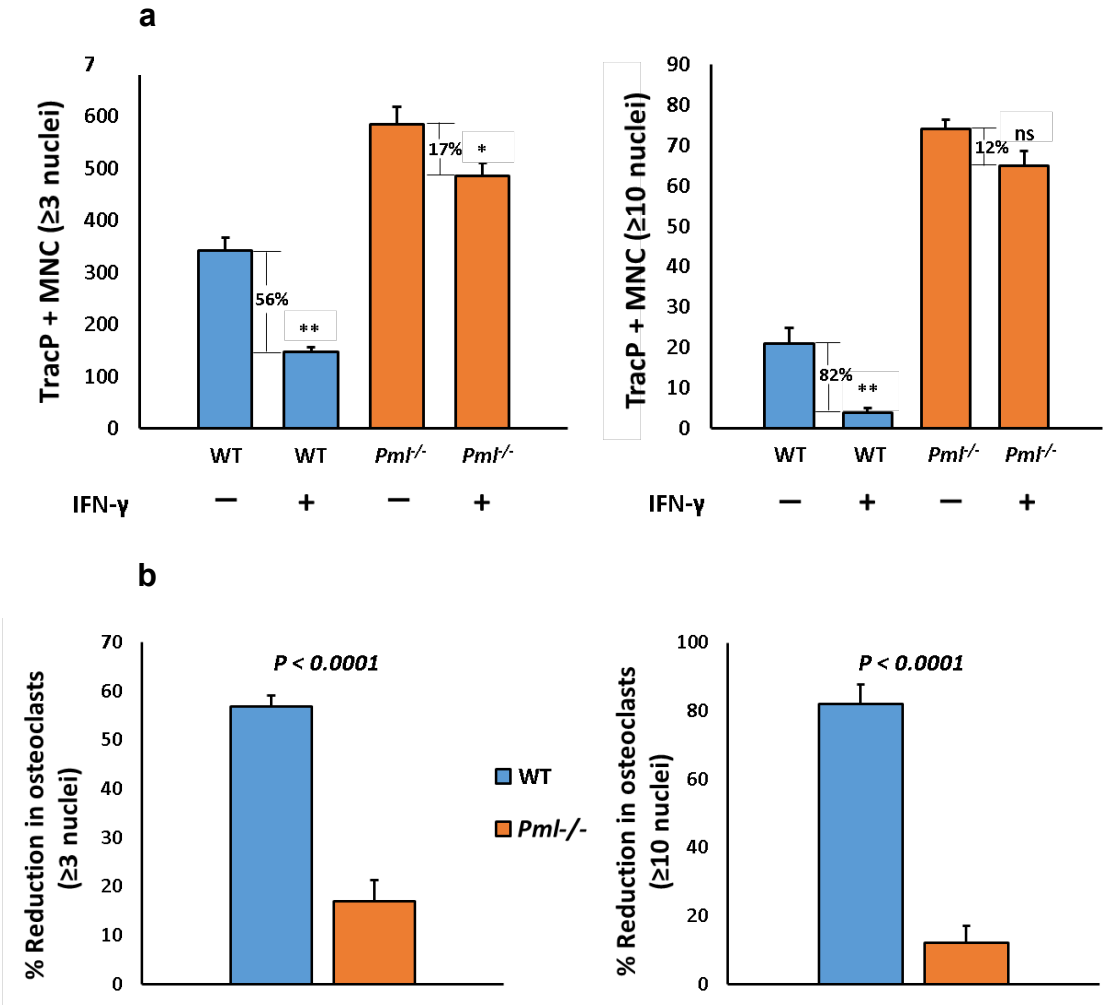

Figure 8.1 Effect of IFN-γ on osteoclast formation and fusion in *Pml* $^{-/-}$ and WT mice.

BMDMs from both genotypes were treated with 5ng/ml IFN-γ for 24 hrs followed by treatment with MCSF and RANKL to generate osteoclasts. a) IFN-γ treatment resulted in increased reduction of TRAcP+ MNC - osteoclasts (≥3 nuclei) or hypernucleated MNC (≥10 nuclei) in WT (blue bars) compared to *Pml* $^{-/-}$ (orange bars) mice. Values are means ± SEM (data from one biological replicate) representative of two independent experiments. *p <0.5; **p<0.01 and ns=not significant. b) Values are expressed as % reduction in osteoclast

numbers from (from one biological replicate) representative of two independent experiments. Osteoclast formation and fusion was significantly reduced in WT compared to *Pml* $^{-/-}$ mice.

Effect of *Pml* gene knockout on the expression of *Nfatc1*, the master regulator of osteoclast was also assessed. *Nfatc1* gene as expected was upregulated in WT as well as *Pml*$^{-/-}$ mice during RANKL mediated osteoclast differentiation. However, *Nfatc1* expression was much higher in *Pml* $^{-/-}$ mice compared to WT in the initial stages of osteoclast development (Fig. 8.2).

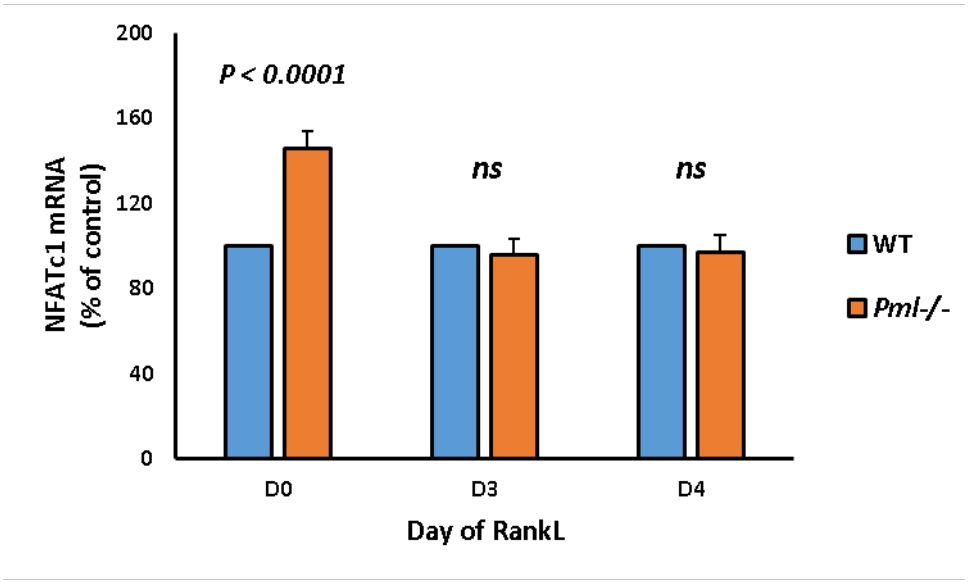

Figure 8.2 Expression analysis of *Nfatc1* by qPCR in *Pml*$^{-/-}$ and WT mice during osteoclast development.

Nfatc1 expression was much higher in *Pml*$^{-/-}$ mice compared to WT in the initial stages of osteoclast development. Values are means ± SEM (cpmbined data) from three independent replicates presented as % of WT. ns =not significant

As mentioned in previous chapter, Cathepsin K was found to be more upregulated in *Pml*$^{-/-}$ mice compared to WT in response to RANKL until later stage of osteoclast differentiation. *Dcstamp*, the master osteoclast fusion regulator, was also found to be highly expressed in *Pml*$^{-/-}$ mice compared to WT in response to RANKL treatment.

8.4 Discussion

PML gene contains binding sites for IFN-γ and IRF-8 in its promoter (Stadler et al. 1995; Dror et al. 2007) and is regulated by IRF-8 in response to IFN-γ activation (Khalfin-Rabinovich et al. 2011). Thus, lack of PML may be rendering IFN-γ and/or IRF-8 ineffective in suppressing osteoclastogenesis.

We found that IFN-γ treatment inhibited osteoclastogenesis in WT mice but the effect was not so pronounced on osteoclasts in *Pml*$^{-/-}$ mice. IFN-γ is known to activate STAT1 (Stark et al. 1998) and failed to inhibit RANKL-induced osteoclastogenesis in *Stat1*$^{-/-}$ mice (Takayanagi et al. 2000) whereas PML positively regulates IFN-γ responses by inducing STAT-1 DNA phosphorylation and DNA binding leading to higher induction of IFN-γ target genes (El Bougrini et al. 2011). *IRF-8* is one of the IFN-γ induced target genes regulated by JAK-STAT1 pathway (Kanno et al. 1993; Dror, Alter-Koltunoff, et al. 2007). Cathepsin K whose levels are enhanced during osteoclast development, is inhibited by IFN-γ in response to RANKL (Kamolmatyakul et al. 2001; Pang et al. 2005).

We found Cathepsin K to be more upregulated in *Pml*$^{-/-}$ mice compared to WT in response to RANKL until the later stages of osteoclastogenesis. This may be a direct effect of PML deficiency on Cathepsin K and/or failure of endogenous IFN-γ to suppress Cathepsin K in absence of PML.

Under basal conditions, *Nfatc1* is expressed at low levels in unstimulated BMDMs whereas osteoclast differentiation in response to RANKL results in marked upregulation of *Nfatc1* (Takayanagi et al. 2002). We saw similar trend for *Nfatc1* in WT as well as *Pml*$^{-/-}$ mice but the expression was much higher in *Pml*$^{-/-}$ mice compared to WT in the pre-osteoclasts. This might contribute to the osteoclast phenotype we see in *Pml*$^{-/-}$ mouse model and could be explained by a direct effect of PML deficiency on NFATc1.

IRF-8 inhibits osteoclastogenesis by interfering with function and expression of NFATc1. (Zhao et al. 2009). This means that osteoclast phenotype we see in *Pml*$^{-/-}$ mouse model could also result from a lack of *PML* which hinders IRF8

from inhibiting NFATc1 during initial stages of osteoclastogenesis. Thus, IRF-8 effect on osteoclastogenesis in *Pml*$^{-/-}$ mice could also be blunted by absence of its downstream target gene *PML*.

Therefore, PML may mediate IFN-γ responses in osteoclast by altering STAT1/IRF-8 and Cathepsin K activity.

Multinucleation and cellular fusion is essential for osteoclasts to effectively resorb bone. DC-STAMP plays a key role in this fusion process (Miyamoto 2006) and we found it to be highly expressed in *Pml* $^{-/-}$ mice compared to WT in response to RANKL treatment. This explains the increased fusion and therefore size of osteoclasts we observe in *Pml*$^{-/-}$ mice compared to WT.

Thus, my study points to a negative role of PML in osteoclast development probably achieved by modulating response of IFN-γ and IRF-8 in association with direct or indirect regulation of osteoclast related genes such as *Ctsk* (Cathepsin K), *Dcstamp* and *Nfatc1* (Fig. 9.3). Osteoclasts are already primed for increased formation, differentiation, fusion and activity due to upregulation of these factors in absence of PML rendering negative regulators ineffective in suppressing osteoclastogenesis.

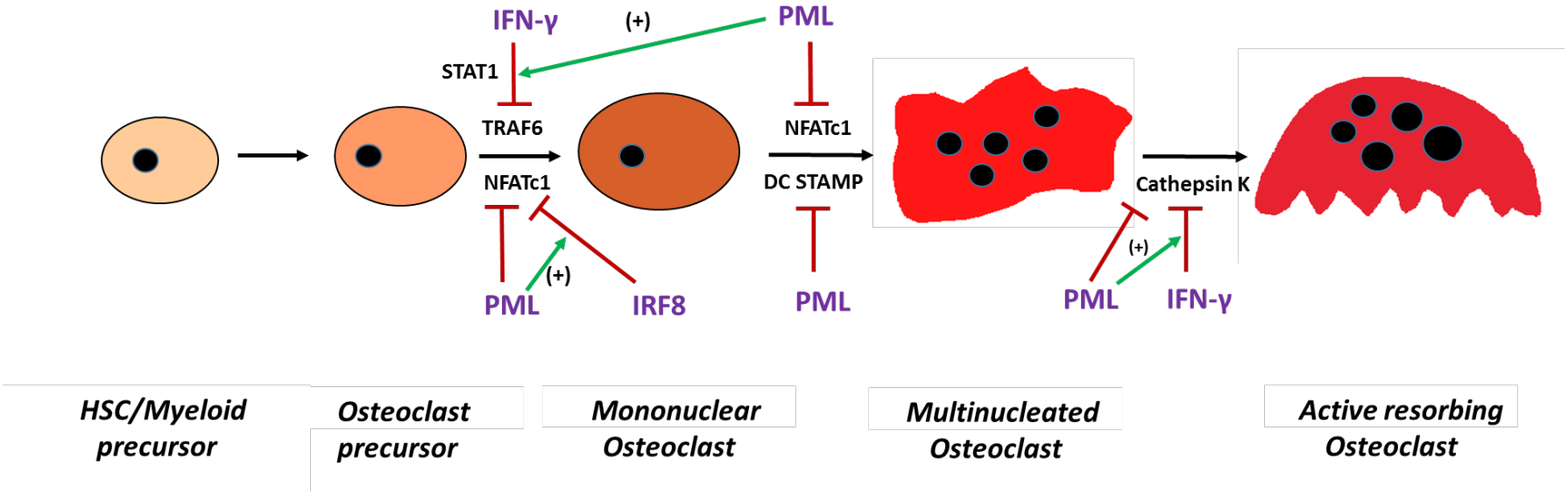

Figure 8.3 Potential role of Pml during osteoclast differentiation.

PML seems to achieve this by controlling IRF-8 and IFN-γ activity as well as regulation of osteoclast related genes such as *Nfatc1*, *Ctsk* and *Dcstamp* as depicted in figure above.

CHAPTER NINE

Discussion, conclusions and future studies

9 Discussion, conclusions and future studies

PDB was first identified in late 19th century (Paget 1877). It is the one of the most common metabolic bone disorder, second only to osteoporosis. PDB is characterised by focal abnormalities of increased bone turnover and abnormal bone remodelling (Ralston et al. 2008).

The disease has a late-onset affecting 1-2% of Caucasians aged 55 years and above and UK has the highest PDB prevalence in the world (Detheridge et al. 1982, Van Staa et al. 2002). Many patients are asymptomatic but others may suffer from bone pain, bone fracture, bone deformity, deafness and secondary osteoarthritis. These complications can be extremely disabling due to loss of mobility and can result in a substantial reduction in quality of life. Its late-onset and asymptomatic presentation means long term permanent skeletal damage may have already occurred by the time it is diagnosed and the current therapeutic modalities only offer symptomatic relief and short term metabolic control but not a cure for the disease. Thus, morbidity and not mortality, is the main concern in relation to this chronic, late-onset bone disease. There have been significant developments in last few decades in understanding pathophysiology of PDB, but its aetiology is still incompletely understood. It is regarded as a complex disease resulting from an interplay between genetic and environmental factors.

PDB has a strong genetic basis. Mutations in *SQSTM1* (which is the only known causal gene for classical PDB), have been found in approximately 10% of sporadic cases and 40% of familial cases which means additional causal genes remain unidentified (Ralston et al. 2008, Ralston and Albagha, 2011). GWAS studies have identified seven other risk loci predisposing to PDB (Ralston et al. 2008; Albagha et al. 2010; Albagha et al. 2011). Identification of causal genetic variants and how they regulate bone metabolism by acting alone or interacting with each other as well as environmental triggers of PDB is crucial to develop a full understanding of this disease. Research in our lab

has focussed on investigating the seven new risk loci and genes within to fully elucidate their role in bone metabolism.

One of these loci (15q24) is a strong genetic susceptibility locus for PDB. Though this locus contains several genes (*LOXL1*, *PML, STOML1, GOLGA6A, ISLR, ISLR2*), targeted DNA sequencing identified PDB associated variants only within PML that suggested it to be the likely candidate gene from this locus.

PML was found to be expressed in primary bone cells osteoblasts and osteoclasts as well as RAW 264.7 cell line and its expression varies during the development and differentiation of these cells.

PML expression was downregulated in patients with PDB. This raises the possibility that genetically determined reduction in *PML* expression is associated with susceptibility to PDB. However, there was no correlation between *PML* expression levels and PDB severity. This could be due to the small sample size of the cohort but also indicates that additional factors (genetic as well as environmental) need to be present for the disease to become fully penetrant and to manifest clinically.

Pml overexpression inhibited osteoclast formation and fusion whereas downregulation by arsenic trioxide promoted osteoclast formation and fusion pointing to a negative regulatory role in osteoclast differentiation. Studies in *Pml* knockout mice validated these findings and osteoclasts from these mice also showed increased activity and survival compared to WT. Thus, PML deficiency resulted in a substantial increase in osteoclast formation, fusion, survival and activity.

IFN-γ treatment failed to suppress osteoclast formation during RANKL mediated osteoclast differentiation. Cathepsin K was found to be more upregulated in *Pml*$^{-/-}$ mice compared to WT in response to RANKL until the later stages of osteoclastogenesis whereas *Nfatc1* expression was much higher in *Pml*$^{-/-}$ mice compared to WT in BMDMs during the initial stages of osteoclast development both of which appear to promote development of the

precursors down the route of osteoclast lineage as well as enhance osteoclast formation and differentiation. *Dcstamp* was found to be highly expressed in *Pml*$^{-/-}$ mice compared to WT thereby leading to increased fusion and therefore size of osteoclasts observed in these mice.

IFN-γ interferes with RANKL-induced osteoclastogenesis by suppressing Cathepsin K expression whereas IRF-8 achieves this by inhibiting NFATc1.

In light of above findings, PML might be implicated in osteoclast signalling by controlling IFN-γ and IRF-8 pathways in association with direct or indirect regulation of osteoclast related genes such as *Ctsk*, *Dcstamp* and *Nfatc1*.

Calvarial osteoblasts cultured *ex vivo* from *Pml*$^{-/-}$ mice showed increased mineralized calcium deposition compared to WT. This probably results from a direct effect of PML deficiency on osteoblast differentiation. This data is consistent with the observation that arsenic Trioxide which degrades PML, also stimulates collagen synthesis and osteoblast differentiation (Xu et al. 2015). Levels of alkaline phosphatase (ALP) mRNA which promotes bone mineralisation were also found to be significantly higher at basal levels (early stages of osteoblast differentiation) in osteoblasts from *Pml*$^{-/-}$ mice compared to WT.

Assessment of bone micro-architecture by μCT in mice revealed no significant differences in bone structure between *Pml*$^{-/-}$ mice and WT controls even after ageing them to 14 months. Thus, bone resorption by osteoclasts is balanced by increase in osteoblast mineralization thereby leading to a normal skeletal phenotype.

In addition to optineurin (OPTN) which has recently been shown to be important for type I interferon (IFN-β) signalling in maintaining bone homeostasis via negative regulation of osteoclastogenesis (Obaid et al. 2015, Wong et al. 2019), PML seems to achieve this by controlling type II interferon signalling (via IFN-γ/IRF-8 axis).

Nagy et al (2008) found significant upregulation of Interferon signalling pathways in monocytes from a small cohort of pagetic patients compared to

controls. At the same time, however, interferons are known to inhibit osteoclast differentiation (Takayanagi et al. 2000, 2002) Thus, mediators of interferon pathways such as OPTN, PML and/or IRF-8 could hold the key to provide an explanation for such observations.

Also, measles virus which induces both Type I (Helin et al. 2001) and IFN-γ (Type II interferon) response (Griffin 2016), has been shown to be strongly correlated with PDB development (Kurihara et al. 2011). Thus, changes in PML may potentially impair antiviral immunity by altering IFN-γ activity thereby increasing susceptibility to PDB.

The above findings further strengthen the case of assigning PDB to an osteoimmunological disorder and at the same time, also open up new therapeutic targets for its treatment and control.

In conclusion, this project has identified Pml as a novel regulator of bone metabolism. PDB patients have reduced levels of *PML* expression. Decreased expression of Pml leads to increased osteoclast differentiation and activity. Lack of PML impairs type II interferon signalling as well as upregulates osteoclast related genes leading to increased bone resorption with a subsequent increase in bone mineralisation by osteoblasts. Thus, genetic variants associated with PDB found within *PML* at the chr15 locus possibly contribute to PDB susceptibility by reducing its expression thereby enhancing osteoclast differentiation and activity.

Future work

It is worth noting that PDB is a late-onset disease characterized by focal osteolytic lesions generally affecting older people and the penetrance increases with age (Ralston et al. 2008) as was evident in *Optn* deficient mice (Wong et al. 2019). So the bone remodeling changes in *Pml* $^{-/-}$ mice may actually manifest at a later age than 14 months when we assessed these mice. *Pml*$^{-/-}$ mice will be assessed for bone turnover, structure and evidence of lesions at 22 months of age to determine how lack of PML affects the bone remodeling process and disease penetrance with more advancing age.

PML is a direct inhibitor of the p38 MAPK which plays an important role in skeletogenesis and bone metabolism by regulating various transcription factors involved in osteoclast and osteoblast development (Shin et al. 2004; Thouverey & Caverzasio 2015). p38 alpha subunit functions downstream of RANK-RANKL interaction to stimulate osteoclast formation, maturation and bone resorption by phosphorylating and transcriptional activation of the p65 NF-kB subunit, MITF, STAT1 and NFATc1 (Thouverey & Caverzasio 2015). At the same time, p38 MAPK signalling positively regulates early osteoblast differentiation, late osteoblast maturation as well as extracellular matrix deposition and mineralisation (Thouverey & Caverzasio 2015). The phenotype of osteoclast and osteoblast we see in our knockout mice could also be arising from lack of interaction between PML and p38 in relation to bone. PML deficiency may result in failure to inhibit p38 which in turn leads to NFATc1 and cathepsin K (IFN γ-STAT1 mediated) upregulation accompanied by increased osteoblast mineralisation. Further studies will be needed to confirm the link between PML and p38-MAPK pathway in relation to bone cell development.

Mutations in *SQSTM1*/p62 are associated with PDB. p62 also localises to PML nuclear bodies (Pankiv et al. 2010). PML is a known repressor of autophagy whereas p62 is degraded by autophagy (Ravikumar et al. 2010; Missiroli et al. 2017). Mice with P394L *SQSTM1* mutation which develop PDB-like lesions show features associated with enhanced autophagosome formation such as increased expression of genes *Atg5, Lc3* and Lc3II protein in osteoclast precursors (Daroszewska et al. 2011). Studies have also found p62 expression to be upregulated in Pagetic osteoclasts (Chamoux et al. 2009).

Interestingly, it was found that autophagy markers *Atg5* and *Lc3* though upregulated in BMDMs, were downregulated post-RANKL stimulation in PML knockout mice (data not shown) which supports the hypothesis that autophagy inhibition may predispose to PDB (Usategui-Martín et al. 2015) leading to protein aggregates and characteristic cytoplasmic/nuclear

inclusions seen in Pagetic osteoclasts (Malkani 1974; Mills et al. 1988; Sieradzan et al. 1999). But our autophagy marker data are conflicting with the P394L *Sqstm1* mice data (Daroszewska et al. 2011) as well as the fact that PML represses autophagy (Missiroli et al. 2017). It appears that PML represses autophagy in macrophages but regulation in osteoclasts is more complex. Further detailed studies in relation to p62 as well as exploring LC3II protein levels and other methods of assessing autophagy may help in dissecting these pathways or interactions further. However, initial findings indicate other factors/pathways to be more important for PDB pathogenesis in these mice compared to autophagy.

NFATc1 is a major downstream target of NF-kB, an essential pathway in osteoclast biology which is repressed by PML (Wu et al. 2003; Kim & Kim 2014; Boyce et al. 2015). RANKL induces *NFATc1* gene via NF-kB and c-Fos signalling pathway in osteoclasts (Kim & Kim 2014). PML transcriptionally represses NF-kB by binding to its target *A20* via the C-terminus (Wu et al. 2002; Wu et al. 2003). Therefore, lack of PML may result in upregulation of NF-kB and its target gene *NFATc1* thereby promoting osteoclast differentiation.

Upregulation of *Nfatc1* in *Pml*$^{-/-}$ mice in response to RANKL when compared to WT was evident only in early stages of osteoclastogenesis. This indicates that activation of NF- kB leading to early induction of *NFATc1* may contribute but makes upregulation of NF-kB alone unlikely to result in osteoclast phenotype in these knockout mice since the upregulation with reference to WT was not sustained in later stages. Further studies are needed to confirm this and establish the exact role of PML in NF-kB signalling in bone, if any.

Thus, in addition to interferon gamma signalling, precise mechanisms underlying osteoclastic gene upregulation (especially role of PML in relation to NF-kB and p38MAPK signalling) and involvement in osteoblast biology needs to be explored further. Studying osteoclast-osteoblast interaction in a co-culture system will be of interest.

PML is important for the PML nuclear body formation which host multiple interactions with a huge array of proteins and thereby play an important regulatory role in multiple cellular processes (Salomoni et al. 2008; Guan & Kao 2015). This could be assessed by studying the presence and characteristics of PDB nuclear inclusions by electron microscopy of osteoclasts generated from *Pml*$^{-/-}$ mice as well as human PBMC derived osteoclasts from PDB cases (if they resemble PML nuclear bodies) and compare them with unaffected controls.

Methylation status at the *PML* locus could be evaluated to determine if control of gene expression at this level is via epigenetic mechanisms and the interaction, if any, between genetic and epigenetic factors.

In recent years, diet as an environmental factor, has gained significant importance in our lives since it affects our gut microbiota (GM) or microbiome. Studies in mice have implicated GM as a regulator of bone mass mainly via its effect on immune system (Ohlsson and Sjögren 2015) which we know in turn, affects osteoclastogenesis. Thus, exploring effects of altered diet/GM in *Pml*$^{-/-}$ mice and other PDB mouse models may improve our understanding of PDB pathogenesis and bone metabolism in general.

Above studies as well as ageing analysis in PML knockout mice will throw further insights into the role of PML in relation to bone metabolism and substantiate its role in accelerated bone remodelling disorders such as PDB.

10 References

Ahmed, A., Wan X., Mitxitorena I., Lindsay A., Pandolfi P. et al., 2017. Regulation of NF-κ B by PML and PML-RARα. *Scientific Reports*, 7, pp.1–9.

Albagha, O.M.E., Visconti M., Alonso N., Wani S. et al., 2013. Common susceptibility alleles and SQSTM1 mutations predict disease extent and severity in a multinational study of patients with Paget's disease. *Journal of Bone and Mineral Research*, 28(11), pp.2338–2346.

Albagha, O.M.E., Wani S., Visconti M., Alonso N. et al., 2011. Genome-wide association identifies three new susceptibility loci for Paget's disease of bone. *Nature Genetics*, 43(7), pp.685–689.

Albagha, O.M.E., Visconti M., Alonso N., Langston A. et al., 2010. Genome-wide association study identifies variants at CSF1, OPTN and TNFRSF11A as genetic risk factors for Paget's disease of bone. *Nature Genetics*, 42(6), pp.520–524.

Albagha, O.M.E. & Ralston, S.H., 2016. *Genetics of Paget's Disease of Bone*, Elsevier Inc., pp.25-35.

Alcalay, M., Tomassoni L., Colombo E., Stoldt S. et al., 1998. The promyelocytic leukemia gene product (PML) forms stable complexes with the retinoblastoma protein. *Molecular and cellular biology*, 18(2), pp.1084–93.

Allen, M.R. & Burr, D.B., 2013. Bone Modeling and Remodeling. *Basic and Applied Bone Biology*, pp.75–90.

Alonso, N., Calero-Paniagua., I. & del Pino-Montes, J., 2017. Clinical and Genetic Advances in Paget's Disease of Bone: a Review. *Clinical Reviews in Bone and Mineral Metabolism*, 15(1), pp.37–48.

Auer, P.L. & Lettre, G., 2015. Rare variant association studies: Considerations, challenges and opportunities. *Genome Medicine*, 7(1), pp.1–11.

Barker, D.D.J.P., 1984. The Epidemiology of Paget's Disease of Bone. *British*

Medical Bulletin, 40(4), pp.396–400.

Baron, R. & Kneissel, M., 2013. WNT signaling in bone homeostasis and disease: from human mutations to treatments. *Nature Medicine*, 19(2), pp.179–192.

Begg, B.S.K., Radley J.M., Pollard J.W., Chisholm OT. et al., 1993. Delayed hematopoietic development in osteopetrotic (op/op) mice. *The Journal of Experimental Medicine*, 177(1), pp.237–242.

Bellido, T., Plotkin L., Bruzzaniti A., 2013. *Bone Cells* in Basic and Applied Bone Biology, 14, Elsevier, pp.27–45.

Bernardi R., Scaglioni P.P., Bergmann S., Horn H.F., et al. 2004. PML regulates p53 stability by sequestering Mdm2 to the nucleolus. *Nat Cell Biol*., 6(7): pp.665–72.

Bernardi, R. & Pandolfi, P.P., 2007. Structure, dynamics and functions of promyelocytic leukaemia nuclear bodies. *Nature Reviews Molecular Cell Biology*, 8(12), pp.1006–1016.

Beyens, G., Van Hul E., Van Driessche K., Fransen E. et al., 2004. Evaluation of the role of the SQSTM1 gene in sporadic Belgian patients with Paget's disease. *Calcified Tissue International*, 75(2), pp.144–152.

Beyens, G., Daroszewska A., de Freitas F., Fransen E. et al., 2007. Identification of sex-specific associations between polymorphisms of the Osteoprotegerin gene, TNFRSF11B, and Paget's disease of bone. *Journal of Bone and Mineral Research*, 22(7), pp.1062–1071.

Bianco, P., Silvestrini G., Ballanti P., Bonucci E., 1992. Paramyxovirus-like nuclear inclusions identical to those of Paget's disease of bone detected in giant cells of primary oxalosis. *Virchows Archive European Journal of Pathology*, 421(5), pp.427–33

Bolland, M.J., Tong P.C., Naot D., Callon KE. et al., 2007. Delayed development of Paget's disease in offspring inheriting SQSTM1 mutations. *Journal of Bone and Mineral Research*, 22(3), pp.411–415

Bolland, M.J. & Cundy, T., 2013. Paget's disease of bone: Clinical review and update. *Journal of Clinical Pathology*, 66(11), pp.924–927.

Borden, K.L., 2002. Pondering the promyelocytic leukemia protein (PML) puzzle: possible functions for PML nuclear bodies. *Molecular and Cellular Biology*, 22(15), pp.5259–5269.

Borden, K.L.B., 2008. Pondering the puzzle of PML nuclear bodies: Can we fit the pieces together using an RNA regulon? *Biochimica et Biophysica Acta - Molecular Cell Research*, p.1783(11), 2145-54.

Boyce, B.F., Xiu Y., Li J., Xing L. et al., 2015. NF-κB-Mediated Regulation of Osteoclastogenesis. *Endocrinology and Metabolism*, 30(1), p.35.

Boyce B., Zuscik M., Xing L., 2013. *Biology of Bone and Cartilage,* in Genetics of Bone Biology and Skeletal Disease. First Edit., Elsevier Inc., pp. 3-24

Boyden B., Mao J., Belsky J., Mitzner L., Farhi A., Mitnick M.A., Wu D., Insogna K., Lifton R.P., 2002. High bone density due to a mutation in LRP5. *New England Journal of Medicine,* 346(20), pp.1513–21.

Burr, D.B. & Akkus, O., 2013. *Bone Morphology and Organization*, in Basic and Applied Bone Biology. Elsevier Inc., pp. 3-25

Celil, A.B. & Campbell, P.G., 2005. BMP-2 and insulin-like growth factor-I mediate osterix (Osx) expression in human mesenchymal stem cells via the MAPK and protein kinase D signaling pathways. *Journal of Biological Chemistry*, 280(36)(9), pp.31353–31359.

Chamoux, E., Couture J., Bisson M., Morissette J. et al., 2009. The p62 P392L mutation linked to Paget's disease induces activation of human osteoclasts. *Molecular endocrinology*, 23(10), pp.1668–1680.

Chen, Y., Wright J., Meng X., Leppard KN., 2015. Promyelocytic Leukemia Protein Isoform II Promotes Transcription Factor Recruitment To Activate Interferon Beta and Interferon-Responsive Gene Expression. *Molecular and Cellular Biology*, 35(10), pp.1660–1672.

Choi, Y.H., Bernardi R., Pandolfi P.P., Benveniste EN., 2006. The promyelocytic leukemia protein functions as a negative regulator of IFN-{gamma} signaling. *Pnas*, 103(49), pp.18715–18720.

Chung I, Osterwald S, Deeg K.I, Rippe K., 2012. PML body meets telomere: the beginning of an ALTernate ending *Nucleus,* 3(3), 263-75.

Clarke, B., 2008. Normal bone anatomy and physiology. *Clinical journal of the American Society of Nephrology : CJASN*.3(3), S131-9.

Corral-Gudino L., del Pino-Montes J., García-Aparicio J., Corral E., Montilla C.A., González-Sarmiento R., 2006. - 511 C/T IL1B gene polymorphism is associated to resistance to bisphosphonates treatment in Paget disease of bone. *Bone*, 38(4), pp.589–594.

Corral-Gudino, L., Del Pino-Montes J., García-Aparicio J., Corral E. et al., 2013. Epidemiology of Paget's disease of bone: A systematic review and meta-analysis of secular changes. *Bone*, 55(2), pp.347–352.

Corral-Gudino, L., Del Pino-Montes J., García-Aparicio J., Alonso-Garrido M. et al., 2010. Paget's disease of bone is not associated with common polymorphisms in interleukin-6, interleukin-8 and tumor necrosis factor alpha genes. *Cytokine*, 52(3), pp.146–150.

Cundy, T., Rutland M.D., Naot D., Bolland M., 2015. Evolution of Paget's disease of bone in adults inheriting SQSTM1 mutations. *Clinical Endocrinology*, 83(3), pp.315–9.

Dahniya, M.H., 1987. Paget's disease of bone in Africans. *The British Journal of Radiology*, 60(710), pp.113–116.

Daroszewska, A., Van't Hof R.J., Rojas J.A., Layfield R. et al., 2011. A point mutation in the ubiquitin-associated domain of SQSMT1 is sufficient to cause a Paget's disease-like disorder in mice. *Human Molecular Genetics*, 20(14), pp.2734–2744.

Datta, H.K., NG WF, Walker JA, Tuck SP. et al., 2008. The cell biology of bone metabolism. *Journal of Clinical Pathology*, 61(5), pp.577–587.

Dellaire G, Bazett-Jones D.P., 2004. PML nuclear bodies: dynamic sensors of DNA damage and cellular stress. BioEssays, 26(9):963–77.

DeSelm, C.J., Miller B.C., Zou W., Beatty W.L. et al., 2011. Autophagy proteins regulate the secretory component of osteoclastic bone resorption. *Developmental Cell*, 21(5), pp.966–74.

Detheridge, F.M., Guyer, P.B. & Barker, D.J.P., 1982. European distribution of Paget's disease of bone. *Br Med J*, 285(6347), pp.1005–1008.

Dickson, S.P., Wang K., Krantz I., Hakonarson H. et al., 2010. Rare Variants Create Synthetic Genome-Wide Associations. *PLoS Biology*, 8(1).

Divisato, G., Formicola D., Esposito T., Merlotti, D. et al., 2016. ZNF687 Mutations in Severe Paget Disease of Bone Associated with Giant Cell Tumor. *American Journal of Human Genetics*, 98(2), pp.275–286.

Donáth, J., Speer G., Poór G., Gergely P Jr., Tabák A. et al., 2004. Vitamin D receptor, oestrogen receptor-α and calcium-sensing receptor genotypes, bone mineral density and biochemical markers in Paget's disease of bone. *Rheumatology*, 43(6), pp.692–695.

Dougall, W.C., Glaccum M., Charrier K., Rohrbach K. et al., 1999. RANK is essential for osteoclast and lymph node development. *Genes and Development*, 13(18), pp.2412-24

Dror, N., Rave-Harel N., Burchert A., Azriel A. et al., 2007. Interferon regulatory factor-8 is indispensable for the expression of promyelocytic leukemia and the formation of nuclear bodies in myeloid cells. *Journal of Biological Chemistry*, 282(8), pp.5633–5640.

El Bougrini, J., Dianoux, L. & Chelbi-Alix, M.K., 2011. PML positively regulates interferon gamma signaling. *Biochimie*, 93(3), pp.389–398.

Falchetti, A., Di Stefano M., Marini F., Del Monte F., Mavilia C. et al., 2004. Two novel mutations at exon 8 of the sequestosome 1 (SQSTM1) gene in an Italian series of patients affected by Paget's disease of bone (PDB). *Journal of Bone and Mineral Research*, 19(6), pp.1013–7.

Florencio-Silva, R., Sasso G.R., Sasso-Cerri E., Simões MJ. et al., 2015. Biology of Bone Tissue: Structure, Function, and Factors That Influence Bone Cells. *BioMed Research International*, 2015.

Franceschi, R.T., Xiao G., Jiang D., Gopalakrishnan R. et al., 2003. Multiple Signaling Pathways Converge on the Cbfa1/Runx2 Transcription Factor to Regulate Osteoblast Differentiation. *Connective Tissue Research*, 44(1), pp.109–116.

Franzoso, G., Carlson L., Xing L., Poljak L., Shores E.W. et al., 1997. Requirement for NF-κB in osteoclast and B-cell development. *Genes and Development*, 11(24), pp.3482-96.

Gao, Y., Huang E, Zhang H., Wang J., Wu N. et al., 2013. Crosstalk between Wnt/β-catenin and estrogen receptor signaling synergistically promotes osteogenic differentiation of mesenchymal progenitor cells. *PLoS ONE*, 8(12), pp.1–13.

Geetha, T. & Wooten, M.W., 2002. Structure and functional properties of the ubiquitin binding protein p62. *FEBS Letters*, pp.19–24.

Gennari, L., Di Stefano M., Merlotti D., Giordano N. et al., 2005. Prevalence of Paget's disease of bone in Italy. *Journal of Bone and Mineral Research*, 20(10), pp.1845–1850.

Gianfrancesco, F., Rendina D., Di Stefano M., Mingione A. et al., 2012. A nonsynonymous TNFRSF11A variation increases NFκB activity and the severity of Paget's disease. *Journal of Bone and Mineral Research*, 27(2), pp.443–52.

Good, D., Busfield F., Fletcher B.H., Duffy DL. et al., 2002. Linkage of Paget disease of bone to a novel region on human chromosome 18q23. *American Journal of Human Genetics*, 70(2), pp.517–25.

Gong, Y., Slee R.B., Fukai N., Rawadi G., Roman-Roman S., Reginato A.M., Wang H., Cundy T., et al., 2001. LRP5 affects bone accrual and eye development. *Cell*, 107(4), pp.513–23.

Griffin, D. 2016. The immune response in measles: Virus control, clearance and protective Immunity. *Viruses*, 8(10), Epub.282.

Gu, J.M., Zhang Z.L., Zhang H., Hu W.W. et al., 2012. Thirteen Chinese patients with sporadic Paget's disease of bone: Clinical features, SQSTM1 mutation identification, and functional analysis. *Journal of Bone and Mineral Metabolism*, 30(5), pp.525–33.

Guan, D. & Kao, H.Y., 2015. The function, regulation and therapeutic implications of tumor suppressor protein, PML. *Cell & Bioscience*, 5(1), p.60.

Guan D., Lim J.H., Peng L., Liu Y., et al. 2014. Deacetylation of the tumor suppressor protein PML regulates hydrogen peroxide-induced cell death. *Cell Death Dis*, 5:e1340.

Guerrini, M.M., Sobacchi C., Cassani B., Abinun M., Kilic S.S. et al., 2008. Human Osteoclast-Poor Osteopetrosis with Hypogammaglobulinemia due to TNFRSF11A (RANK) Mutations. *American Journal of Human Genetics*, 83(1), pp.64–76.

Guma, M., Rotés D , Holgado S , Monfort J , Olivé A et al., 2002. Paget's disease of bone: study of 314 patients. *Medicina Clinica*, 119(14), pp. 537-540.

Hassan, E., Maeda Y., Taipaleenmaki H., Zhang W., Jafferji M. et al., 2012. miR-218 directs a Wnt signaling circuit to promote differentiation of osteoblasts and osteomimicry of metastatic cancer cells. *The Journal of Biological Chemistry* , 287(50), pp.42084–92.

Hayakawa F., Abe A., Kitabayashi I., Pandolfi P.P., Naoe T., 2008. Acetylation of PML is involved in histone deacetylase inhibitor-mediated apoptosis. *J Biol Chem*; 283: pp.24420–24425.

Helin, E., Vainionpää R., Hyypiä T., Julkunen I., Matikainen S. 2001. Measles virus activates NF-kappa B and STAT transcription factors and production of IFN-alpha/beta and IL-6 in the human lung epithelial cell line A549. *Virology* , 290(1), pp.1–10.

Hennies, H.C., Kornak U., Zhang H., Egerer J., Zhang X. et al., 2011. Gerodermia osteodysplastica is caused by mutations in SCYL1BP1, a Rab-6 interacting golgin. *Nature Genetics* , 40(12), pp.1410–1412.

Hocking, L.J., Lucas G.J., Daroszewska A., Mangion J. et al., 2002. Domain-specific mutations in sequestosome 1 (SQSTM1) cause familial and sporadic Paget's disease. *Human Molecular Genetics*, 11(22), pp.2735–9.

Hocking, L.J., Herbert C.A., Nicholls R.K., Williams F. et al., 2001. Genomewide search in familial Paget disease of bone shows evidence of genetic heterogeneity with candidate loci on chromosomes 2q36, 10p13, and 5q35. *American Journal of Human Genetics*, 69(5), pp.1055–1061.

Huang Q., Li F., Liu X., Li W. et al., 2011 Caspase 3-mediated stimulation of tumor cell repopulation during cancer radiotherapy. *Nat Med*., 17(7):860–6.

Huang, H., Fu S., Zhong W., Huang H. 2013. PML overexpression inhibits proliferation and promotes the osteogenic differentiation of human mesenchymal stem cells. *Oncology Reports*, 30(6), pp.2785–2794.

Insogna, K L, Sahni, M., Grey A.B., Tanaka S. et al, 1997. Colony-stimulating factor-1 induces cytoskeletal reorganization and c-src-dependent tyrosine phosphorylation of selected cellular proteins in rodent osteoclasts. *Journal of Clinical Investigation*, 100(10), pp.2476–2485.

Jeganathan, S., Fiorino, C., Naik, U., Sun, H.S. et al., 2014. Modulation of osteoclastogenesis with macrophage M1- and M2-inducing stimuli. *PLoS One*, 9(8):e104498.

Jin, W., Chang M., Paul E.M., Babu G. et al., 2008. Deubiquitinating enzyme CYLD negatively regulates RANK signaling and osteoclastogenesis in mice. *Journal of Clinical Investigation*, 118(5), pp.1858–1866.

Johnson-Pais, T.L., Wisdom J.H., Weldon K.S., Cody J.D. et al., 2003. Three Novel Mutations in SQSTM1 Identified in Familial Paget's Disease of Bone. *Journal of Bone and Mineral Research*, 18(10), pp.1748–53.

Kajiho, H., Saito K., Tsujita K., Kontani K. et al., 2003. RIN3: a novel Rab5

GEF interacting with amphiphysin II involved in the early endocytic pathway. *Journal of Cell Science*, 116(20), pp.4159–68.

Kamolmatyakul, S., Chen, W. & Li, Y.P., 2001. Interferon-gamma down-regulates gene expression of cathepsin K in osteoclasts. *Journal of Dental Research*, 80, pp.351–355.

Kanis, J.A., 1992. Pathophysiology and Treatment of Paget's Disease of Bone. *Martin Dunitz*, Vol 1, pp.1–293.

Kawasaki A., Matsumura I., Kataoka Y., Takigawa E. et al., 2003. Opposing effects of PML and PML/RAR alpha on STAT3 activity. *Blood*, 101, pp.3668–3673.

Kearns, A.E., Khosla, S. & Kostenuik, P.J., 2008. Receptor activator of nuclear factor κB ligand and osteoprotegerin regulation of bone remodeling in health and disease. *Endocrine Reviews*, 29(2), pp.155-92

Khalfin-Rabinovich, Y., Weinstein, A. & Levi, B.Z., 2011. PML is a key component for the differentiation of myeloid progenitor cells to macrophages. *International Immunology*, 23(4), pp.287–296.

Khan M.M., Nomura T., Kim H., Kaul S.C. et al., 2001. Role of PML and PML-RAR alpha in Mad-mediated transcriptional repression. *Mol.CellI.*, 7(6):1233–43.

Kim, H.J., Kim N., Yang Y., Scarborough E. et al., 2013. Prion-like domain mutations in hnRNPs cause multisystem proteinopathy and ALS performed the experiments provided patient clinical material, clinical evaluation, or evaluation of patient clinical material. *Nature*, 495(7442), pp.467–473.

Kim, J.H., Seong S., Kim K., Kim I. et al., 2016. Downregulation of runx2 by 1, 25-dihydroxyvitamin D3 induces the transdifferentiation of osteoblasts to adipocytes. *International Journal of Molecular Sciences*, 17(5).

Kim, J.H. & Kim, N., 2014. Regulation of NFATc1 in Osteoclast Differentiation. *Journal of Bone Metabolism*, 21(4), p.233-241.

Kini and Nandeesh, 2012. *Physiology of bone formation, remodeling and metabolism* in Radionuclide and hybrid bone imaging. Springer, pp. 29-58

Kohli, S. & Kohli, V., 2011. Role of RANKL-RANK/osteoprotegerin molecular complex in bone remodeling and its immunopathologic implications. *Indian Journal of Endocrinology and Metabolism*, 15(3), pp.175–81.

Komori T, Yagi H., Nomura S., Yamaguchi A., Sasaki K. et al., 1997. Targeted disruption of Cbfa1 results in a complete lack of bone formation owing to maturational arrest of osteoblasts. *Cell*, 89(5), pp.755-64.

Kong, Y.Y., Yoshida H., Sarosi I., Tan H.L. et al., 1999. OPGL is a key regulator of osteoclastogenesis, lymphocyte development and lymph-node organogenesis. *Nature*, 97(6717), pp.315-23.

Kuo, TR. & Chen, CH., 2017. Bone biomarker for the clinical assessment of osteoporosis: recent developments and future perspectives. *Biomarker Research*, 5(1), p.18.

Kurihara, N., Hiruma Y., Yamana K., Michou L. et al., 2011. Contributions of the measles virus nucleocapsid gene and the SQSTM1/p62P392L mutation to paget's disease. *Cell Metabolism*, 13(1), pp.23–34.

Lacey, D.L., Timms E., Tan H.L., Kelley MJ. et al., 1998. Osteoprotegerin ligand is a cytokine that regulates osteoclast differentiation and activation. *Cell*, 93(2), pp.165–176.

Lallemand-Breitenbach, V., Jeanne M., Benhenda S., Nasr R., Lei M. et al., 2008. Arsenic degrades PML or PML-RARα through a SUMO-triggered RNF4/ ubiquitin-mediated pathway. *Nature Cell Biology*, 10(5), pp.547–54.

Lango, A.H., Estrada K., Lettre G., Berndt S.I., Weedon M.N. et al., 2011. Hundreds of variants clustered in genomic loci and biological pathways affect human height. *Nature*, 467(7317), pp.832–838.

Langston A.L, Campbell M.K., Fraser W.D., MacLennan G.S., Selby P.L, Ralston S.H., 2010 Randomized trial of intensive bisphosphonate treatment

versus symptomatic management in Paget's disease of bone. *Journal of Bone and Mineral Research,* 25(1), pp. 20–31

Laurin, N., Brown J.P, Lemainque A., Duchesne A., Huot D. et al., 2001. Paget Disease of Bone: Mapping of Two Loci at 5q35-qter and 5q31. *The American Journal of Human Genetics*, 69(3), pp.528–543.

Laurin, N., Brown J.P., Morissette J., Raymond V., 2002. Recurrent Mutation of the Gene Encoding sequestosome 1 (SQSTM1/p62) in Paget Disease of Bone. *The American Journal of Human Genetics*, 70(6), pp.1582–1588.

Layfield, R. & Hocking, L.J., 2004. SQSTM1 and Paget's Disease of Bone. *Calcified Tissue International*, 75(5), pp.347–57.

Lehembre F., Muller S., Pandolfi P.P., Dejean A., 2001. Regulation of Pax3 transcriptional activity by SUMO-1-modified PML. *Oncogene*, 20: pp.1–9.

Lever, J.H., 2002. Paget's Disease of Bone in Lancashire and arsenic pesticide in cotton mill wastewater: a speculative hypothesis. *Bone*, 31(3), pp.434–36.

Li, J., Sarosi I., Yan X.Q., Morony S., Capparelli C. et al., 2000. RANK is the intrinsic hematopoietic cell surface receptor that controls osteoclastogenesis and regulation of bone mass and calcium metabolism. *Proceedings of the National Academy of Sciences of USA*, 97(4), pp.1566–71.

Lim J.H., Liu Y., Reineke E., Kao H.Y., 2011. Mitogen-activated protein kinase

extracellular signal-regulated kinase 2 phosphorylates and promotes Pin1 protein-dependent promyelocytic leukemia protein turnover. *J. Biol Chem*, 286(52): pp.44403–11.

Lin, H.K., Bergmann, S. & Pandolfi, P.P., 2004. Cytoplasmic PML function in TGF-β signalling. *Nature*, 431(7005), pp.205–11.

Lombardi, G., Di Somma C., Rubino M., Faggiano A. et al., 2011. The roles of parathyroid hormone in bone remodeling: prospects for novel therapeutics. *Journal of endocrinological investigation*, 34(7supp) pp.18–22.

Lucas, G.J.A., Daroszewska, A. & Ralston, S.H., 2006. Contribution of genetic factors to the pathogenesis of Paget's disease of bone and related disorders. *Journal of Bone and Mineral Research*, 21(SUPPL. 2), pp.31–7.

Malkani, R, Rebel A., Basle M., Bregeon C. et al, 1974. Ultrastructural characteristics of osteoclasts in Paget's disease. *Rev Rhum Mal Osteoartic*, 41, pp.767–771.

Matthews, B.G., Naot D., Bava U., Callon K.E. et al., 2009. Absence of somatic SQSTM1 mutations in Paget's disease of bone. *Journal of Clinical Endocrinology and Metabolism*, 94(2), pp.691–4.

McCarthy, T.L., Chang W.Z., Liu Y., Centrella M., 2003. Runx2 Integrates Estrogen Activity in Osteoblasts. *Journal of Biological Chemistry*, 278(44), pp.43121–9.

Mellis, D.J., Itzstein C., Helfrich M.H., Crockett J.C. et al., 2011. The skeleton: A multi-functional complex organ. The role of key signalling pathways in osteoclast differentiation and in bone resorption. *Journal of Endocrinology*, 211(2), pp.131–143.

Merchant, A., Smielewska M., Patel N., Akunowicz J.D. et al., 2009. Somatic mutations in SQSTM1 detected in affected tissues from patients with sporadic paget's disease of bone. *Journal of Bone and Mineral Research*, 24(3), pp.484–94.

Mills, B.G., Yabe, H. & Singer, F.R., 1988. Osteoclasts in human osteopetrosis contain viral-nucleocapsid-like nuclear inclusions. *Journal of Bone and Mineral Research*, 3(1), pp.101–6.

Misra, S., Misra S.R., Vineet D.A., Baskaran P., 2013. Paget disease of bone: A classic case report. *Contemporary Clinical Dentistry*, 4(2), pp.227–30.

Missiroli, S., Bonora M., Patergnani S., Giorgi C., 2017. Novel function of the tumor suppressor PML at ER-mitochondria sites in the control of autophagy. *Oncotarget*, pp.1–2.

Miyamoto, T., 2006. The dendritic cell-specific transmembrane protein DC-

STAMP is essential for osteoclast fusion and osteoclast bone-resorbing activity. *Modern Rheumatology*, 16(6), pp.341–342.

Miyauchi, Y., Ninomiya K., Miyamoto H., Sakamoto A. et al., 2010. The Blimp1–Bcl6 axis is critical to regulate osteoclast differentiation and bone homeostasis. *The Journal of Experimental Medicine*, 207(4), pp.751–762.

Myint, Y.Y., Miyakawa K., Naito M., Shultz L.D. et al., 1999. Granulocyte / Macrophage Colony-Stimulating Factor and Interleukin-3 Correct Osteopetrosis in Mice with Osteopetrosis Mutation, *American Journal of Pathology*, 154(2), pp.553–566.

Nagabhushana A., Bansal M., Swarup G., 2011. Optineurin is required for CYLD-dependent inhibition of TNFα-induced NF-κB activation. *PLoS ONE*, 6(3).

Nagy, Z.B., Gergely, P., Donáth, J., Borgulya, G., Csanád, M., and Poór G., 2008. Gene expression profiling in Paget's disease of bone: upregulation of interferon signaling pathways in pagetic monocytes and lymphocytes *Journal of Bone and Mineral Research*, 23(2), pp.253-259.

Nakashima, K., Zhou X., Kunkel G., Zhang Z., Deng J.M., Behringer R.R., de Crombrugghe B., 2002. The novel zinc finger-containing transcription factor osterix is required for osteoblast differentiation and bone formation. *Cell*, 108(1), pp.17–29.

Nakatsuka, K., Nishizawa, Y. & Ralston, S.H., 2003. Phenotypic characterization of early onset Paget's disease of bone caused by a 27-bp duplication in the TNFRSF11A gene. *Journal of Bone and Mineral Research*, 18(8), pp.1381–5.

Nalbandian, A., Donkervoort S., Dec E., Badadani M. et al., 2011. The multiple faces of valosin-containing protein-associated diseases: Inclusion body myopathy with Paget's disease of bone, frontotemporal dementia, and amyotrophic lateral sclerosis. *Journal of Molecular Neuroscience*, 45(3), pp.522–531.

Neale, S., Schulze E., Smith R., Athanasou N.A., 2002. The influence of serum cytokines and growth factors on osteoclast formation in Paget's disease. *QJM : monthly journal of the Association of Physicians*, 95(4), pp.233–40.

Negishi-Koga, T., Shinohara M., Komatsu N., Bito H. et al., 2011. Suppression of bone formation by osteoclastic expression of semaphorin 4D. *Nature Medicine*, 17(11), pp.1473–1480.

Nisole, S., Maroui M.A., Mascle X.H., Aubry M., Chelbi-Alix M.K., 2013. Differential Roles of PML Isoforms. *Frontiers in Oncology*, 3(May), pp.1–17.

Obaid, R., Wani S.E., Azfer A., Hurd T. et al., 2015. Optineurin Negatively Regulates Osteoclast Differentiation by Modulating NF-κB and Interferon Signaling: Implications for Paget's Disease. *Cell Reports*, 13(6), pp.1096–1102.

Ohlsson, C. and Sjögren K., 2015. Effects of the gut microbiota on bone mass. *Trends in Endocrinology and metabolism*, 26(2), pp. 69-74.

Ooi, C.G. & Fraser, W.D., 1997. Paget's disease of bone. *Postgraduate Medical Journal*, 73(856), pp.69–74.

OpenStax Anatomy & Physiology, 2016. Anatomy & Physiology 2016.

Osterberg, P.H., Wallace R.G., Adams D.A., Crone R.S. et al., 1988. Familial expansile osteolysis. A new dysplasia. *The Journal of bone and joint surgery. British volume*, 70(2), pp.255–60.

Otto F., Thornell A.P., Crompton T., Denzel A., Gilmour K.C. et al., 1997. Cbfa1, a candidate gene for cleidocranial dysplasia syndrome, is essential for osteoblast differentiation and bone development. *Cell*, 89(5), pp.765-71.

Paget J. 1877. On a Form of Chronic Inflammation of Bones (Osteitis Deformans). *Medico-Chirurgical Transactions*, 60, pp.37–64.9.

Pang, M., Martinez A.F., Jacobs J., Balkan W., Troen B.R., 2005. RANK ligand and interferon gamma differentially regulate cathepsin gene expression

in pre-osteoclastic cells. *Biochemical and Biophysical Research Communications*, 328(3), pp.756–763.

Pankiv, S., Lamark T., Bruun J.A., Øvervatn A., Bjørkøy G., Johansen T., 2010. Nucleocytoplasmic shuttling of p62/SQSTM1 and its role in recruitment of nuclear polyubiquitinated proteins to promyelocytic leukemia bodies. *Journal of Biological Chemistry*, 285(8), pp.5941–5953.

Pearson M. and Pelicci P.G., 2000 PML interaction with p53 and its role in apoptosis and replicative senescence. *Oncogene*, 20: pp.7250–7256.

Poór, G., Donáth J., Fornet B., Cooper C., 2006. Epidemiology of Paget's disease in Europe: The prevalence is decreasing. *Journal of Bone and Mineral Research*, 21(10), pp.1545–9.

Ralston, S.H., 2017. Bone structure and metabolism. *Medicine (United Kingdom)*, 45(9), pp.560–564.

Ralston, S.H., Corral-Gudino L., Cooper C., Francis R.M. et al., 2019. Diagnosis and Management of Paget's Disease of Bone in Adults: A Clinical Guideline. *Journal of Bone and Mineral Research*, 34(4), pp.579–604.

Ralston, S.H., 2008. Juvenile Paget's disease, familial expansile osteolysis and other genetic osteolytic disorders. *Best Practice and Research: Clinical Rheumatology*, 22(1), pp.101–111.

Ralston, S.H., 2013. Paget's Disease of Bone. *New England Journal of Medicine*, 368(7), pp.644–650.

Ralston, S.H. & Albagha, O.M.E., 2011. Genetic determinants of Paget's disease of bone. *Annals of the New York Academy of Sciences*, 1240(1), pp.53–60.

Ralston, S.H. & Albagha, O.M.E., 2012. Genetics of Paget's Disease of Bone. *Genetics of Bone Biology and Skeletal Disease*, 4(1.2), p.295.

Ralston, S.H., Langston, A.L. & Reid, I.R., 2008. Pathogenesis and management of Paget's disease of bone. *The Lancet*, 372(9633), pp.155–

163.

Ralston, S.H. & Layfield, R., 2012. Pathogenesis of paget disease of bone. *Calcified Tissue International*, 91(2), pp.97–113.

Raschke, W.C., Baird S., Ralph P., Nakoinz I., 1978. Functional macrophage cell lines transformed by abelson leukemia virus. *Cell*, 15(1), pp.261–267.

Ravikumar, B., Sarkar S., Davies J.E., Futter M., Garcia-Arencibia M. et al., 2010. Regulation of Mammalian Autophagy in Physiology and Pathophysiology. *Physiological Reviews*, 90(4), pp.1383–435.

Rea, S.L., Sarkar S., Davies J.E., Futter M., Garcia-Arencibia M. et al., 2013. New insights into the role of sequestosome 1/p62 mutant proteins in the pathogenesis of paget's disease of bone. *Endocrine Reviews*, 34(4), pp.501–524.

Reid, I.R., Lyles K., Su G., Brown J.P., Walsh J.P.et al., 2011. A single infusion of zoledronic acid produces sustained remissions in paget disease: Data to 6.5 years. *Journal of Bone and Mineral Research*, 26(9), pp.2261–2270.

Rendina, D., De Filippo G., Ralston S.H., Merlotti D. et al., 2015. Clinical characteristics and evolution of giant cell tumor occurring in Paget's disease of bone. *Journal of Bone and Mineral Research*, 30(2), pp.257–263.

Ritchie, R.O., Buehler, M.J. & Hansma, P., 2009. Plasticity and toughness in bone. *Physics Today*, 62(6), pp.41–47.

Roodman, G. & Windle, J., 2005. Science in medicine-Paget disease of bone. *The Journal of Clinical Investigation*, 115(2), pp.200–7.

Rosenberg, N., Rosenberg, O. & Soudry, M., 2012. Osteoblasts in Bone Physiology – Mini Review. *Rambam Maimonides Medical Journal*, 3(2), pp.1–7.

S. Niida, M. Kaku, H., Amano, H., Yoshida, H., Kataoka, S., Nishikawa, K. Tanne, N., Maeda, S., Nishikawa, H.K., 1999. Vascular Endothelial Growth

Factor Can Substitute for Macrophage Colony-stimulating Factor in the support of osteoclastic bone resoption. *J. Exp. Med*, 190(2), pp.293–298.

Salem, S., Gao C., Li A., Wang H. et al., 2014. A novel role for interferon regulatory factor 1 (IRF1) in regulation of bone metabolism. *Journal of Cellular and Molecular Medicine*, 18(8), pp.1588–1598.

Salomoni, P., Ferguson B.J., Wyllie A.H., Rich T., 2008. New insights into the role of PML in tumour suppression. *Cell Research*, 18(6), pp.622–640.

Salomoni P., Bernardi R., Bergmann S., Changou A., et al., 2005. The promyelocytic leukemia protein PML regulates c-Jun function in response to DNA damage. *Blood*, 105(9):3686–90.

Salomoni, P. & Pandolfi, P.P., 2002. The role of PML in tumor suppression. *Cell*, 108(2), pp.165–170.

Scaglioni P.P., Yung T.M., Cai L.F., Erdjument-Bromage H., et al. 2006. A CK2-dependent mechanism for degradation of the PML tumor suppressor. *Cell*, 126(2): pp.269–83.

Seitz, S., Priemel, M., Zustin, J., Beil, F.T. et al., 2009. Paget's disease of bone: histologic analysis of 754 patients. *Journal of Bone and Mineral Research*, 24(1), pp.62–69

Selby, P., Davie M.W., Ralston S.H., Stone M.D. et al., 2002. Guidelines on the management of Paget's disease of bone. *Bone*, 31(3), pp.366–373.

Sharma, H., MacDuff E., Jane M.J., Reid R., 2005. Sarcomatous change in the Pagetoid tibiae. *International Orthopaedics*, 29(5), pp.319–325.

Shen, X., Ying H., Qiu Y., Park J.S., Shyam R. et al., 2011. Processing of optineurin in neuronal cells. *Journal of Biological Chemistry*, 286(5), pp.3618–29.

Shimoyama, A., Wada M., Ikeda F., Hata K. et al., 2007. Ihh/Gli2 Signaling Promotes Osteoblast Differentiation by Regulating Runx2 Expression and Function. *Molecular Biology of the Cell*, 18(7), pp.2411–8.

Shin, J., Park B., Cho S., Lee S. et al., 2004. Promyelocytic leukemia is a direct inhibitor of SAPK2/p38 mitogen-activated protein kinase. *Journal of Biological Chemistry*, 279(39), pp.40994–41003.

Shtutman, M., Zhurinsky J., Oren M., Levina E., Ben-Ze'ev A., 2002. PML is a target gene of beta-catenin and plakoglobin, and coactivates beta-catenin-mediated transcription. *Cancer research*, 62(20), pp.5947–54.

Sieradzan, K.A., Mechan A.O., Jones L., Wanker E.E., Nukina N., Mann D.M., 1999. Huntington's disease intranuclear inclusions contain truncated, ubiquitinated huntingtin protein. *Experimental Neurology*, 156(1), pp.92–9.

Silva, I.A.L., Conceição N., Gagnon É., Brown J.P., Cancela M.L., Michou L., 2018. Molecular effect of an optn common variant associated to paget's disease of bone. *PLoS One*, 13(5), pp.1–16.

Singer, F.R., 2015. Paget's disease of bone-genetic and environmental factors. *Nature Reviews Endocrinology*, 11(11), pp.662–671.

Smits, P., Bolton A.D., Funari V., Hong M. et al., 2010. Lethal Skeletal Dysplasia in Mice and Humans Lacking the Golgin GMAP-210. *New England Journal of Medicine*, 362(3), pp.206–16.

Sobacchi, C., Frattini A., Guerrini M.M., Abinun M. et al., 2007. Osteoclast-poor human osteopetrosis due to mutations in the gene encoding RANKL. *Nature Genetics*, 39(8), pp.960–962.

Sofaer, J.A., Holloway, S.M. & Emery, A.E., 1983. A family study of Paget's disease of bone. *Journal of Epidemiology & Community Health*, 37(3), pp.226–231.

Sparks, A.B., Peterson S.N., Bell C., Loftus B.J. et al., 2001. Mutation screening of the TNFRSF11A gene encoding receptor activator of NF kappa B (RANK) in familial and sporadic Paget's disease of bone and osteosarcoma. *Calcif Tissue Int*, 68(3), pp.151–5.

van Staa, T.P., Selby P., Leufkens H.G., Lyles K., Sprafka J.M., Cooper C., 2002. Incidence and natural history of Paget's disease of bone in England and

Wales. *Journal of bone and mineral research*, 17(3), pp.465–71.

Stadler, M., Chelbi-Alix M.K., Koken M.H., Venturini L. et al., 1995. Transcriptional induction of the PML growth suppressor gene by interferons is mediated through an ISRE and a GAS element. *Oncogene*, 11(12), pp.2565–73.

Takata, S., Hashimoto J., Nakatsuka K., Yoshimura N. et al., 2006. Guidelines for diagnosis and management of Paget's disease of bone in Japan. *Journal of Bone and Mineral Metabolism*, 24(5), pp.359–367.

Takayanagi, H., Kim S., Koga T., Nishina H. et al., 2002. Induction and activation of the transcription factor NFATc1 (NFAT2) integrate RANKL signaling in terminal differentiation of osteoclasts. *Developmental Cell*, pp.889–901.

Takayanagi, H., Kim S., Matsuo, K., Suzuki, H. et al., 2002. RANKL maintains bone homeostasis through c-Fos-dependent induction of interferon-beta. *Nature*, 416(6882), pp.744-749.

Takayanagi, H., Ogasawara K., Hida S., Chiba T. et al., 2000. T-cell-mediated regulation of osteoclastogenesis by signalling cross-talk between RANKL and IFN-γ. *Nature*, 408(6812), pp.600–5.

Tamura, T., Kurotaki, D. & Koizumi, S. ichi, 2015. Regulation of myelopoiesis by the transcription factor IRF8. *International Journal of Hematology*, 101(4), pp.342–351.

Tan A., Goodman K., Walker A., Hudson J. et al, 2017. Long-Term Randomized Trial of Intensive Versus Symptomatic Management in Paget's Disease of Bone: The PRISM-EZ Study. *Journal of Bone and Mineral Research*, 32(6), pp.1165–1173.

Tanaka, S., Takahashi N., Udagawa N., Tamura T. et al., 1993. Macrophage colony-stimulating factor is indispensable for both proliferation and differentiation of osteoclast progenitors. *Journal of Clinical Investigation*, 91, pp.257–263.

Teitelbaum, S.L. & Ross, F.P., 2003. Genetic regulation of osteoclast development and function. *Nature Reviews Genetics*, 4(8), pp.638–649.

Teramachi, J., Nagata Y., Mohammad K., Inagaki Y. et al., 2016. Measles virus nucleocapsid protein increases osteoblast differentiation in Paget's disease. *Journal of Clinical Investigation*, 126(3), pp.1012–1022.

Thouverey, C. & Caverzasio, J., 2015. Focus on the p38 MAPK signaling pathway in bone development and maintenance. *BoneKey Reports*, 4(JUNE), pp.1–8.

Tiegs, R.D., Lohse C.M., Wollan P.C., Melton L.J., 2000. Long-term trends in the incidence of Paget's disease of bone. *Bone*, 27(3), pp.423–427.

Tomé M., López-Romero P., Albo C., Sepúlveda J.C., Fernández-Gutiérrez B. et al., 2011. miR-335 orchestrates cell proliferation, migration and differentiation in human mesenchymal stem cells. *Cell Death and Diferentiation*, 18(6), pp.985–95.

Tsuzuki S., Towatari M., Saito H, Enver T., 2000. Potentiation of GATA-2 activity through interactions with the promyelocytic leukemia protein and the t (15, 17)-generated PML-retinoic acid receptor alpha oncoprotein. *Mol Cell Biol*, 20(17):6276–86.

Usategui-Martín, R., García-Aparicio J., Corral-Gudino L., Calero-Paniagua I. et al., 2015. Polymorphisms in autophagy genes are associated with paget disease of bone. *PLoS ONE*, 10(6), pp.1–9.

Vallet, M., Soares D.C., Wani S., Sophocleous A. et al., 2014. Targeted sequencing of the Paget's disease associated 14q32 locus identifies several missense coding variants in RIN3 that predispose to Paget's disease of bone. *Human Molecular Genetics*, 24(11), pp.3286–3295.

Vallian S, Chin K.V., Chang K.S., 1998. The promyelocytic leukemia protein interacts with Sp1 and inhibits its transactivation of epidermal growth factor receptor promoter. *Mol. Cell. Biol.*, 18: 7147–7156.

Vincent, C., Kogawa M., Findlay D.M., Atkins GJ. 2009. The generation of

osteoclasts from RAW 264.7 precursors in defined, serum-free conditions. *Journal of Bone and Mineral Metabolism*, 27(1), pp.114–119.

Wada, T., Nakashima T., Hiroshi N., Penninger J.M., 2006. RANKL-RANK signaling in osteoclastogenesis and bone disease. *Trends in Molecular Medicine*, 12(1), pp.17–25.

Wang Z.G., Ruggero D., Ronchetti S.., Zhong S., et al., 1998. PML is essential for multiple apoptotic pathways. *Nat Genet*, 20(3): pp.266–72

Wang, Z.G., Delva L., Gaboli M., Rivi R. et al., 1998. Role of PML in cell growth and the retinoic acid pathway. *Science*, 279(5356), pp.1547–1551.

Watts, G.D.J., Wymer J., Kovach M.J., Mehta S.G. et al., 2004. Inclusion body myopathy associated with Paget disease of bone and frontotemporal dementia is caused by mutant valosin-containing protein. *Nature Genetics*, 36(4), pp.377–81.

Westra, H.J., Peters M. J., Esko T., Yaghootkar H., Schumann C. et al., 2013. Systematic identification of trans eQTLs as putative drivers of known disease associations. *Nature Genetics*, 45(10), pp.1238–43.

Whyte, M.P, Mills B.G., Reinus W.R., Podgornik M.N. et al., 2000. Expansile skeletal hyperphosphatasia: A new familial metabolic bone disease. *Journal of Bone and Mineral Research*, 15(12), pp.2330–44.

Whyte, M.P., Obrecht S.E., Finnegan P.M., Jones J.L. et al., 2002. Osteoprotegerin Deficiency and Juvenile Paget's Disease. *New England Journal of Medicine*, 347(3), pp.175–84.

Wong, S.W., Huang B.W., Hu X., Ho Kim E. et al., 2019. Global deletion of Optineurin results in altered type I IFN signaling and abnormal bone remodeling in a model of Paget's disease. *Cell Death & Differentiation*. Epublication.

Wood, A.R., Esko T., Yang J., Vedantam S. et al., 2014. Defining the role of common variation in the genomic and biological architecture of adult human height. *Nature Genetics*, 46(11), pp.1173–86.

Wu W.S., Xu Z.X., Ran R., Meng F., 2002. PML inhibits Nur77-mediated transcription through specific functional interactions. *Oncogene*, 21(24): pp.3925–33

Wu J., Zhou L.Q., Yu W., Zhao Z.G., et al., 2014. PML4 facilitates erythroid differentiation by enhancing the transcriptional activity of GATA-1. *Blood*, 123(2):261–70.

Wu W.S., Xu Z.X., Chang K.S., 2002. The promyelocytic leukemia protein represses A20-mediated transcription. *J Biol Chem*.; 277(35):31734–9.

Wu, M., Chen, G. & Li, Y.P., 2016. TGF-β and BMP signaling in osteoblast, skeletal development, and bone formation, homeostasis and disease. *Bone Research*, 4.Ecollection.

Wu, W.S., Xu Z.X., Hittelman W.N., Salomoni P. et al., 2003. Promyelocytic Leukemia Protein Sensitizes Tumor Necrosis Factor α-Induced Apoptosis by Inhibiting the NF-κB Survival Pathway. *Journal of Biological Chemistry*, 278(14), pp.12294–12304.

Wu, W.S., Xu, Z.X. & Chang, K.S., 2002. The promyelocytic leukemia protein represses A20-mediated transcription. *Journal of Biological Chemistry*, 277(35), pp.31734–31739.

Xu, W.X., Liu S.Z., Wu D., Qiao G.F., Yan J. et al., 2015. Sumoylation of the tumor suppressor promyelocytic leukemia protein regulates arsenic trioxide-induced collagen synthesis in osteoblasts. *Cellular Physiology and Biochemistry*, 37(4), pp.1581–1591.

Yagi, M., Miyamoto T., Sawatani Y., Iwamoto K. et al., 2005. DC-STAMP is essential for cell–cell fusion in osteoclasts and foreign body giant cells. *The Journal of Experimental Medicine*, 202(3), pp.345–51.

Yasuda, H., Shima N., Nakagawa N., Mochizuki S.I., Yano K., Fujise N., Sato Y, Goto M. et al., 1998. Identity of OCIF and OPG. A mechanism by which OPG/OCIF inhibits osteoclastogenesis in vitro. *Endocrinology*, 139(3), pp.1329–37.

Yoshida, H., Hayashi S., Kunisada T., Ogawa M. et al., 1990. The murine mutation osteopetrosis is in the coding region of the macrophage colony stimulating factor gene. *Nature*, 345, pp.442–444.

Zeller, T., Wild P., Szymczak S., Rotival M., Schillert A., Castagne R. et al., 2010. Genetics and beyond-The transcriptome of Human Mondocytes and disease susceptibility. *Plos One*, 5(5), e10693.

Zhao, B., Takami M., Yamada A., Wang X., Koga T. et al., 2009. Interferon regulatory factor-8 regulates bone metabolism by suppressing osteoclastogenesis. *Nature Medicine*, 15(9), pp.1066–1071.

Zhao, B. & Ivashkiv, L.B., 2011. Negative regulation of osteoclastogenesis and bone resorption by cytokines and transcriptional repressors. *Arthritis Research and Therapy*, 13(4), pp.1–10.

Zhou, X., Zhang Z., Feng J.Q., Dusevich V.M., Sinha K., Darnay B.G., de Crombrugghe B., 2010. Multiple functions of osterix are required for bone growth and homeostasis in postnatal mice. *Pnas*, 107(29), pp.12919–24.

Zhu, G., Wu C.J., Zhao Y., Ashwell J.D., 2007. Optineurin Negatively Regulates TNFα- Induced NF-κB Activation by Competing with NEMO for Ubiquitinated RIP. *Current Biology*, 17, pp.1438–1443.

Zhu, J., Koken M.H., Quignon F., Chelbi-Alix M.K. et al., 1997. Arsenic-induced PML targeting onto nuclear bodies: implications for the treatment of acute promyelocytic leukemia. *Proceedings of the National Academy of Sciences of the United States of America*, 94(April), pp.3978–3983.

Zimmermann, E.A., Köhne T., Bale H.A., Panganiban B. et al., 2015. Modifications to nano- and microstructural quality and the effects on mechanical integrity in Paget's disease of bone. *Journal of Bone and Mineral Research*, 30(2), pp.264–73.

11 Appendices

Appendix 1. TRAcP Staining of osteoclasts

Solutions for TRAcP staining were prepared as follows:

Naphthol-AS-BI-phosphate

10 mg/ml Naphthol-AS-BI-phosphate in N.N-Dimethylformamide

Veronal buffer

1.17 g sodium acetate (anhydrous) and 2.94g sodium barbiturate, both dissolved in 100 ml of dH_2O

Acetate buffer

0.82 g sodium acetate anhydrous dissolved in 100 ml of dH_2O and pH adjusted to 5.2 with 0.6 ml glacial acetic acid which is made up to 100 ml with dH_2O

Pararosanilin

1g Pararosanilin added to 20ml dH_2O followed by 5ml concentrated HCl. Solution heated carefully in a waterbath while stirring until fully dissolved and filtered after cooling to room temperature.

Sodium Nitrite

4g of sodium nitrite in 100mls dH_2O

TRAcP staining solution was prepared fresh by mixing solution A and B as mentioned below. Solution B was prepared prior to fixing the cells since it needs time to bind before being added to Solution A and the mix filtered through 0.2um filter.

Solution A

150 ml of Napthol-AS-BI-phosphate

750 ml of Veronal buffer

900 ml Acetate buffer

900 ml Acetate buffer with 100 mM Sodium Tartrate

Solution B

120 ml of Pararosanilin

120 ml of Sodium Nitrite (4%)

Appendix 2. Nrecon software reconstruction parameters

Parameter	*Description*	*Setting*
Smoothing	Smoothens images and removes noise	Width, 1 pixel
Beam hardening factor	Corrects for absorption of lower-energy X-ray on the outside of specimen	10%
Ring artefact reduction	Corrects for the non-linear behaviour of pixels causing ring artifacts	10

Appendix 3. CTAn software analysing parameters

Parameter	*Description*	*Setting*
Smoothing/Filtering	Smoothes images and removes noise	Median filter, 2D space Radius: 1
Threshold	Segment the foreground from background to binary images	Global, Low level 80-100, High level 255
Despeckle	Remove speckles from binary images	Remove white speckles, <150 voxels, Image
3D Model	Creates 3D surface from binary images	Adaptive rendering, file saved as .p3g
3D Analysis	Calculates 3D parameters of binary images	Output of Trabecular thickness, number and separation as well as cortical thickness

Appendix 4. Immunohistochemistry Envision protocol

FFPE tissue blocks were obtained with help of Prof. Donald Salter from NHS Lothian tissue archive and included samples from patients with PDB, Giant cell tumour as well as tissue microarrays for initial optimisation of primary antibody (PML) concentration for IHC. Samples were processed for FFPE by fixing them in neutral buffered formalin for 24 hours at RT. Post-fixation, bone tissue was decalcified and samples passed through a series of graded ethanol and xylene washes and then infiltrated with molten paraffin wax and embedded into blocks. The FFPE samples were then processed for IHC at Division of Pathology Histology services by Helen Caldwell. Briefly, FFPE blocks were cut into thin sections of 4um thickness using a Leica microtome, placed in a floatation bath to flatten them and transferred to positively charged Superfrost slides and baked overnight in a low temperature oven. Envision Immuno protocol was then performed using heat induced epitope retrieval technique with the following steps:

1. Dewax sections in xylene under hood through graded alcohols and finally to water, the sequence being two successive Xylene washes for 5 mins each followed by EtOH 100% (2min), then EtOH 100%(2min), then EtOH 80%(2min), then EtOH 50%(2min) with final wash in tap water.

2. Perform antigen retrieval on slides by treating them with antigen retrieval solution (0.1Msodium citrate and 0.1M citric acid; pH 6) in pressure cooker, heated in a microwave for 5 minutes, leave to cool for at least 20 minutes on a paper.

3. Wash slides in PBS-Tween (0.1%) twice for 5 minutes.

4. Treat sections in 3% hydrogen peroxide in water for 10 minutes which blocks endogenous peroxidases in tissue.

5. Wash slides with PBS-Tween (0.1%) for 5 minutes.

6. Add slides to Sequenza rack.

7. Block with Dako Total Protein blocking solution from Agilent for 30 minutes.

8. Incubate sections in PML H-238 sc-5621 primary antibody diluted 1:200 with Dako antibody diluent for 1 hour at room temperature.

9. Wash with PBS-Tween (0.1%) twice.

10. Incubate section with Dako envision labelled polymer (secondary antibody) from Agilent for 30 minutes.

11. Wash slides with PBS-Tween (0.1%) twice.

12. Add DAB substrate diluted in DAB buffer until colour develops to visualise.

13. Wash sections in tap water.

14. Counterstain with Hematoxylin for 10 minutes and wash successively with water, then ethanol 50%, 80% & 100% twice followed by three consecutive Xylene washes (5 mins each).

15. Sections were mounted using DPX mounting medium (Sigma) using cover slip and analysed using Olympus BX51 or Zeiss inverted microscope.

Appendix 5. Protein isolation and Western blot reagents

RIPA lysis buffer

1% Triton 100X, 0.5% (w/v) Sodium Deoxycholate, 50 mM Tris-HCl (pH 7.4), 0.1% (w/v) Sodium Dodecyl Sulphate (SDS) and 150 mM Sodium Chloride were dissolved in dH_2O. Stored at 4°C.

This was reconstituted with Protease inhibitor, Phosphatase inhibitor, 0.5M EDTA and 1M Sodium Fluoride (NaF) prior to extracting protein from cultured cells/tissue.

Electrophoresis running buffer

100 ml of 10X TGS Buffer (Biorad) in 900 ml of dH_2O. Stored at room temperature.

Samples loading protein buffer (5X stock)

5.2 ml of 1M Tris-HCl pH adjusted to 6.8, 3 g SDS, 1 g of DL-Dithiothreitol (DTT), 6.5 ml glycerol and 130 ul of 10% (w/v) Bromophenol Blue. Stored at -20°C.

1X TBS

50ml of 20X TBS Buffer (Thermoscientific Pierce) in 950 ml dH_2O. Stored at room temperature.

TBST

0.1% (v/v) Tween-20 in TBS prepared as above. Stored at room temperature.

Stripping buffer

2% (w/v) SDS and 62.5 mM Tris-HCl (pH 6.7). Make up with dH_2O. Stored at 4°C. Then, finally add 1mM DTT prior to use.

Appendix 6. Apparatus, Software, Consumables and reagents

Apparatus	Supplier
Axiovert 200 inverted microscope	Carl Zeiss, UK
Axiovert 40 CFL inverted microscope	Carl Zeiss, UK
Balance	Fisherbrand and Ohaus, Switzerland
Bench top centrifuge	Sigma, Germany
Bench top Eppendorf centrifuge	Sigma, Germany
Bio2 safety cabinet	Envair, UK
Bio-Tek Synergy HT plate reader	Fisherscientific, UK
BX51 microscope	Olympus, UK
Captair Bio flow RNA workstation	Erlab, US
CFX Connect real time PCR machine	Biorad, UK
Class II biological safety cabinet	Nuaire, UK
CO_2 Incubators Cell 240	Heraeus, Germany
Fridge / Freezer	Lec, UK
Fume hood	Envair, UK
Gel tanks, Criterion	Biorad, UK
Heat block	Grant, UK
Horizontal electrophoresis tanks	Fisherscientific, UK
Hot plate / stirrer	Thistlescientific, UK
Icemaker	Scotsman AF103
MJ Research thermocycler	GRI, UK
Nanodrop ND-8000	Thermoscientific, UK
Odysssey Fc Imaging system	Li-cor, UK
Pipettes (2,20,100,200,1000ul)	Nichipet, Gilson, Eppendorf, UK
Powerpack basic	Biorad, UK
QImaging Retiga CCD camera	Media cybernetics, UK

Rocking table / Shaker	Biometra, Germany
Skyscan 1172 uCT system	Skyscan, Belgium
Syngene GelDoc Imaging system	Fisherscientific, UK
Tetrad 2 thermocycler	Biorad, UK
Transblot Turbo blotting system	Biorad, UK
Vortex	Fisherscientific, UK
Waterbath Grant OLS	Thistlescientific, UK
Software	**Supplier**
BioTek Gen5 plate reader software	Biotek, UK
Burrows-Wheeler Alignment tool	Wellcome Trust Sanger Institute, UK
CFX manager software	Biorad, UK
Chromas Pro	Technelysium Pty Ltd, UK
GATK	Broad Institute, US
Genesys software, Syngene	Synoptics, UK
Genetools software, Syngene	Synoptics, UK
Image studio lite ver 3.1	Li-cor, UK
ImageJ	NIH, US
Microsoft Word, Powerpoint, Excel, Windows	Microsoft, US
Mutation surveyor V3.30	Softgenetics, US
Opticon monitor 3.1 software	GRI, UK
PLINKSeq	Harvard, NIH, US
Polyphen 2	Harvard, NIH, US
QCapture Pro software	Media cybernetics, UK
SIFT	Genome Institute, Singapore
Skyscan 1172 MicroCT software	Skyscan, Belgium
Skyscan CTAn software	Skyscan, Belgium
Skyscan CTVol software	Skyscan, Belgium
Skyscan Dataviewer software	Skyscan, Belgium

Skyscan NRecon software	Skyscan, Belgium
SPSS 22	IBM, US
Other reagent / consummable	**Supplier**
0.5ml, 1ml and 2ml eppendorf tubes	Greiner, UK
1ml Pasteur pipette	Fisher scientific, UK
96 well PCR plates	Thermo scientific, UK
96 well, 12 well, 24 well tissue culture plate	Corning, UK
Adhesive PCR plate seals	Thermo Fisher scientific, UK
Agarose	Bioline, UK
Alamar Blue reagent	Invitrogen, UK
Alizarin Red S	Sigma Aldrich, UK
Ammonium hydroxide	Sigma Aldrich, UK
Arsenic Trioxide	Sigma Aldrich, UK
Axygen microcentrifuge tubes	Axygen Corning, UK
BCA protein assay	Sigma Aldrich, UK
BSA (Bovine serum albumin)	Sigma Aldrich, UK
Calcein	Sigma Aldrich, UK
Cell dissociation buffer	Gibco, UK
Cell scrapers	Sarstedt, UK
Cetylpyridinium chloride	Sigma Aldrich, UK
Clarity western ECL substrate	Biorad, UK
Collagenase IA	Sigma Aldrich, UK
Copper II sulfate	Sigma Aldrich, UK
Cover slips	SLS, UK
DEPC treated water	Thermo Fisher scientific, UK
DMSO	Sigma Aldrich, UK
DNA ladders (100bp, LMW and 1kb)	New England Biolabs, UK
dNTPs	Thermo Fisher scientific, UK
DPX mounting medium	Sigma Aldrich, UK

DTT (Dithiothreitol)	Sigma Aldrich, UK
EDTA (Ethylenediamine tetraacetic acid)	Sigma Aldrich, UK
Ethanol Absolute for molecular biology	Fisher scientific, UK
Falcon (15ml and 50ml)	Greiner, UK
FCS (Fetal calf serum)	Hyclone, UK
Filter sterile (0.45um)	Merck Millipore, UK
Forceps	World precision instruments, UK
Genticin	Lifetech, UK
Glacial acetic acid AnalR	Sigma Aldrich, UK
Glycerol	VWR, UK
Hanks's solution HBSS	Sigma Aldrich, UK
HCl (Hydrochloric acid) AnalR	BDH, UK
Interferon gamma	Lifetech, UK
Jet-PEI macrophage	Polyplus, UK
Kaleidoscope ladder	Biorad, UK
Kisol foil	Taab Lab, UK
L-Glutamine	Invitrogen, UK
Magic Mark	Invitrogen, UK
Methanol	Thermo Fisher scientific, UK
MicroAmp 8-cap flat PCR strip	Thermo Fisher scientific, UK
Mini Protean TGX gels	Biorad, UK
M-CSF	Prospec Tany, US
N,N-Dimethylformamide	Fisher scientific, UK
Naphthol-AS-BI-phosphate	Sigma Aldrich, UK
Needles (19,21,25G)	BD, US
Neubauer's chamber	Hawksley, UK
Nitrile gloves	Fisher scientific, UK
Optical flat 8 cap strips	Bioplastics, UK
Orange G	Sigma Aldrich, UK

Paraformaldehyde	Taab Lab, UK
Pararosanilin	Sigma Aldrich, UK
Penicillin	Invitrogen, UK
PBS tablets	Invitrogen, UK
PCR primers	Invitrogen, UK
Petri dishes	BD, UK
Phosphatase inhibitor cocktail	Sigma Aldrich, UK
Pipette tips (all sizes)	Starlab, UK
Protease inhibitor cocktail	Sigma Aldrich, UK
Protein BSA standards prediluted	Thermo Fisher scientific, UK
qPCR nonskirted 96 well white plates	Bioplastics, UK
qScript cDNA supermix	Quanta bioscience, US
RANKL	R&D systems
RNA later solution	Sigma, Thermoscientic, UK
Scalpel	VWR, UK
Scissors	S. Murray & Co. Ltd, UK
SensiFAST No-ROX qPCR mix	Bioline, UK
Silver nitrate	Sigma Aldrich, UK
Silver nitrite	Sigma Aldrich, UK
Sodium acetate anhydrous	Sigma Aldrich, UK
Sodium barbiturate	BDH, UK
Sodium carbonate	Sigma Aldrich, UK
Sodium chloride	Sigma Aldrich, UK
Sodium deoxycholate	Sigma Aldrich, UK
Sodium dodecyl sulphate (SDS)	Biorad, UK
Sodium fluoride	Sigma Aldrich, UK
Sodium hypochlorite	Sigma Aldrich, UK
Sodium phosphate	Sigma Aldrich, UK
Sodium tartrate dibasic dihydrate	Sigma Aldrich, UK
Stripettes (2ml, 5ml, 10ml, 25ml and 50ml)	Costar, UK
Streptomycin	Invitrogen, UK

SYBR Safe DNA gel stain	Thermo Fisher scientific, UK
Syringes (all sizes)	BD, UK
Taq polymerase and accessory kit reagent	Qiagen, UK
Taqman 18s Gene expression rRNA mix	Applied biosystems, UK
Tissue culture flasks (25 and 75 cm^2)	Greiner, UK
Tris	Biorad, UK
Tris-EDTA buffer	Sigma Aldrich, UK
Triton X-100	Sigma Aldrich, UK
Trypsin/EDTA	Sigma Aldrich, UK
Tween 20	Biorad, UK
Universal probe library	Roche, UK
Vitamin C	BDH Lab, UK
Xylene AnalR	Sigma Aldrich, UK
β Glycerol -2- phosphate	Sigma Aldrich, UK

Appendix 7. Summary of protein coding variants found at 15q24 locus by Targeted Sequencing

Gene	*Variant ID*	*Position (hg19)*	*Reference Allele*	*Sample Allele*	*Gene Region*	*Protein Variant*	*Function*	*AF Cases (%)[a]*	*AF Controls (%)[a]*	*P-value*	*SIFT Function Prediction*	*PolyPhen-2 Function Prediction*
LOXL1	N/A	74219158	G	A	Exonic	p.A12T	missense	0.0	1.0	0.26		Benign
	N/A	74219308	G	A	Exonic	p.V62M	missense	0.0	1.0	0.26	Tolerated	Benign
	rs1048661	74219546	G	T	Exonic	p.R141L	missense	23.6	24.0	0.79	Tolerated	Benign
	rs3825942	74219582	G	A	Exonic	p.G153D	missense	13.4	17.0	0.34	Damaging	Benign
	rs138183635	74219602	G	C	Exonic	p.A160P	missense	0.7	0.0	0.53	Tolerated	Possibly Damaging
	rs41429348	74220000	C	T	Exonic	p.D292D	synonymous	2.9	3.0	0.26		
	rs13329473	74239525	C	T	Exonic	p.F489F	synonymous	0.4	0.0	0.73		
STOML1	rs34353835	74277666	C	T	Exonic	p.P261P; p.P174P; p.P211P; p.P219P	synonymous	6.5	1.0	0.03		
	rs10851866	74277795	T	C	Exonic	p.A176A; p.A131A; p.A218A; p.A168A	synonymous	35.1	42.0	0.19		
	rs370609840	74281464	G	A	Exonic	p.N125N; p.N38N; p.N83N	synonymous	0.4	0.0	0.73		
PML	rs17849259	74315358	C	T	Exonic	p.A264A	synonymous	0.4	1.0	0.46		
	rs140050477	74315485	C	T	Exonic	p.R307C	missense	0.0	1.0	0.26	Damaging	Possibly Damaging
	rs148158604	74325040	G	C	Exonic	p.G461A	missense	0.4	0.0	0.73	Tolerated	Benign
	rs386449354	74327684	G	A	Exonic	p.A628T; p.A580T	missense	0.4	0.0	0.73		Benign
	rs75056290	74327819	C	T	Exonic	p.R673C; p.R625C	missense	0.4	0.0	0.73		Benign
	rs140648301	74327949	A	G	Exonic	p.Q716R; p.Q668R	missense	0.4	0.0	0.73		Benign
	rs144170102	74327973	G	A	Exonic	p.R724Q; p.R676Q	missense	0.7	0.0	0.53		Benign
	rs743580	74328116	A	G	Exonic	p.S724G; p.S772G	missense	31.5	39.0	0.05		Benign
	rs146867846	74328125	C	A	Exonic	p.Q775K; p.Q727K	missense	0.4	0.0	0.73		Benign
	rs743581	74328141	G	T	Exonic	p.G780V; p.G732V	missense	23.9	33.0	0.01		Benign
	rs743582	74328206	G	C	Exonic	p.A802P; p.A754P	missense	6.5	7.0	0.17		Benign
	N/A	74328261	C	A	Exonic	p.P820Q; p.P772Q	missense	0.0	1.0	0.26		Possibly Damaging
	rs5742915	74336633	T	C	Exonic	p.F645L	missense	43.1	36.0	0.005	Tolerated	Benign

	rs61751122	74336656	C	T	Exonic	p.A652A	synonymous	2.2	2.0	0.31		
	rs61751123	74336725	C	T	Exonic	p.A675A	synonymous	1.4	0.0	0.57		
	rs111398700	74336874	A	G	Exonic	p.K725R	missense	1.1	1.0	0.28	Tolerated	Benign
	rs61751124	74337073	C	G	Exonic	p.P791P	synonymous	0.4	1.0	0.46		
ISLR2	rs3743207	74425410	T	C	Exonic	p.D105D	synonymous	0.7	2.0	0.28		
	rs3889598	74425505	C	T	Exonic	p.S137F	missense	0.7	2.0	0.28	Damaging	Benign
	rs141520519	74426925	C	T	Exonic	p.G610G	synonymous	0.7	1.0	0.43		
	rs140851809	74427231	G	A	Exonic	p.E712E	synonymous	0.4	0.0	0.73		
ISLR	rs76808097	74467585	T	C	Exonic	p.M129T	missense	0.0	1.0	0.26	Damaging	Possibly Damaging
	rs11854957	74467796	C	T	Exonic	p.A199A	synonymous	15.6	19.0	0.30		
	rs1052622	74467856	G	A	Exonic	p.T219T	synonymous	43.8	44.0	0.70		
	rs150108021	74467878	C	T	Exonic	p.L227L	synonymous	0.0	1.0	0.26		
	rs150921456	74468105	G	A	Exonic	p.P302P	synonymous	1.1	2.0	0.61		
	rs140374543	74468266	G	C	Exonic	p.G356A	missense	1.1	0.0	0.56	Tolerated	Benign
	rs149028569	74468321	C	T	Exonic	p.N374N	synonymous	0.0	1.0	0.26		
	rs140714071	74468355	G	A	Exonic	p.V386I	missense	0.4	0.0	0.73	Tolerated	Possibly Damaging

[a]Allele Frequency (AF) calculated by (number of alleles observed/total number of alleles) and shown as percentage.

Appendix 8. Summary of potential regulatory variants found at 15q24 locus by Targeted Sequencing

Gene	*Variant ID*	*Position (hg19)*	*Reference Allele*	*Sample Allele*	*Gene Region*	*AF Cases (%)[a]*	*AF Controls (%)[a]*	*P-value*	*Regulatory site*	*Regulator*
LOXL1	rs12708513	74218178	G	C	Promoter	50.0	50.0	1	Promoter Loss	Hltf; ZEB1
	rs16958477	74218466	A	C	Promoter	33.3	39.0	0.72	Promoter Loss; ENCODE TFBS	ZNF263; Tcfcp2l1
	N/A	74218479	T	A	Promoter	0.4	0.0	0.73	ENCODE TFBS	ZNF263
	rs139557020	74218509	C	G	Promoter	1.4	2.0	0.65	Promoter Loss; ENCODE TFBS	ZNF263; Pax2
STOML1	rs2304715	74284406	C	G	Intronic	35.9	35.0	0.64	ENCODE TFBS	POLR2A
	rs28454082	74284780	C	G	Promoter; Intronic	0.4	0.0	0.73	Promoter Loss; ENCODE TFBS	NFKB1; ZNF263; ZNF143; STAT1; STAT2; SP2
	N/A	74284784	G	C	Promoter; Intronic	0.0	1.0	0.26	Promoter Loss; ENCODE TFBS	NFKB1; ZNF263; ZNF143; STAT1; STAT2 SP2
	rs28575231	74284801	C	G	Promoter; Intronic	0.4	0.0	0.73	Promoter Loss; ENCODE TFBS	NFKB1; ZNF263; ZNF143; STAT1; STAT2 ; SP2
	rs11633520	74284805	C	G	Promoter; Intronic	38.8	39.0	0.64	ENCODE TFBS	ZNF263;NFKB1; ZNF143; STAT1 STAT2; SP2
	rs79233608	74285177	G	A	Promoter; Intronic	8.3	1.0	0.004	Promoter Loss	GATA2; Esrrb; ETS1
	rs111819443	74285446	G	A	Promoter; Intronic	0.0	1.0	0.26	Promoter Loss	MZF1_1-4
	rs185313180	74285530	C	A	Promoter; Intronic	0.4	0.0	0.73	Promoter Loss	TFAP2A
STOML1; PML	rs2301272	74286482	C	T	Promoter; Intronic	2.2	3.0	0.70	Promoter Loss	Mafb; ETS1
STOML1; PML	rs2301273	74286882	C	T	Promoter; Intronic	1.8	3.0	0.44	Promoter Loss; ENCODE TFBS	ZNF263; ZNF143; SP1; SP2; IRF1
STOML1; PML	rs5742914	74286929	C	T	Promoter; 5'UTR	7.6	17.0	0.02	Promoter Loss; ENCODE TFBS	ZNF263; STAT1; SP1; SP2; IRF1
STOML1; PML	rs371460626	74287381	C	T	Promoter; Intronic	0.4	0.0	0.73	Promoter Loss; ENCODE TFBS	REST; EBF1; FOXC1
LOC283731; ISLR2	rs79925446	74420796	C	T	Promoter; ncRNA	0.4	1.0	0.46	ENCODE TFBS	SUZ12

ISLR2	rs2279379	74421010	C	G	Promoter	17.8	25.0	0.08	Promoter Loss	ETS1; TFAP2A
	rs183039083	74421025	C	T	Promoter	0.7	0.0	0.53	Promoter Loss	TFAP2A; MZF1_1-4
	N/A	74421254	C	T	Promoter	0.4	0.0	0.73	Promoter Loss	Mafb; TFAP2A; Klf4
LOC283731; ISLR2	rs80172572	74421336	C	A	Promoter; ncRNA	6.5	6.0	0.18	ENCODE TFBS; Promoter Loss	SUZ12; ZNF354C
LOC283731; ISLR2	N/A	74421440		G	Promoter; ncRNA	0.0	1.0	0.26	ENCODE TFBS; Promoter Loss	SUZ12; SP1
LOC283731; ISLR2	rs75640427	74421442	G	A	Promoter; ncRNA	0.7	0.0	0.53	ENCODE TFBS; Promoter Loss	SUZ12; SP1
ISLR2	rs28665184	74422047	C	G	Promoter; 5'UTR	0.4	0.0	0.73	ENCODE TFBS	SUZ12; GATA2
	rs142361296	74422822		Insertion C	Intronic; 5'UTR	1.8	1.0	0.34	ENCODE TFBS	SUZ12
	N/A	74422822		Insertion N	Intronic; 5'UTR	1.1	0.0	0.56	ENCODE TFBS	SUZ12
ISLR	N/A	74465485	G	A	Promoter	0.0	1.0	0.26	Promoter Loss; ENCODE TFBS	E2F1; CTCF
ISLR	rs71434225	74465522	A	Deletion A	Promoter	10.5	12.0	0.13	Promoter Loss; ENCODE TFBS	CTCF; FOXA1
	N/A	74465522	AA	Deletion AA	Promoter	4.0	3.0	0.76	Promoter Loss; ENCODE TFBS	CTCF; FOXA1
	rs111365628	74466130	G	A	Promoter; 5'UTR	0.0	1.0	0.26	ENCODE TFBS; Promoter Loss	TFAP2A; POLR2A
	rs923118	74466271	G	T	Promoter; 5'UTR	15.6	19.0	0.30	ENCODE TFBS; Promoter Loss	TFAP2A; Myc; Mycn; POLR2A
	rs1385650	74466466	G	A	Promoter; Intronic	44.9	44.0	0.37	Promoter Loss	Arnt::Ahr; HIF1A::ARNT
	rs73431458	74466703	G	A	Promoter; Intronic	9.1	5.0	0.40	Promoter Loss	TFAP2A

[a]Allele Frequency (AF) calculated by (number of alleles observed/total number of alleles) and shown as percentage.